ΙΔΡΥΜΑ ΤΕΧΝΟΛΟΓΙΑΣ ΚΑΙ ΕΡΕΥΝΑΣ

UNIVERSITY OF CRETE

Postgraduate Program
Molecular Biology and Biomedicine

Study of transcription circuits and enhancers involved in neural stem cell fate in Drosophila

Postgraduate thesis

Boumpa Vasiliki

Professor: Delidakis Christos
Supervisor: Theodorou Vasiliki

Heraklion, 2022

Table of contents

Abstract

The nervous system of Drosophila consists of the central and peripheral nervous systems. Neurogenesis is regulated by proneural genes (acute-scute complex: acute, scute, lethal of scute and asense), which drive cells to a neural fate, and neurogenic genes (Notch signalling and Enhancer of split complex), which drive to the epidermal fate. Neuroblasts, the stem cells of the nervous system, divide asymmetrically, resulting in a new neuroblast and a ganglion mother cell (GMC). The GMC divides to produce neurons and glia. During the development of an organism, the genome gives rise to different cell types, each expressing a subset of genes that define its identity. Important in this process are enhancers, which are cis-regulatory elements and determine transcription in each cell type. Their study is important as they bind transcription factors and cofactors and drive gene transcription to desired levels and not to basal level, which results from promoters. In this thesis, transcriptional circuits and enhancers were studied, involved in the embryonic neural stem cells fate, as well as their dependence on proneural genes was examined. Specifically, the enhancers and the genes they control were studied in the wild type and in deficiency environment lacking the three proneural genes except from asense. The results showed that some enhancers and genes are completely dependent on the absent proneural transcription factors, while other enhancers and genes respond in the presence of asense and are activated. Regarding the transcriptional circuits, the ability of deadpan, a transcriptional repressor and neuroblast marker, to repress neural fate repressors, one of the genes of the Enhancer of split complex, was investigated. The results show that deadpan does not suppress the neurogenic gene studied. Deeper study is needed both on the activity of the enhancers, and on the action of deadpan and the transcriptional circuits involved in the neuroblasts fate.

Περίληψη

Το νευρικό σύστημα της Drosophila αποτελείται από το κεντρικό και το περιφερειακό νευρικό σύστημα. Η νευρογένεση ρυθμίζεται από τα προνευρικά γονίδια (acute-scute complex: acute, scute, lethal of scute και asense), που καθοδηγούν τα κύτταρα προς τη νευρική τύχη, και τα νευρογόνα γονίδια (Notch signaling και Enhancer of split complex), που καθοδηγούν προς την επιδερμική τύχη. Οι νευροβλάστες, τα βλαστικά κύτταρα του νευρικού συστήματος, διαιρούνται ασύμμετρα, με αποτέλεσμα ένα νέο νευροβλάστη και ένα ganglion mother cell (GMC). Το GMC διαιρείται παράγοντας νευρώνες και γλοία. Κατά τη διάρκεια της ανάπτυξης ενός οργανισμού, το γονιδίωμα δημιουργεί διαφορετικούς κυτταρικούς τύπους, με τον καθένα να εκφράζει ένα υποσύνολο γονιδίων, που ορίζουν την ταυτότητά του. Σημαντικοί σε αυτή τη διαδικασία είναι οι ενισχυτές, που είναι cis-ρυθμιστικά στοιχεία και καθορίζουν τη μεταγραφή σε κάθε κυτταρικό τύπο. Η μελέτη τους είναι σημαντική καθώς προσδένουν μεταγραφικούς παράγοντες και συμπαράγοντες και οδηγούν τη μεταγραφή του γονιδίου σε επιθυμητά επίπεδα και όχι απλά στο βασικό επίπεδο, που προκύπτει από τους υποκινητές. Στην παρούσα διπλωματική εργασία μελετήθηκαν μεταγραφικά κυκλώματα και ενισχυτές, που εμπλέκονται στη γένεση των εμβρυικών νευρικών βλαστοκυττάρων και των παραγόμενων κυττάρων, καθώς και η εξάρτηση τους από τα προνευρικά γονίδια. Πιο συγκεκριμένα, οι ενισχυτές και τα γονίδια που ελέγχουν μελετήθηκαν στον άγριο τύπο και σε περιβάλλον έλλειψης των τριών προνευρικών μεταγραφικών παραγόντων παρουσία του asense, και από τα αποτελέσματα προκύπτει πως κάποιοι ενισχυτές και γονίδια εξαρτώνται πλήρως από τα απόντα προνευρικά γονίδια, ενώ άλλοι ενισχυτές και γονίδια αποκρίνονται στην παρουσία του asense και ενεργοποιούνται. Όσον αφορά στα μεταγραφικά κυκλώματα, ερευνήθηκε η ικανότητα του deadpan, ενός μεταγραφικού καταστολέα και νευροβλαστικού δείκτη, να καταστέλλει τους καταστολείς της νευρικής τύχης, δηλαδή ένα από τα γονίδια του Enhancer of split συμπλόκου. Από τα αποτελέσματα της παρούσας εργασίας προκύπτει πως το deadpan δεν καταστέλλει το νευρογόνο γονίδιο που μελετήθηκε. Περισσότερη μελέτη χρειάζεται τόσο για τη δράση και την ενεργότητα των ενισχυτών, όσο και για τη δράση του deadpan και των μεταγραφικών κυκλωμάτων που ενέχονται στη γένεση νευροβλαστών.

Introduction

History about Drosophila

Drosophila melanogaster is a small fly, also known as fruit or vinegar fly, often found near rotting fruit. Drosophila pertain to the order *Diptera* and family *Drosophilidae*. The fruitfly is used in experimental procedures since 1909, when Dr. Morgan used it for genetic experiments and confirmed the chromosome theory of inheritance. During the following years, a wide range of molecular, developmental and biological techniques were applied to Drosophila. Many of them were firstly achieved in *D. melanogaster* and then applied to other organisms. Indeed, Nobel Prizes in Physiology or Medicine were awarded to scientists for their pioneer work in Drosophila.

D. melanogaster is used as a model organism for over a century due to its advantages. First of all, it is small, easily handled and maintenance does not cost. Drosophila has a short life span and produces a large number of progenies. Last, genome sequencing is almost complete and a plethora of experimental data and discoveries are available.

Nowadays, Drosophila is a powerful model organism used in host-pathogen interaction, evolutionary and human diseases studies. In addition, laboratories worldwide study regulation of gene expression, developmental procedures, neuronal processes, behaviour and more biological questions based on fruitfly (Hales et al., 2015; Yamaguchi & Yoshida, 2018).

Life cycle of Drosophila

Drosophila is a holometabolous insect, which means that the organism goes through a complete metamorphosis. This developmental procedure can be divided in four stages: the egg (embryo), larva, pupa and adult fly.

The first stage of the insect life cycle is the egg, whose fertilization is followed by highly synchronised nuclear division cycles forming an embryo with a multi-nuclear syncytial blastoderm. After that, most nuclei move to the surface of the embryo and further divide. Cellular blastoderm is the next step of the procedure, as the nuclei cellularise. Last, embryo proceed to segmentation. The duration of this step is about one day (Yamaguchi & Yoshida, 2018).

After the embryo stage, three larval stages are following, named first, second, and third instar. There is a molting event at each stage transition. At the first two instars larvae live within the food, while the third instar larva begins wandering. The first two instars last on average one day each, whereas the third instar typically requires two days. Thus, 5 days after fertilization, larval development is complete (Hales et al., 2015).

After larval stage is pupal stage in which most tissues undergo autophagy and cell death, except from larval imaginal disks, which proliferate, differentiate and produce organs and external structures of the fly. This procedure is guided by ecdysone, a steroid hormone, that mediates gene expression shifts from the larval to adult fly pattern. The organism is within a hard, protective chitin-based pupal case for about five days (Hales et al., 2015).

The adult fly emerges from the pupal case in a process termed eclosion and become sexually mature after eight to twelve hours, allowing the life cycle to repeat itself. The life span varies from sixty to eighty days, depending on the conditions the fly is raised.

In total, the process from a fertilized egg to an adult requires on average nine to ten days at 25°C. However, temperature can greatly influence the speed of this process, with flies cultured at 18°C requiring about nineteen days to become adults (Hales et al., 2015).

Each developmental stage provides information for different scientific questions. For instance, the embryo may be used in studies on fundamental developmental biology by examining pattern formation, cell fate determination, organogenesis, central/peripheral neuronal development, and axon pathfinding. On the other hand, the larva, particularly the wandering third instar larva, is commonly used to study developmental and physiological processes as well as learning and memory. Adult fly is a model organism that shares similarities with mammals and human. For this

reason is widely studied. The Drosophila adult has organs, such as heart, gut, reproductive tract and brain, similar to mammalian ones, providing a powerful model for studying complex behaviours and drug testing.

Drosophila genome

The genome size of *D. melanogaster* is approximately 180 Mb, with 2/3 (120 Mb) representing the euchromatic region and 1/3 (60 Mb) the heterochromatic region. The genome is organised in four sets of chromosomes, the X and Y acrocentric sex chromosomes, two large metacentric autosomal chromosomes (2 and 3), and the very small acrocentric autosomal chromosome 4. The Y chromosome is mostly composed by heterochromatin and it has very few genes, regulating spermatogenesis. Female flies carry two X chromosomes and males carry a single X and Y chromosome. Sex is determined by the balance between the X chromosome and autosome in Drosophila: X: A = 1 is female and X:A = 0.5 is male.

Annotation of the genome currently identifies 17.726 genes, 13.907 of which are protein coding that encode 21.953 unique polypeptides. The remaining 3821 identified loci are genes encoding various types of non-coding RNA (such as rRNA, tRNA, snRNA, miRNA) and 315 for pseudo-genes (Yamaguchi & Yoshida, 2018).

Balancer chromosomes

Genetic crosses of Drosophila flies have become easy due to balancer chromosomes. Balancer chromosomes consist of extensive inversions through the entire chromosome that prevent the recovery of chromosome exchange events. In this way the maintenance of the sequences in the balancer and balanced chromosome is achieved. Their actual role is not the prevention of crossovers, but the inhibition of the recovery of exchanged chromatids (Kaufman, 2017). Balancer chromosomes are used to stably maintain lethal and sterile mutations in the *Drosophila* stock without the selection process. They, also, carry dominant visible mutations in order to facilitate the selection of the flies carrying the balancer in crossing schemes (Yamaguchi & Yoshida, 2018)

Embryogenesis of Drosophila

Embryonic development is a continuous process with profound modifications of the egg within a specific period of time. Although, embryologists have organised this procedure into a series of different stages. All subdivisions are artificial, yet very useful providing a temporal framework, to which embryogenetic events can be referred (Figure 1I).

In detail, the embryo development begins with the ovulation, a procedure that makes an oocyte available for fertilization. When an oocyte released from the ovary meets the released sperm from storage, a successful fertilization is accomplished. This procedure takes place in the uterus of a female *D. melanogaster*. Before that, females mate males and store sperm within specialized regions of the female reproductive tract,

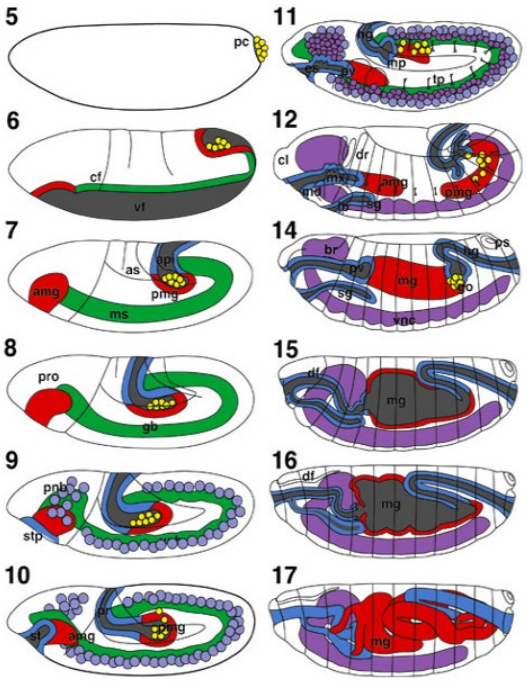

Figure 1I: The stages of embryogenesis (Hartenstein 1993, Atlas of Drosophila Development).

called seminal receptacles and spermathecae. Females store sperm in order to prolong sperm availability, as sperm is not immediately used for fertilization. Sperm storage also has important consequences for female fecundity and fertility. After mating females tend to not mate again for several days but they still can store sperm from more than one male. Fertilization does not occur until the egg is ready to be laid. Before fertilization, oocytes are arrested in metaphase of meiosis I and are activated again after the merge of the two gametes, which happens at the ovulation stage. This is the first stage of embryogenesis, which ends up with two cleavage divisions of the zygote. Characteristic of the stage 2 is the third to eighth cleavage divisions. At third stage, two more divisions take place, nuclei migrate at the periphery of the embryo and pole cells form. These pole cells are the ancestor germ cells, divide asynchronously once or twice and they enter cell-cycle quiescence. The fourth stage includes three more cleavage divisions and the maternal to zygotic transition and zygotic control of the mitotic cycles. Up to this point, divisions are synchronous, fast and are not followed by cytoplasmic divisions. As a result, embryo is a syncytial blastoderm, consisting of about 6000 nuclei. During the stage five, blastoderm cell formation takes place and divisions start to be asynchronous. Stage 6 and stage 7 are short stages in which gastrulation begins and completes. During gastrulation, the three germ layers are generated, as cells within the polar caps and the mid-ventral part of the blastoderm invaginate. Most of the cells that remain at the surface represent the ectoderm, the invaginating cells form the endoderm and the mesoderm. A narrow mid-dorsal partition of the blastoderm gives rise to the amnioserosa, a thin membrane that covers the germ band dorsally. Gastrulation coincides with the beginning of germ-band elongation, a movement that pushes the posterior tip of the germ band upward and then toward anterior. At the stage eight, dominates the germ-band elongation, but also several furrows are formed. The deepest one is the cephalic furrow. Following gastrulation (stages 9-10), the germ band elongates further until stage 11 and the ectoderm gives rise to different organ primordia, foregut and hindgut, CNS and, epidermis. The cephalic furrow is still present, the other transient furrows have all disappeared. The stage 11 is characterized by the parasegmental furrows that subdivide the germ band into metameric units. Stage 12 begins when the germ band starts the retraction and ends when germ-band retraction is complete. During stage 12, important morphogenetic events take place in the endoderm and mesoderm. The next stage is about the end of germ-band retraction and cells in most organ primordia begin to differentiate. Additionally, dorsal closure and head involution take place. At the following stage the head involution leads to definitive changes in the head region, as dorsal closure progresses. By the end of stage 15, dorsal closure is completed, as well as the amnioserosa degenerates. By stage 17, head involution is completed and the embryonic surface has reached its final, larval morphology. During this stage, the cuticle gets thicker and cuticle specializations, such as ventral denticles, become visible (Hartenstein 1993; Campos-Ortega and Volker Hartenstein 1997).

Drosophila embryonic CNS

The central nervous system (CNS) of an embryo can be subdivided into the brain and ventral nerve cord (VNC). CNS is an organ with segmentation, and each segment is referred to as a neuromere. The embryonic brain consists of three cerebral neuromeres: protocerebrum, deutocerebrum, and tritocerebrum. The VNC contains three subesophageal neuromeres: the mandibular, maxillary, and labial neuromeres (S1, S2, S3), three thoracic neuromeres (T1–T3), seven complete abdominal neuromeres (A1–7), and three reduced terminal neuromeres (A8–A10). In the CNS, each neuromere has two bilaterally symmetric hemi-neuromeres (lateral CNS), and, in the VNC, these hemi-neuromeres are separated by a set of specialized midline cells. CNS neurons extend axons that connect with other neurons, muscles, and the gut. Within the CNS, axons assemble into one of two longitudinal connectives that run along the anterior-posterior (A–P) axis of the CNS in each neuromere.

At the stage of cellularization (stage 5), the ventral-lateral region of the trunk is specified to become neurogenic ectoderm, which gives rises to both the CNS and epidermis. A specialized group

of neuroectodermal cells, mesectoderm, lies at the midline and generates CNS midline neural precursors and midline glia. The lateral neuroectoderm on either side of the mesectoderm comprises most of the CNS and gives rise to neuroblasts (NBs) and epidermal precursors.

NBs are neuronal stem cells that emerge at precise positions, and have a distinct cell fate (Figure 2I). Enlargement and delamination of NBs from the ectoderm occur in a pulse mode five times (S1–S5). NBs formation starts at the stages 8-9, and lasts until the late stage 11. S1 NBs are born within a medial and lateral columnar domain of the ventral neurectoderm (mVN and lVN, respectively). From each of these columns, four regularly spaced NBs delaminate per hemi-neuromere. Two additional S1 NBs derive from the neurectodermal domain enclosed by mVN and lVN, called the intermediate ventral neurectoderm (iVN). Thus, the early pattern of S1 NBs forms a regular, orthogonal grid of three columns (medial, intermediate, lateral NBs), and four rows (A, B, C, D) in each half-segment. Shortly after S1, five S2 NBs delaminate from the intermediate column, followed by six S3 NBs originating from the medial and lateral columns. S4 and S5 NBs are more numerous and, based on their position within the map, delaminate from the intermediate domain of the neurectoderm. Aside from these NBs, a double row of cells, called mesectoderm or "midline", located in between the medial columns of either side, also gives rise to neural progenitors, the majority developing into neurons, and some into glia cells. Each NB emerges from a group of five to seven cells, which form a proneural cluster. This proneural cluster is coordinated by transcription factors (TFs) in order to each cell acquire a fate.

Prepatterning genes, responsible for activating proneural genes, are expressed in regular longitudinal and transverse stripes. Among the former are the homeobox genes ventral nerve cord defective (vnd), intermediate neuroblasts defective (ind), and muscle-specific homeobox gene (msh), whose expression domain coincides with the medial, intermediate, and lateral column of the neurectoderm, respectively. The transverse rows A–D coincide with the expression domains of the pair rule and segment polarity genes, and proneural gene expression in these rows is directly controlled by pair rule genes (Hartenstein & Wodarz, 2013).

The proneural basic helix-loop-helix (bHLH) transcription factor genes that constitute the Achaete scute complex: achaete (ac), scute (sc), and lethal of scute [l(1)sc] as well as asense (ase) play key roles in neural precursor formation (Alonso & Cabrera, 1988; Villares & Cabrera, 1987). Combinations of ac, sc, l'sc are expressed in NB prior to delamination, while ase is expressed in all NBs after their formation (Gonzalez et al., 1989). The HLH motif allows the forming of homo- or heterodimers with other bHLH proteins. The b domain allows the binding of the complex in specific DNA sequences. The ac, sc, l'sc predominantly form heterodimers with the ubiquitously expressed bHLH protein Daughterless (Da). These dimers bind to specific E-box sequences (CANNTG), mostly found in enhancer regions. The binding of these dimers promotes the expression of neuronal capacity genes (Cabrera & Alonso, 1991). Proneural gene expression precedes NB formation and they are initially expressed in all cells of a proneural cluster. During neurogenesis, most cells within the cluster begin to increase in size, but, subsequently, only one cell continues to enlarge in order to become a neuroblast. The surrounding cells acquire the fate of epidermal cells and the expression of proneural genes is downregulated in them. How a particular cell in a cluster becomes a NB is not precisely known for the CNS, but the Notch signaling pathway is required for the selection of one cell in each proneural cluster to become a NB, through a process known as lateral inhibition. Loss of function mutants in components of the Notch signalling pathway result in hypertrophy of the CNS at the expense of the epidermis (Lehmann et al., 1983). In detail, Notch it is the receptor of the ligand Delta, both encode transmembrane proteins, whose extracellular domain contains multiple epidermal growth factor (EGF)-like repeats required for binding of the two molecules. Upon this conjunction, Notch intracellular part is cleaved and enters the nucleus. Suppressor of Hairless [Su(H)] transcription factor is directly bound by the Notch intracellular domain and, as a result, activates the transcription of Enhancer of split E(spl) bHLH genes. E(spl) contains seven genes encoding bHLH transcription factors (mδ, mγ, mβ, m3, m5, m7, m8). These genes are expressed in the neurectoderm prior to NB appearance; as NBs delaminate, these genes become restricted to the surface ectoderm. At that moment, AS-C genes (transiently) being upregulated in delaminating

NBs, and E(spl) genes being expressed in the undifferentiated ectoderm. The E(spl) TF proteins repress proneural gene expression in the adjacent cells, which allows these cells remain undifferentiated. It is worthy to mention that, Hairless (H) a nuclear protein that represses the binding of Su(H) to its target genes, but plays no role in early neurogenesis (Hartenstein & Wodarz, 2013).

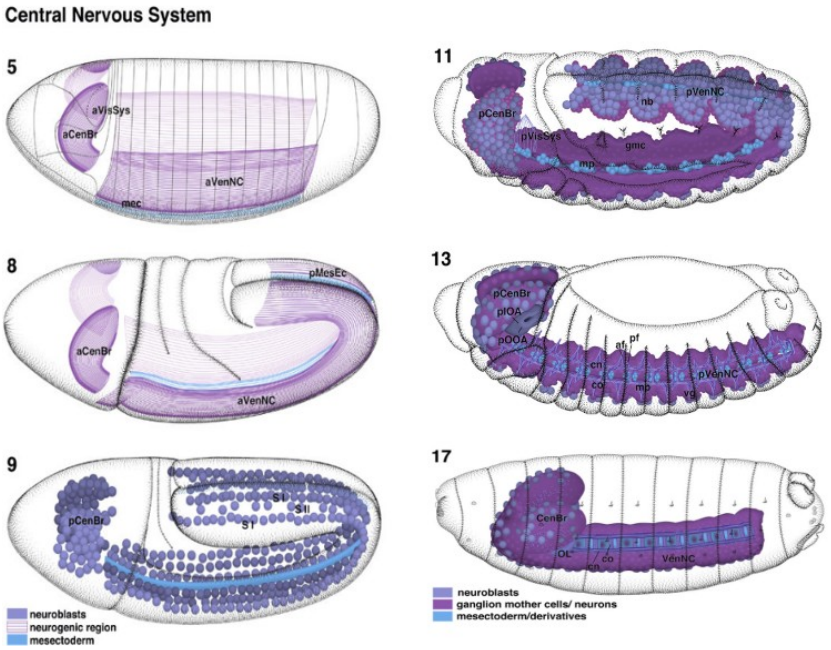

Figure 2I: Central nervous system of Drosophila embryos in indicative stages. (Hartenstein 1993, Atlas of Drosophila Development).

NB asymmetric divisions

Following delamination, NBs divide asymmetrically, generating another NB and a ganglion mother cell (GMC) (Figure 3I). The newly born NB continues its fate as a stem cell, while the GMC divides mainly once in order to generate neurons and/or glia cells. Prerequisite for proper division is NB polarity. In other words, spindle orientation and asymmetric localization of cell fate determinants are important. During NB division the mitotic spindle rotates by 90°, in order to orientate vertically to the plane of the overlying neuroectodermal epithelium. As a result, the GMC is always pinched off at the basal pole of the NB. Determinants that are in the apical side include proteins of the PAR/aPKC complex, Inscutable (Insc) and its partner, Partner of Inscuteable (Pins). Gene products of the tumor suppressor genes lethal giant larvae (lgl), discs large (dlg) and scribble (scrib) are required for the basal localization of cell fate determinants without affecting localization of the apical complex. Several proteins and mRNAs are localized to the basal pole of the NB and are segregated to the GMC (Ohno, 2001; Wodarz, 2002).

One of these factors, the homeobox transcription factor Prospero (Pros) activates differentiation genes and suppresses self-renewal genes. The protein Numb, which is a Notch signaling inhibitor, and the Brain tumor (Brat) protein, which is a translation inhibitor that prevents proliferation and induces differentiation are also part of the basal determinants. Two adaptor proteins are responsible for anchoring the aforementioned proteins in the NB basal cortex, Miranda (Mira) and Partner of Numb (Pons). The first binds to Pros and Brat, while the latter binds to Numb. In conclusion, apical cortex complexes pass on to the developing Nbs, while basal determinants are transmitted to the emerging and differentiating GMCs (Wodarz & Huttner, 2003).

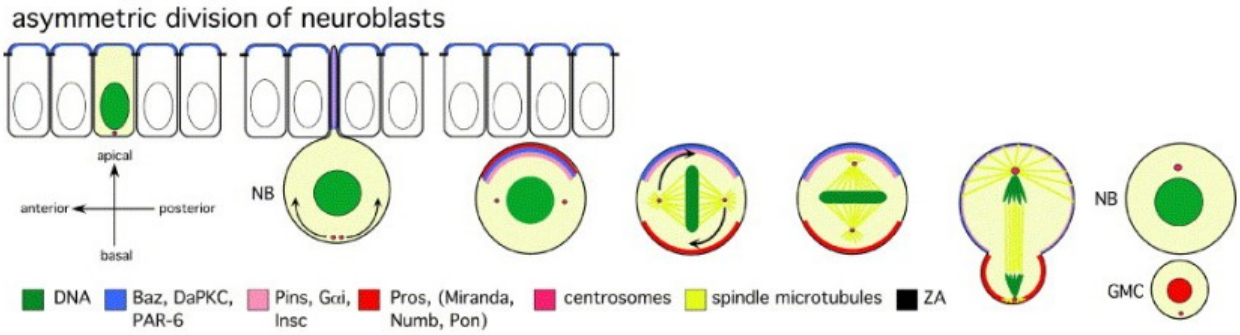

Figure 3I: Neuroblasts delamination of the neuroectoderm and asymmetric division (Wodarz & Huttner, 2003).

Loss of function of ASC

As it was referred, the achaete-scute complex (AS-C) consists of the transcription factors ac, sc and l'sc, which are expressed in the neuroectoderm in proneurals clusters, as well as the transcription factor ase, which is expressed in the delaminating NB. Loss of function of ac or sc removes specific subsets of external sense organ (bristles), but the phenotype is viable. In contrary, the deletion of the l'sc is embryonic lethal. The ase null mutation is viable and fertile with subtle bristle defects (García-Bellido & De Celis, 2009; Jarman et al., 1993). All the above means that these paralogous proteins can compensate for each other's loss, with the exception of l(1)sc, which is irreplaceable.

The depletion of all genes of AS-C is called *Df(1)B57*. In AS-C mutant embryos, the emerging NBs are smaller, reduced in number (up to 25%), have restricted progeny and often go for apoptosis at stage 11 (Jiménez & Campos-Ortega, 1990). Furthermore, in embryos lacking AS-C, NBs are mitotically stalled, so they do not proliferate, and they do not initiate expression of a large part of the neural TF program on time. This phenomenon, which begins in st10-11, is reversed by late st11,when mutant NBs start expressing almost all their NB markers (Theodorou et al., 2022). Lastly, AS-C null mutants show nervous system hypoplasia, which is represented by absence of neuromeres in the VNC and lack of neuronal axonal projections (Jiménez & Campos-Ortega, 1990).

The depletion of the three TFs present in the proneural cluster: ac, sc and l'sc is called *Df(1)sc19*. In this background, NB stalling was still evident during stage 9, until early stage 10. Ase, which is not depleted in this deficiency, exhibited a small delay in expression. The marker of NBs, Dpn, as well as the marker of GMCs, pros, rebounded soon after Ase expression, earlier than in *Df(1)B57* (Theodorou et al., 2022). What is more, the late CNS hypoplasia was also improved in *Df(1)sc19* (Martin-Bermudo et al., 1993). Therefore, the endogenous expression of Ase in the delaminated neuroblasts can greatly improve NB functionality (Theodorou et al., 2022).

Larva CNS

L1 larva CNS consists of a brain and a ventral nerve cord (VNC), that contain 15.000 cells, including 1000 glia. The last NBs divide at embryonic stage 14-15. After that stage, only GMC divisions are present for another 2-3 hours. Neuroblasts become mitotically inactive and reduce their size, so that they cannot be recognized in first instar brains (Figure 4I). Although, a small set of neuroblasts, including the four mushroom body neuroblasts and one of the basal anterior neuroblasts, escape the general quiescence of NBs activity and continue the proliferation during the early larval period. One day after, in the second instar larva, the remainder of the neuroblasts are reactivated, so that during the third instar the whole neuroblasts are proliferating. Just like their embryonic counterparts, NBs as well as GMCs are located at the brain surface. One major difference is the orientation of the mitotic spindle in secondary neuroblasts, as it appears to be more variable than in primary NBs. This could in part be due to the fact that the mechanism controlling spindle orientation could be quite different, and as a result mitotic spindle is from parallel to perpendicular relative to the brain surface. Embryonic NBs are in contact with the ectoderm, while

secondary NBs in the larva are surrounded by a glial layer. Thus, glia-Neuroblast interactions may control the mitotic spindle orientation, as well as the start and frequency of mitosis. Protein complexes such as members of the Par complex, including Baz, Par,6 and aPKC, localized to the apical side, along with Inscuteable, while Miranda and Prospero localized to the basal crescent of the NBs remind the NBs polarity of the embryos (Crews, 2019; Hartenstein et al., 2008). The majority of about 114 lineages identified in the adult central brain are generated by type I NBs. However, there are eight postembryonic NBs in medial regions of the central brain, that follow a different division pattern. These type II NBs give rise to intermediate neural precursors, which in self-renewing asymmetric divisions produce GMCs and neurons as well as glia (Apitz & Salecker, 2014). While NBs generally stop dividing during early pupal development, a recent study provided evidence for continued neurogenesis in the adult medulla, albeit at low levels (Fernández-Hernández et al., 2013).

After the mitotic dormancy of the NBs, the same neuroblasts that had proliferated to form primary neurons during the embryonic period become active again and produce a stereotyped set of secondary lineages, generating 90% of neurons in the adult CNS. Except from these NBs, in the lateral surface of the brain there are two primordia, called the outer and inner proliferation centers (OPC and IPC, respectively) generating newly born NBs. The superficially located OPC generates neurons in the lamina and medulla, while the centrally located IPC gives rise to lobula plate and lobula neurons. By the end of the second instar larval stage, the OPC expands to approximately 700 and the IPC to 400 cells, constituting of neuroepithelial cells, NBs, other neural progenitor types and newly produced postmitotic neurons (Apitz & Salecker, 2014).

During late embryogenesis primary neurons form dendritic and axonal arborizations that, together with sheath-like processes formed by glial cells, establish the neuropile compartments of the larval brain. Similar to primary axons, axons of a given secondary lineage fasciculate with each other, thereby forming discrete bundles, secondary axon tracts (SATs). Most secondary neurons do not differentiate in the larva. Thus, SATs remain unbranched bundles until the pupal period, when secondary lineages form proximal branches (dendrites) and terminal branches (axons) that, together with remodelled primary neurons become integrated, into the adult brain (Larsen et al., 2009).

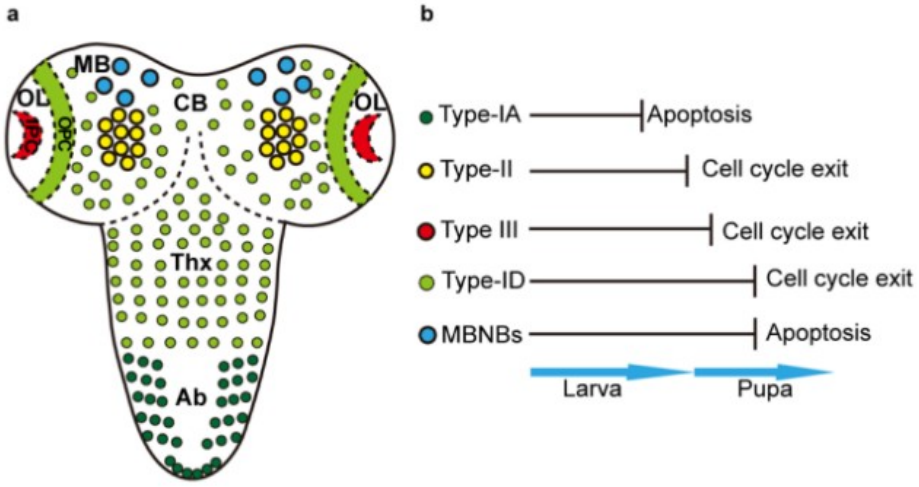

Figure 4I: Neuroblasts in the larval CNS. (a) Distinct types and distribution of developmental NB. (b) NB termination via cell cycle exit or apoptosis. CB: central brain; MB: mushroom bodies; OL: optic lobes; OPC: outer proliferation centre; IPC: inner proliferation centre; Thx: VNC thorax; Ab: VNC abdomen (G. Li & Hidalgo, 2020).

Drosophila PNS

Drosophila has a range of sense organs, both external and internal. External sense (es) organs are mostly mechano- and chemo-sensory receptors, while internal sense organs include the chordotonal (ch) organs which function as strain receptors, as well as other types of organs. The sensory organs arise from the peripheral nervous system (PNS) in a very precise and reproducible

pattern in the larva of Drosophila (Ghysen & Dambly-Chaudiere, 1989). The Drosophila PNS receives and transduces stimuli from the environment to the CNS, in order to promote appropriate larval and adult behaviour. Somatosensory system receive diverse inputs, and this is reflected in the many different morphologies of the sensory organs (sensilla). Somatosensory neurons reside along the inner surface of the epidermis. In the trunk, sensory organs are distinguished in dorsal (d), lateral (l), ventral' (v') and ventral (v) clusters. These clusters consist of neurons that are classified as type I sensilla-neurons with single ciliated dendrites and type II multidendritic neurons. The sensillum lineage results from a sensory organ precursor (SOP) cell, which divides in a stereotyped pattern. SOPs appear in the epidermal ectoderm of the embryo at a stage NBs are about to stop delaminating. Unlike NBs, SOPs do not delaminate fully. In the external sensory organs, the SOP, also known as the pI cell, carries out four cell divisions to generate a total of five cells, pIIa division produces two "outer cells": the external bristle and its socket, and pIIb lineage generate three "inner cells". pIIb undergoes another asymmetric cell division, which gives rise to a multidendritic neuron and pIIIb. pIIIb in turn generates a sheath cell and an external sensory neuron (Hartenstein, 1988; Singhania & Grueber, 2014). At stage 17, all sensilla have differentiated and embryo starts moving. That is possible as sensory axons have reached their target in the CNS, and motor axons have grown toward the musculature. The next step is the degeneration of larval sensilla during metamorphosis. The imaginal discs and histoblasts, which form the adult epidermis, produce another complete set of adult sensilla. The first precursors of adult sensilla appear during the late third larval instar (Hartenstein 1993).

Similar to the NBs, SOPs are selected from the ectoderm when proneural and neurogenic genes act. Actually, prepatterning and proneural genes establish proneural clusters in which neurogenic genes set up the mechanism for SOPs (Hartenstein & Wodarz, 2013). Proneural factors include members of the Achaete-Scute complex, atonal (ato) and absent md neurons and olfactory sensilla (amos). The ASC complex is required in proneural clusters that produce external sensory organs and multidendritic neurons. ato in turn controls the production of chordotonal organs and a subset of multidendritic neurons, and amos the production of the last multidendritic neurons (Singhania & Grueber, 2014).

Lateral inhibition is a key procedure in PNS, as well (Figure 5I). Delta ligand and Notch receptor are expressed in all cells. Delta levels are upregulated in the SOP cell, which results in higher Notch signaling in non-SOP cells. The Notch intracellular domain collaborates with the Suppressor of Hairless protein to promote expression of Enhancer of split in non-SOP cells. E(spl) acts together with the transcriptional repressor Groucho to cease the expression of the achaete. On the contrary, ın the future SOP, Gro, H and Su(H) repress E(spl), so that proneural gene expression can persist. Positive feedback loop is accomplished with high-level expression of proneural genes and Senseless activating proneural gene transcription in the SOP (Singhania & Grueber, 2014).

Glial cells are important for neuronal survival and for guiding developing sensory axons to the CNS. Glia in the PNS are a diverse cell population, deriving from both glial specific lineages and mixed lineages known as neuroglioblasts, which give rise to neurons and glia (Singhania & Grueber, 2014).

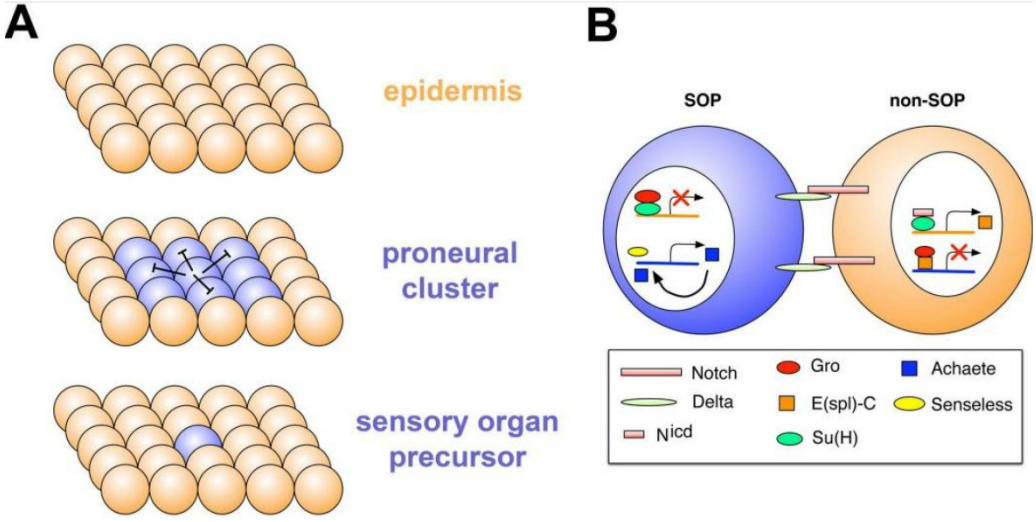

Figure 5I: Sensory organ precursor specification. A) From the proneural cluster a single sensory organ precursor emerges, which inhibits proneural gene expression in surrounding cells, a process termed lateral inhibition. B) Molecular basis for lateral inhibition (for more details see the text) (Singhania & Grueber, 2014).

Enhancers

Throughout the process of development, from a single genome arise different cell types expressing a subset of genes, which define their unique identity. This is possible with differential transcription in each cell cluster. Transcription starts with the recruitment of RNA polymerase II and auxiliary factors to core promoters, short DNA sequences near transcription start sites (TSS). Core promoters are sufficient to drive the transcription at a basal level, but they require cis-regulatory elements or enhancers for full activity(Catarino & Stark, 2018). The notion of enhancers first appeared about forty years earlier and since then they are intensively studied (Banerji et al., 1981). Enhancers can act from both proximal and distal positions, binding transcription factors and co-factors to recruit and activate RNA polymerase II at target gene promoters (Catarino & Stark, 2018). An enhancer typically ranges from a hundred base pairs to a few kilobases of DNA, and usually contains many binding sites for transcription factors. A single gene can interact with many enhancers, and they often work independently. Indeed, an enhancer can provide material for adaptive evolution, when complete or partial loss of an enhancer or accumulation of nucleotide substitutions in an enhancer can result in the loss or gain of certain body structures (Koshikawa, 2015).

Given the importance of the enhancers, their prediction and reliable identification in large genomes has been a challenge. TF binding, histone modifications and DNA accessibility has been used to predict enhancers. Chromatin immunoprecipitation coupled to sequencing (ChIP-seq) is now used routinely to map TF binding. Histone modifications include histone H3 Lys4 monomethylation (H3K4me1) found at enhancers, H3K4 trimethylation (H3K4me3) at promoters, and H3K27 acetylation (H3K27ac) at active enhancers and promoters. DNA regions free from nucleosomes are accessible to TFs as well as the RNA polymerase II, but also other genomic regions such as insulators or promoters are also accessible. Although, the aforementioned characteristics help the finding of new enhancers, there are active enhancers that lack them. Therefore, enhancer prediction approaches typically consider more features to increase the specificity toward active enhancers (Catarino & Stark, 2018). Except from ChIP-seq and DHS-seq (deep sequencing of deoxyribonuclease I hypersensitive sites) analysis, which define the opened genomic regions. new methods have developed in Drosophila melanogaster, in order to find new enhancers. Among them are the STARR-sequncing and STAP-sequencing. STARR-seq (self-transcribing active regulatory region sequencing) is able to assess enhancer strengths quantitatively and to discover regulatory elements directly based on their ability to enhance transcription, even when silenced endogenously (Arnold et al., 2013), while STAP-seq (self-transcribing active core

promoter sequencing) determines the responsiveness of genomic sequences to enhancers (Arnold et al., 2016).

Of particular interest, a recent study utilizing STARR-seq identified two distinct enhancer classes in Drosophila. One class is promoter-proximal and interacts specifically with a housekeeping core promoter, whereas the second class is located distal to promoters and interacts with a developmentally regulated core promoter (Zabidi et al., 2015). One step further, Cubenãs-Potts et al., 2017 found functional differences between enhancers that activate housekeeping versus developmental genes. Housekeeping enhancers are marked by H3K4me3, associate with Topologically Associating Domains (TAD) borders, and associate with multi-TSS in clustered promoters increasing the transcriptional output. In contrast, developmental enhancers are marked by H3K4me1, associate with chromatin loop anchors and are more commonly associated with single TSS-contacts (no promoter clusters).

Cell culture of NBs

Drosophila primary cultures have been used for decades to investigate various aspects of neural development and function. Primary cultures have several advantages over established cell lines, such as the S2, Kc and clone 8, as these cells have unknown origin and how they became immortal is often unclear (Bai et al., 2009). Previous studies have shown that, based on their morphology, there are at least five distinct types of cells in Drosophila primary cultures prepared from embryos: the neuron, the muscle, the epithelial (fat-body cells), a macrophage-like (haemocytes) and a fibroblastic cell type (Shields & Sang, 1970). The embryonic NBs culture is a powerful tool for studying the release from lateral inhibition, neuroectodermal signals (extrinsic signals) or cell-to-cell signals. Lüer and Technau, 2009 have taken single progenitor cells (st7-8) and cultured them for 16 to 20 hours, which corresponds to the time required for normal embryos to fully develop (st 16-17). Their data indicate that presumptive NBs have already acquired a high degree of commitment in the neuroectoderm, and are able to cell-autonomously express specific characteristics of their lineages when grown in primary culture. On the other hand, delaminated NBs require extrinsic signals from the overlying neuroectoderm during interphase to regulate spindle position and apical protein localization (Broadus & Doe, 1997). However, individual NBs in vitro divide asymmetrically in a normal stem cell mode, producing a chain of progeny cells that inherit differential cell fates (Lüer & Technau, 2009). Despite the higher exposure to extrinsic signals in the larval than in embryonic CNS, the location of asymmetric cell determinants remains mainly dependent on intrinsic signals, and the proper apical-basal orientation in the larval neural tissue and the plane of division seem dependent on extrinsic signals to the cell (Ceron et al., 2006).

Larva wing disk

The Drosophila wing disc has led the studies of many biological issues. Interestingly, is one of the most intensively studied organs in biology and as a result there is detailed understanding of its development.

In Drosophila, as well as all the holometabolous insects, which undergo complete metamorphosis, most of the adult structures, such as the head and thorax, result from imaginal disks (Figure 6I). Imaginal disks are clusters of undifferentiated cells that are maintained during larval stages. They are named after the final adult stage. The wing imaginal disc (henceforth, wing disc) gives rise to the wing and wing hinge, and also the dorsal half of the body wall in the second thoracic segment (T2). The body wall consists of the back of the thorax, the notum, and part of the lateral sides of the thorax, the pleura. The imaginal discs grow extensively during the larval stages, increasing their size over 1.000-times. This could happen as they divide many times in order to increase their cell numbers and size, remaining diploid.

Larval two wing discs (left and right) arise from cells in the lateral epidermis of T2 at embryonic stages 11–13. Thoracic imaginal disc primordia (TP) (stage 11) are specified,

expressing the transcription factor Distal-less (Dll). The TP give rise to both leg and wing disc cells. At the next stages, wing disc primordia starts the expression of the transcription factors Snail (Sna) and Vestigial (Vg). Last at the stage 14, wing primordia cells migrate dorsally and are separated from leg primordia (Cohen et al., 1993; Requena et al., 2017).

As the thoracic primordia splits into leg and wing primordia, Wingless (Wg), Decapentapligic (Dpp), and epidermal growth factor receptor (EGFR) act in different ways to further specify the clusters of cells. Dpp is expressed in a lateral stripe just dorsal to the TP, and promotes wing primordium fate, as well as, at lower levels, proximal leg fate. On contrary, EGFR signaling from more ventral cells represses wing primordium fate, while promoting leg fate. Dpp also represses Wg expression through upregulation of Dorsocross (Doc) transcription factors. This results in lower levels of Wg signaling, which promotes wing disc fate at the cost of leg disc fate. Thus, two bilaterally symmetric clusters of about 25–30 embryonic cells form wing disc primordia (Requena et al., 2017)

At the late third instar, wing disk consists of four main regions, the wing pouch, the proximal wing and wing hinge, the notal region, and the peripodial epithelium. The wing pounch is an oval-shaped part of the wing disk that gives rise to the wing blade, while the wing hinge gives rise to structures at the base of the wing. The notum is responsible for the back of the fly in the thorax and peripodial epithelium contributes to some pleura formation. At this point, the wing margin (the edge of the wing) has different gene expression patterns in distinct cell types. The margin maintenance is due to continued Notch activation along the dorso-ventral boundary, and Notch in turn is activated by a feedback loop between dorso-ventral boundary cells, which express Wg in response to Notch activation, and flanking cells, which express Notch ligands in response to Wg signaling. Furthermore, proneural genes like achaete (ac) and senseless (sens) are upregulated by Wg signaling in cells adjacent to the Wg stripe on the dorso-ventral boundary. These stripes of proneural gene expression then are limited to cell clusters, which give rise to the sensory organ precursor cells that will later form wing margin bristles (Tripathi & Irvine, 2022).

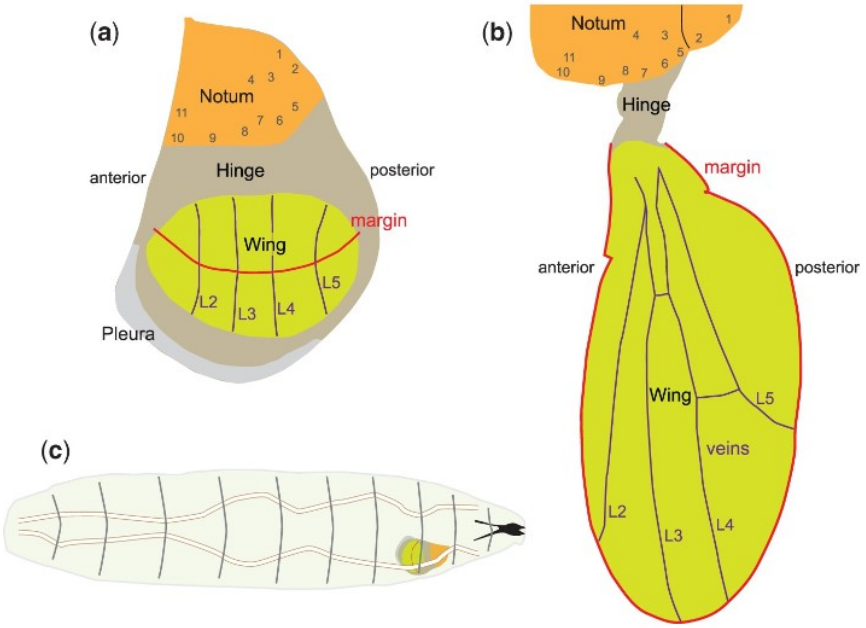

Figure 6I: The wing imaginal disc. a) Schematic of late third instar wing disc, b) schematic of adult wing, hinge, and half notum and c) schematic of third instar larva with approximate location of the wing disc indicated (Tripathi & Irvine, 2022).

Purpose of this study

The purpose of this undergraduate thesis was the study of transcription circuits and putative enhancers involved in neural stem cells in Drosophila. The previous study of the enhancers, named

KV lines, in *Df(1)B57* led to the investigation of the behaviour of these enhancers as well as the genes they regulate in *Df(1)sc19*. These experiments would shed light in the capabilities of the transcription factor ase, which is the solely acting in the CNS. After this, the circuits involved in NBs fate, and especially the relationship between the NB marker Dpn and the suppressorsof the NB fate, the E(spl) genes. In addition to these circuits, the neuroblasts cell culture would give us insight about their division patterns and their progeny.

The previously referred enhancer lines were examined in larval brains with X-gal staining, in order to test the expression strength of each enhancer. One enhancer was selected in order to study the possible effect in Notch induced clones. What is more, another one proneural deficiency was selected so as to see the dependency of Notch tumors on it. Lastly, Notch over-expression could be influenced by downregulation of the pumilio gene?

Results

Study of putative enhancers targeted by proneural TFs in deficiency background

The results from Theodorou et al. (2022), who studied the enhancers in *Df(1)B57* (absence of ac, sc, l'sc and ase) background, led to the investigation of KV lines in *Df(1)sc19* (presence of ase, absence of the other proneurals). The endogenous expression of Ase aided the functionality of NBs in *Df(1)sc19*, thus the investigation of the role of this transcription factor in the activity of enhancers was the first biological question addressed in this thesis. When it was possible the proteins, encoded by the genes the enhancers activate, were studied for comparison. The KV19 line was PNS specific and the KV29 line exhibited weak expression both in X-gal staining (see results below) and Theodorou et al. (2022), so they were not studied further. Unlike NB expression, all enhancers that drove PNS expression displayed activity in the *Df(1)B57* mutant in the ASC-independent sensory organs, most likely due to the activity of the atonal and amos, proneural factors exclusive to PNS primordia (Huang et al., 2000; Jarman & Groves, 2013; Theodorou et al., 2022).

The strategy that was followed for studying the KV lines was to collect females sc19/FM7KrGFP and cross them with males of the KV lines. The desired offspring was the male carrying the *Df(1)sc19* in hemizygosity with the genotype: sc19/y ; KV/+ (1 out of 4 offsprings). The rest progeny that were in heterozygous (females sc19/+ ; KV/+) or had not the deficiency (females +/FM7 ; KV/+ or males FM7/y ; KV/+) were the wild type embryos and were studied as controls. For this reason, it was important to distinguish the balancer FM7KrGFP with the immunostaining against GFP and the females with the immunostaining against the sex lethal (sxl) protein, that stains ubiquitously the female embryos.

KV1 (inscutable)

The gene of inscutable (insc) encodes an adaptor protein required for asymmetric cell division of NBs. It interacts with the microtubule binding protein, mud, and the adaptor protein partner of incutable (pins). It also binds to the apical complex proteins bazooka, par-6 and aPKC (Kraut et al., 1996; Kraut & Campos-Ortega, 1996; Schober et al., 1999).

Immunostaining in Figure 1 shows the expression of the enhancer through the β-galactosidase pattern (red) in a wild type (wt) embryo and a *Df(1)sc19* embryo at stage 10. The enhancer seemed to be active in most neuroblasts in the CNS, brain as well as in the PNS precursors at wt embryos. Embryos with *Df(1)sc19* showed a small delay in the activation of the enhancer, but eventually the KV1 enhancer was activated in CNS and PNS at late stage 10. This enhancer is the only one rebounded in *Df(1)B57* embryos at stage 11 (Theodorou et al., 2022).As a result, asense contributed to KV1 earlier activation.

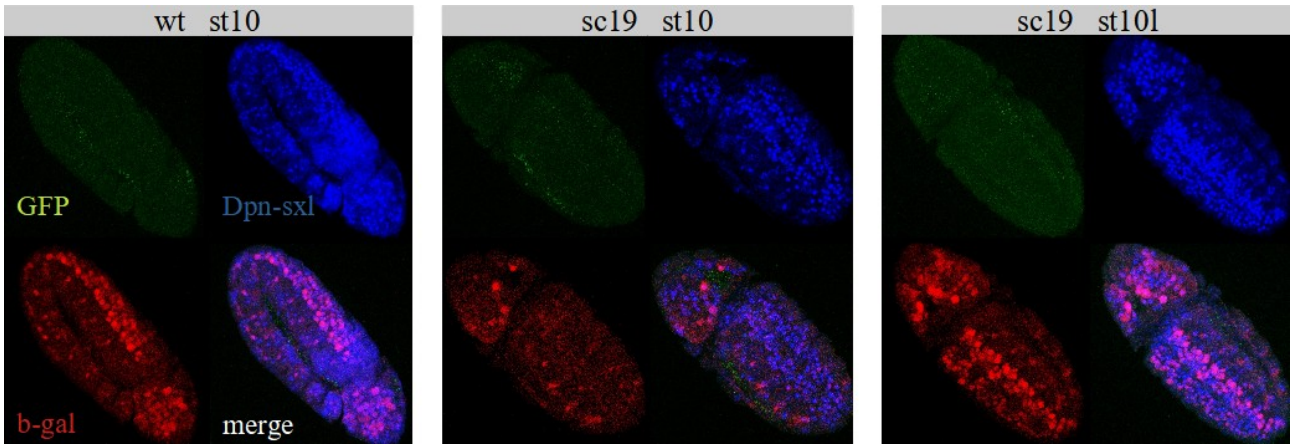

Figure 1: Immumostaining of KV1 of wild type (wt) and *Df(1)sc19* embryos at the developmental stage 10. Antibodies: g anti-GFP 488 (green), rb anti-b-gal 555 (red), gp anti-dpn and m anti-sxl 647 (blue). The lack of GFP indicates the absence of the FM7, KrGFP chromosome in all three embryos.

KV4 (phyllopod)

Phyllopod (phyl) encodes an ubiquitin ligase adaptor and it is required for ac- and sc-dependent external sensory (es) organ development. Its expression is directly activated by Ac and Sc (Pi et al., 2004). Indeed, phyl is required in two stages of es organ development, the formation of SOP cells and cell fate specification of SOP progeny, acting downstream of Notch signaling (Pi et al., 2001).

Figure 2 shows that wt embryos expressed b-galactosidase in a subset of NBs in CNS, brain and in PNS, but *Df(1)sc19* embryos lost its expression. In more detail, *Df(1)sc19* stage 11 embryos did not have signal in CNS and PNS exhibited signal in less clusters. Mutant embryos at st13 showed no signal in CNS and PNS signal was again in less clusters than in wt. Theodorou et al. (2022) found that KV4 is not activated in *Df(1)B57* embryos (st10). Thus, the presence of ase can not rescue the phenotype and activate the enhancer in the CNS and in clusters in the PNS. It is important to say that, KV4 is an enhancer with capability of activation of the gene phyllopod in CNS and PNS, and its remaining PNS expression in the absence of ASC is dependent on the other proneurals (ato and amos) in chordotonal and md precursors.

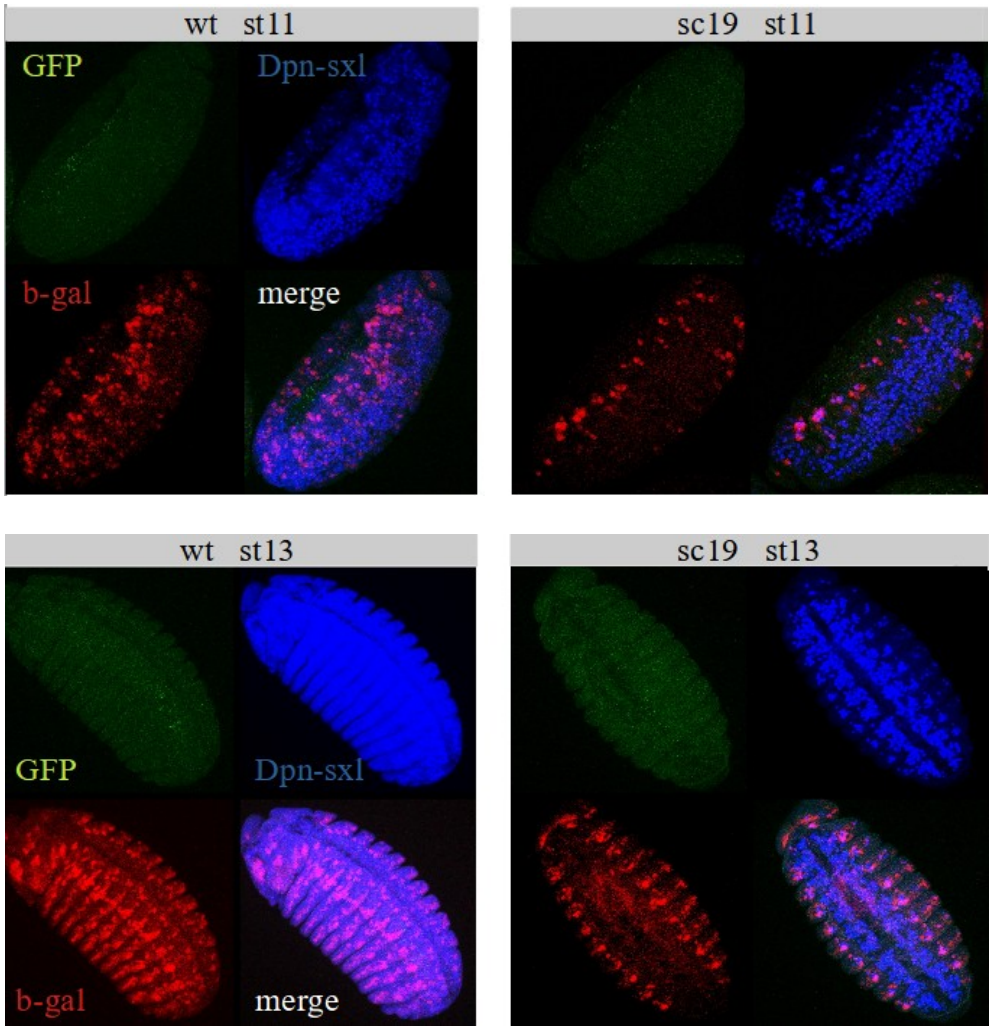

Figure 2: Immumostaining of KV4 of wild type (wt) and *Df(1)sc19* embryos at the developmental stages 11 and 13. Antibodies: g anti-GFP 488 (green), rb anti-b-gal 555 (red), gp anti-dpn and m anti-sxl 647 (blue).

KV8 (brain tumor)

The protein Brain tumor (brat) acts as a tumor suppressor in the larval Drosophila brain, but how it suppresses tumor formation is not completely understood. Upon neuroblast division, Brat is

enriched in one daughter cell where its NHL domain directly binds to specific motifs in the 3'UTR of dpn and zelda (zld) mRNA to mediate their degradation. Zelda (Zld) is expressed in neuroblasts and required to allow re-expression of Dpn. Thus, Brat as a translation repressor promotes differentiation (Reichardt et al., 2018). Furthermore, Brat is partitioned into GMCs via direct interaction with the Miranda scaffolding protein, promoting once more neuronal differentiation (Lee et al., 2006).

Firstly, the protein Brat tagged with GFP (BratGFP) was studied in wt and in both deficiencies embryos. The protein normally is expressed ubiquitously in the ectoderm and upon NB division it accumulates in the cytoplasm of the GMC. The ectodermal pattern was not affected by both deficiencies, but the GMC pattern was affected, as the NB divisions and the GMC birth were affected. As a result, the protein was found where NBs had divide and GMCs were born (Figure 3 and 4). In other words, *Df(1)B57* and *Df(1)sc19* affect NBs division and GMC birth, and BratGFP is found, only where divisions have rebounded.

Theodorou et al. (2022) studied the enhancer KV8 in wt and *Df(1)B57* embryos (stage 10) and found that its broad neuroblast expression was lost in the mutant background. This experiment was conducted again, in order to examine more embryos in later developmental stages (Figure 5). Wild type embryos showed CNS (subset of NBs) and PNS signal, but mutant embryos at stage 10 lost their neuroblast expression, as researchers have shown. The examination of the later stages revealed that the enhancer was activated from transcription factors independent from the proneural TFs at stage 12. The CNS signal finally rebounded (st12), while the PNS was never lost.

Then, the enhancer KV8 was studied in *Df(1)sc19* (Figure 6). *Df(1)sc19* affected its activity, as its expression levels were extremely reduced in CNS, but not in PNS. The TF ase was capable of turning on the enhancer at stage 10 in very few NBs. Later developmental stages were not analyzed. We expect that they will show stronger KV8 expression, as the enhancer was slightly activated in st10, as well as it was finally rebounded in *Df(1)B57* embryos, too.

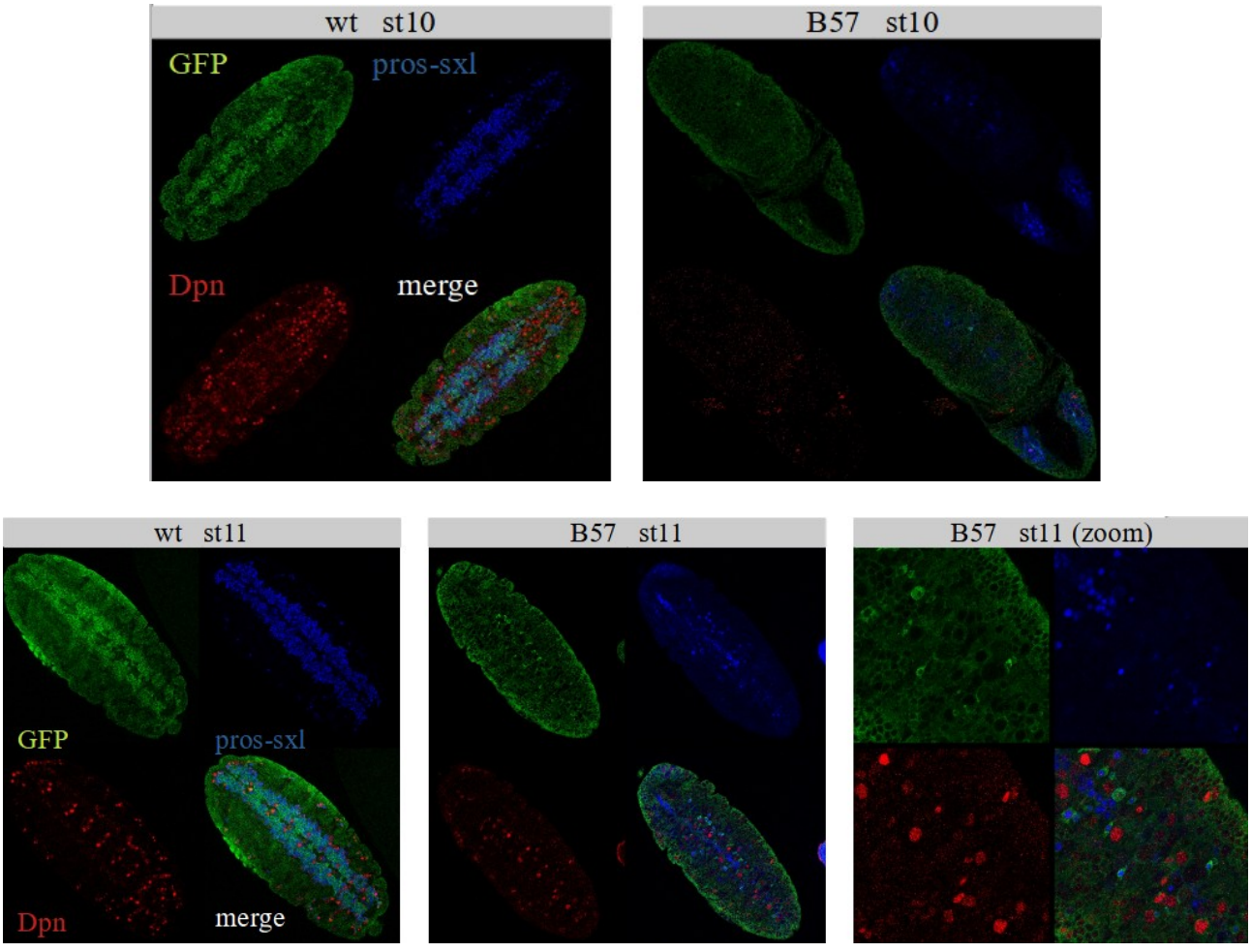

Figure 3: Immumostaining of bratGFP of wild type (wt) and *Df(1)B57* embryos at the developmental stages 10 and 11. Antibodies: rb anti-GFP 488 (green), gp anti-dpn 555 (red), m anti-pros and m anti-sxl 647 (blue). Note that Dpn is not abundantly seen in the wt embryos, as we are presenting sections at the GMC layer.

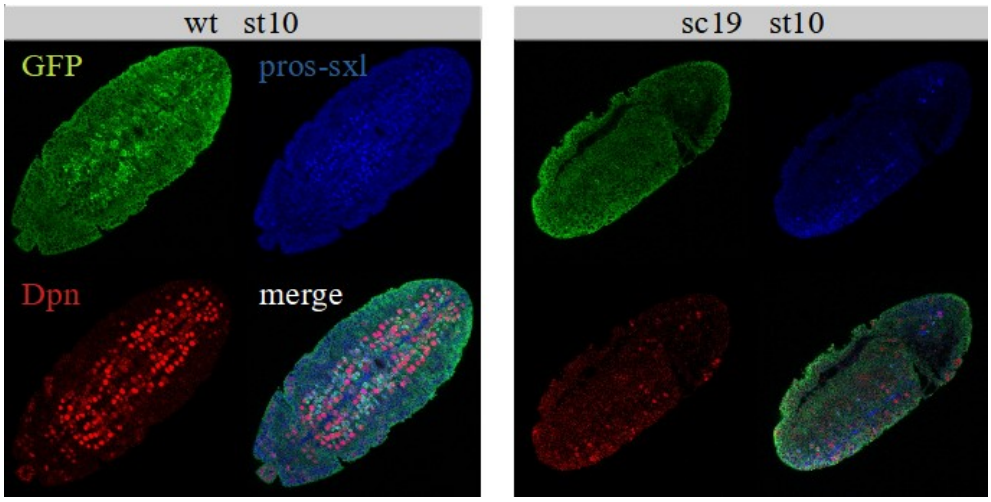

Figure 4: Immumostaining of BratGFP of wild type (wt) and *Df(1)sc19* embryos at the developmental stage 10. Antibodies: rb anti-GFP 488 (green), gp anti-dpn 555 (red), m anti-pros and m anti-sxl 647 (blue).

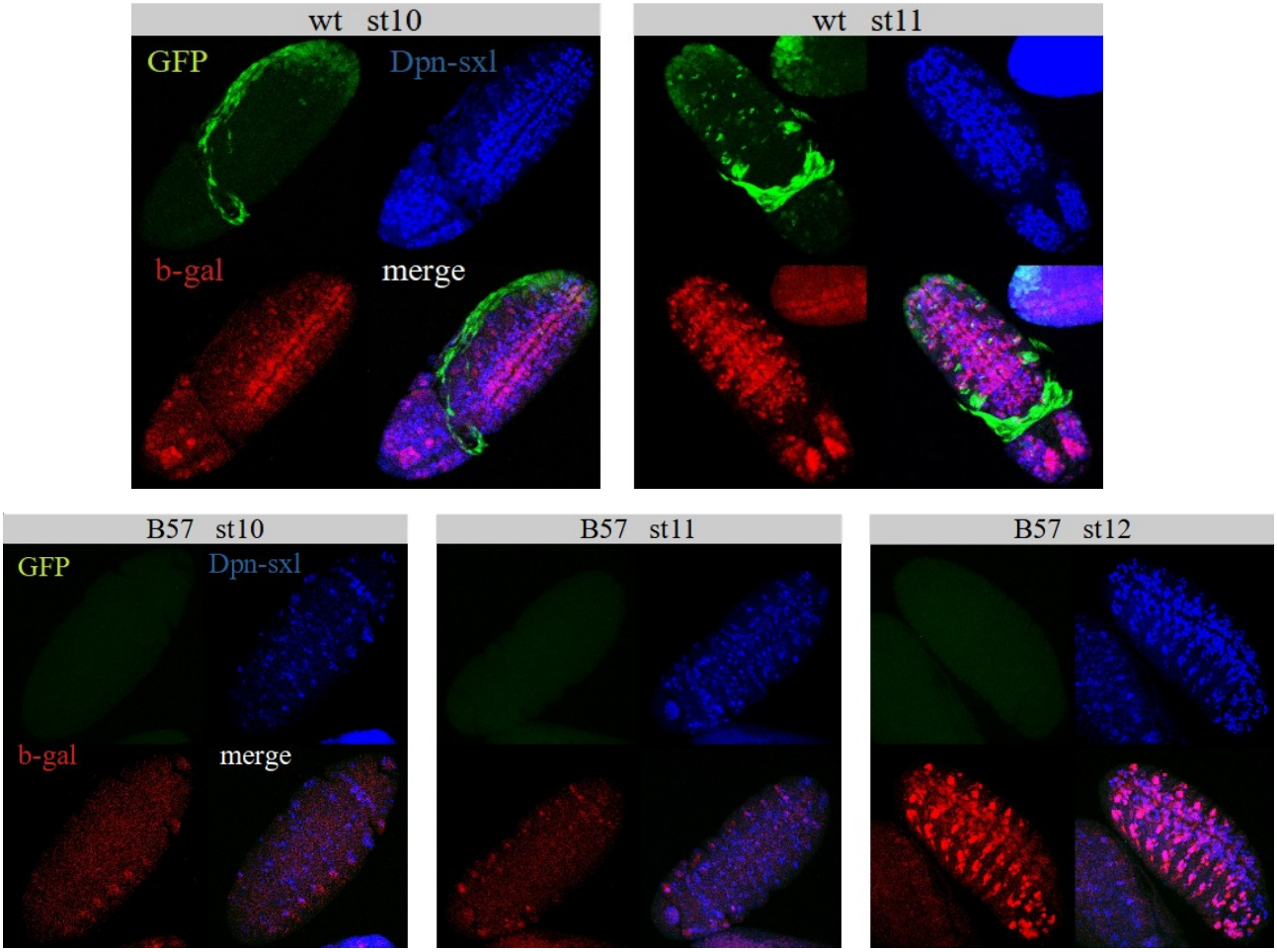

Figure 5: Immumostaining of KV8 of wild type (wt) and *Df(1)B57* embryos at the developmental stage 10, 11 and 12. Antibodies: g anti-GFP 488 (green), rb anti-b-gal 555 (red), gp anti-dpn Cy5 and m anti-sxl 647 (blue).

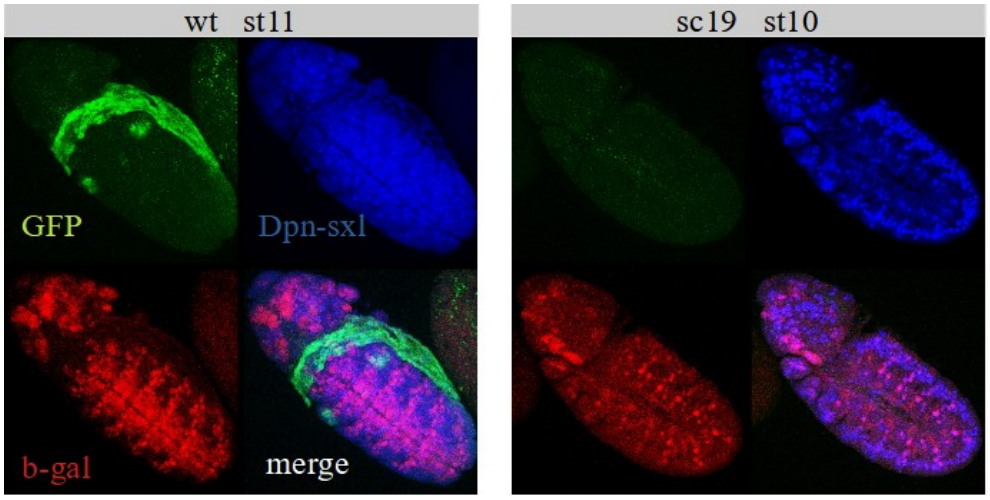

Figure 6: Immumostaining of KV8 of wild type (wt) and *Df(1)sc19* embryos at the developmental stage 10. Antibodies: g anti-GFP 488 (green), rb anti-b-gal 555 (red), gp anti-dpn Cy5 and m anti-sxl 647 (blue).

KV10 (scratch)

The Drosophila scratch (scrt) gene is a transcription factor belonging to the Snail superfamily. As such, it promotes neuronal cell fates by suppressing expression of genes promoting non-neuronal cell fates. In PNS mechanosensory lineages in the larva, it directly blocks the transcription of Notch target genes by displacing proneural transcription activators from DNA binding sites (Ramat et al., 2016; Roark et al., 1995).

The activity of the protein scratchGFP in wt and in *Df(1)sc19* was the next question to answer. Figure 7 shows that the expression pattern of the scratch was in neuroblasts and newly born GMCs in the CNS and in PNS precursors at stages 10 and 10 earlier, in wt and mutant embryos. The immunostaining showed slightly differences in the expression pattern of the protein in st10 mutant embryos, indicating a small delay of its expression. The protein in *Df(1)B57* showed stronger delay in stage 9 and a slighter delay in stage 11 (Theodorou et al., 2022), both of them were stronger than the delay in *Df(1)sc19.*

In wt embryos (stages 10-13) of KV10 line was detected gradually strong NBs and PNS signal, which was lost drastically only in CNS in stage10 mutants (Figure 8). *Df(1)B57* embryos at the same stage showed only PNS signal (Theodorou et al., 2022). Thus, ase cannot rescue the phenotype, at least at this stage. Apparently, the activity of the enhancer in the next stages have to be studied further.

The different results in protein and KV10 expression, showed that more enhancers cooperate for the expression of the protein and they are proneural independent. KV10 is among them, but shows proneural dependency.

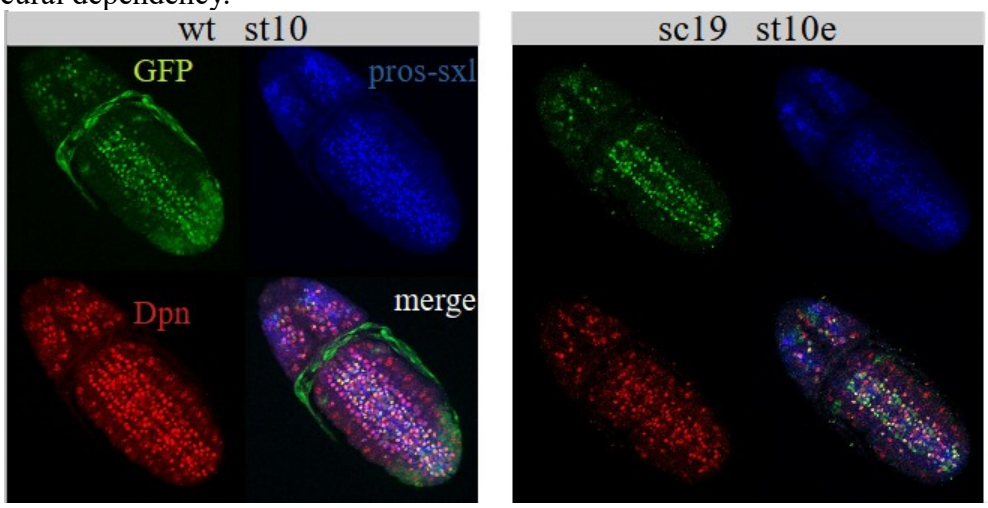

Figure 7: Immumostaining of scratch-GFP protein of wild type (wt) and *Df(1)sc19* embryos at the developmental stage 10. Antibodies: g anti-GFP 488 (green), gp anti-dpn 555 (red), m anti-pros and m anti-sxl 647 (blue).

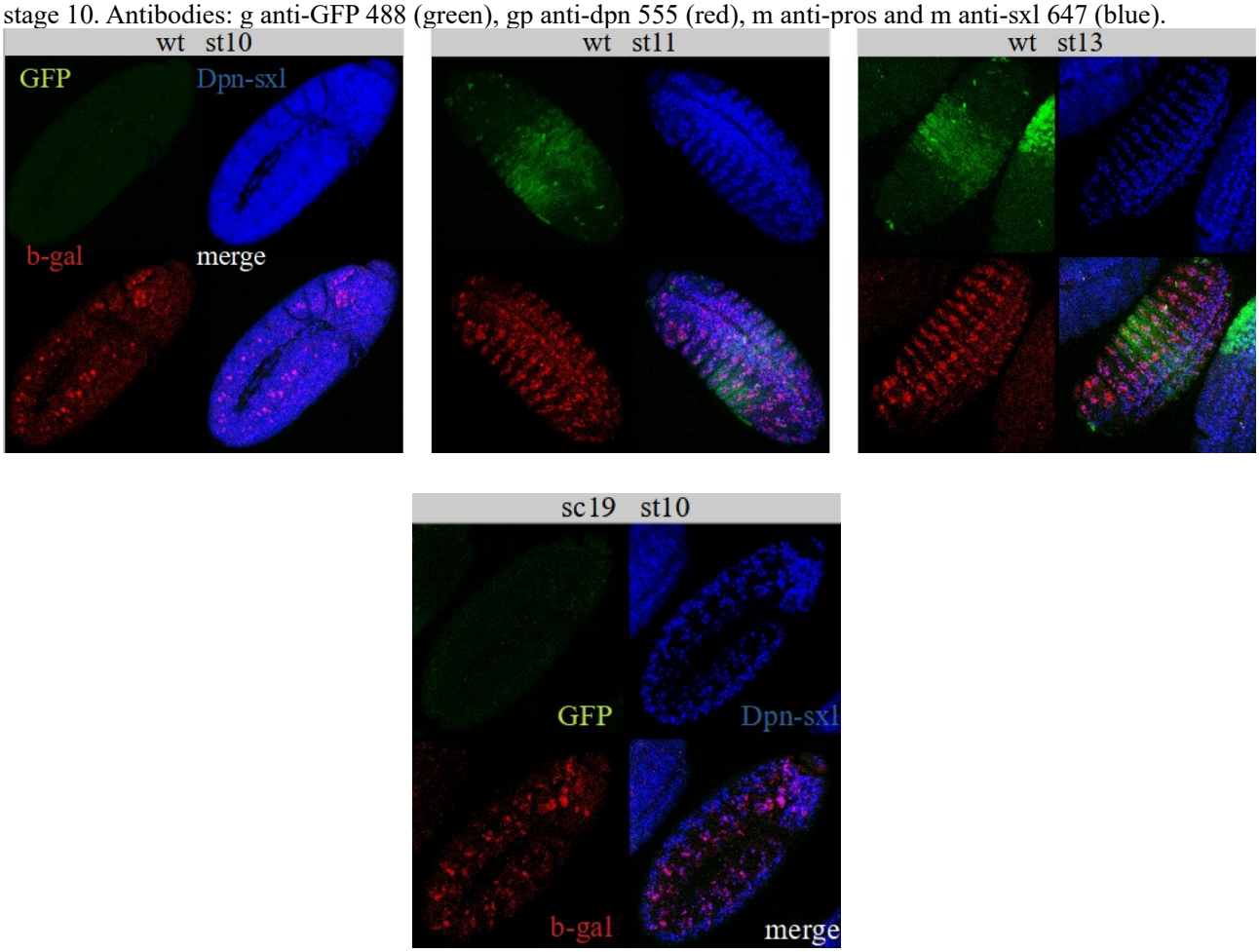

Figure 8: Immumostaining of KV10 of wild type (wt) and *Df(1)sc19* embryos at the developmental stage 10,11 and 13. Antibodies: g anti-GFP 488 (green), rb anti-b-gal 555 (red), gp anti-dpn and m anti-sxl 647 (blue).

KV14 and KV15 (nervy 1 and 2)

nervy (nvy) throughout embryogenesis appears at CNS and PNS precursors. nvy is a neuroblast marker in CNS and specifically expressed in the SOP, where it interacts with Daughterless (Da) and affects the expression of ac and sc targets, as a transcriptional repressor (Feinstein et al., 1995; Wildonger & Mann, 2005). Furthermore, an other controversial role of nervy, a member of the myeloid translocation gene family of A kinase anchoring proteins (AKAPs), is the regulation of repulsive axon guidance (Terman & Kolodkin, 2004).

The nervy-GFP protein, as well as the enhancer of nervy KV14 were studied during my rotation and the results are shown in the Figures 10 and 11, respectively. KV15 was not further studied, because in X-gal staining and in Theodorou results, the signal was detected only in PNS, and as it was referred in the PNS there are, also, other proneurals (ato and amos) in chordotonal and md precursorss.

The nvyGFP protein in wt embryos (st10-13) appeared in a subset of NBs and in PNS. The embryos at the same stages with the *Df(1)sc19* in their genetic background showed only PNS expression, the CNS signal was lost (Figure 10). The nvyGFP embryos also showed a weak ubiquitous signal deeper than NBs layer, that it seemed not to be affected by *Df(1)sc19*. *Df(1)B57* embryos at stages 9 and 11 studied by Theodorou et al. (2022) showed only PNS signal as well, and CNS signal never rebounded.

The staining results of KV14 showed CNS and PNS signal in wt embryos. The CNS signal was lost in *Df(1)sc19* embryos (st10 and 11) (Figure 11). In *Df(1)B57* neuroblasts, nvy-KV14

expression was abolished throughout neurogenesis similar to the Nvy protein (Theodorou et al., 2022).

Even though, the enhancer could be studied more extensively, the presence of ase was not capable of turning on neither the enhancer till stage 11, nor the nervy-GFP protein till the stage 13, in the CNS. One can conclude that these two elements are asense-independent, but show fully dependency on the rest proneural transcription factors for their activity.

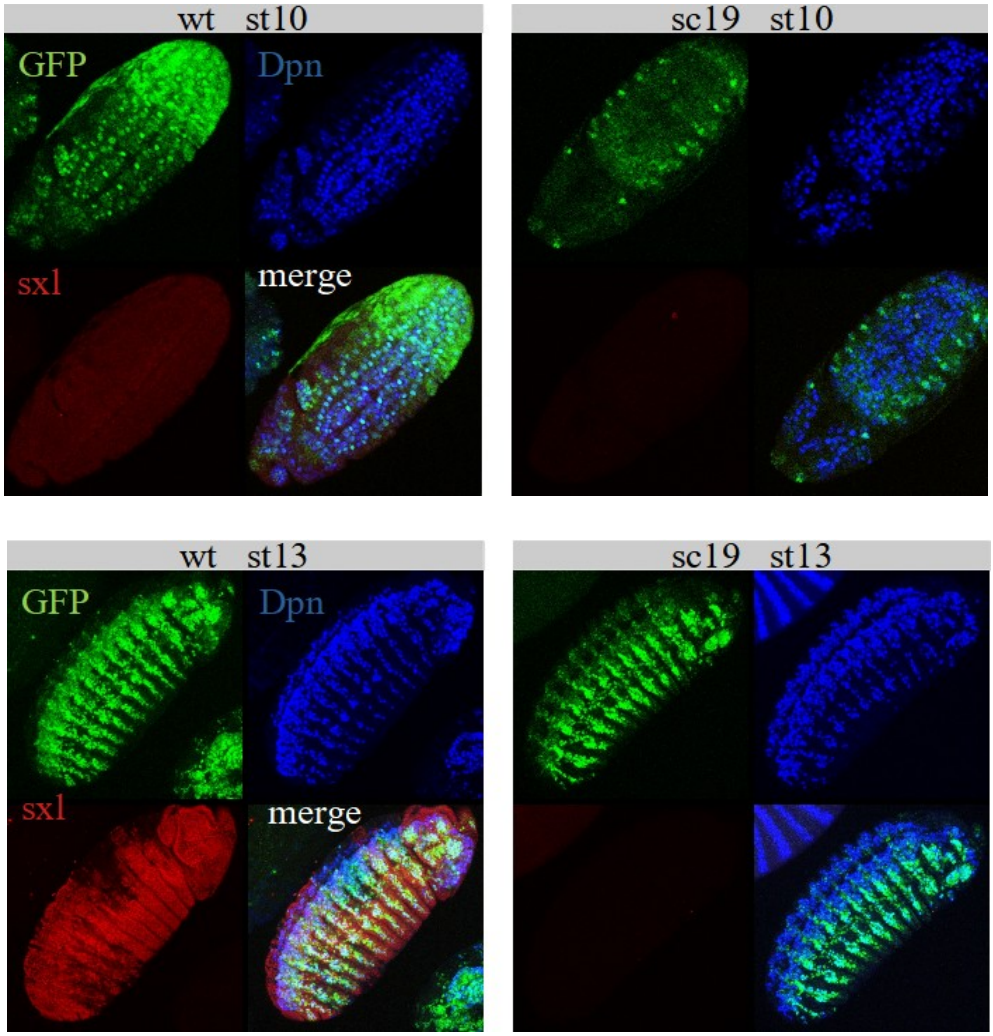

Figure 10: Immumostaining of nervy-GFP protein of wild type (wt) and Dfsc19 embryos at the developmental stages 10 and 13. Antibodies: g anti-GFP 488 (green), m anti-sxl 555 (red), gp anti-dpn 647 (blue).

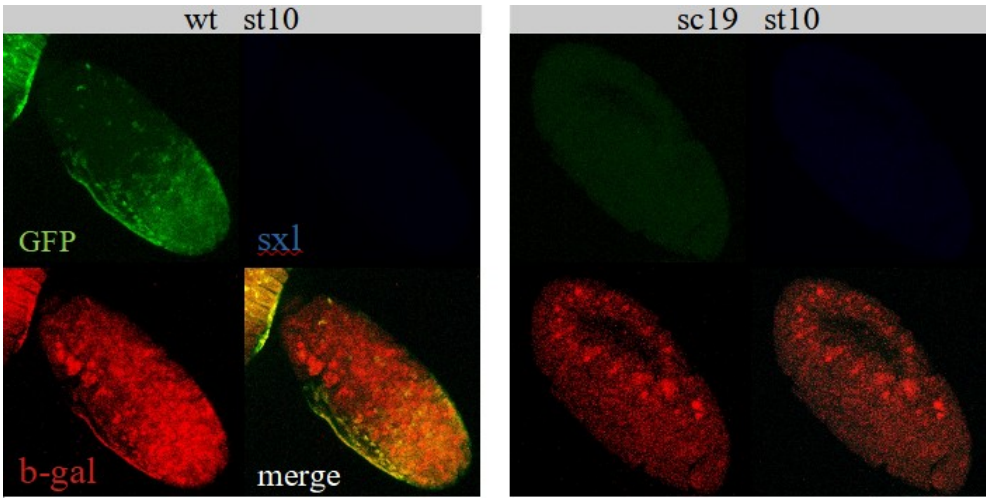

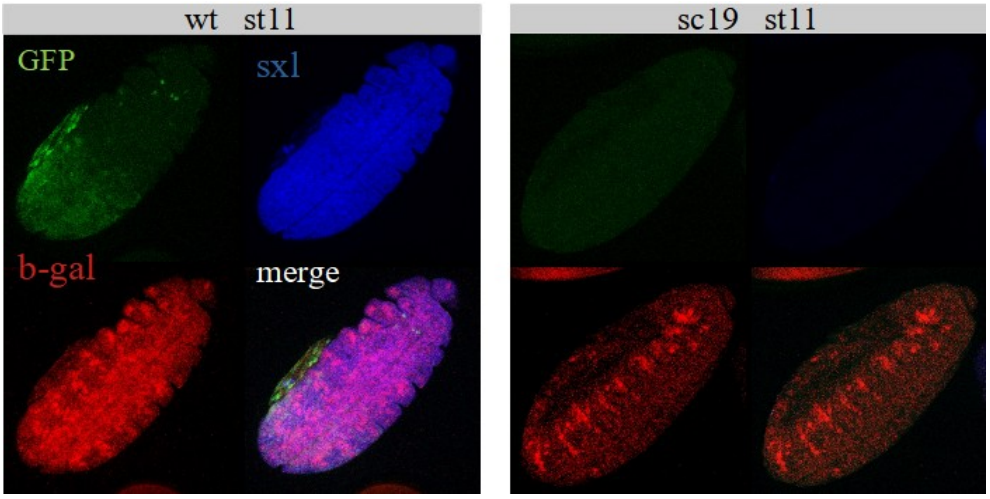

Figure 11: Immumostaining of KV14 of wild type (wt) and Dfsc19 embryos at the developmental stage 10 and 11. Antibodies: g anti-GFP 488 (green), rb anti-b-gal 555 (red), m anti-sxl 647 (blue).

KV21 (target of poxneuro)

The Drosophila genome encodes a single neurogenin family member, based on the conservation of family-defining residues in the bHLH domains, the target of poxneuro (tap). Its role is not well understood. Although, tap is normally expressed in a large subset of GMCs, as well as in precursor cells in the PNS, during embryogenesis. Furthermore, tap is not a proneural protein in Drosophila but is required for proper axonal growth and guidance of neurons of the mushroom body (Theodorou et al., 2022; Yuan et al., 2016).

Concerning the tap-GFP protein, Figure 12 shows its expression levels in wt and *Df(1)sc19* background. At stage 10, wt and sc19 embryos had a ring-like expression pattern. By stage 12, both embryos had stronger expression of the protein. At stage 13, the expression levels seemed equal again. tap is expressed in a large set of GMCs, not in NBs and in some PNS precursors. Figure 12, especially the embryo at stage 10 in zoom, confirm the GMC presence and the NB absence. Last, wt embryos at stages 12 and 13 showed an expression pattern in PNS, which is partially or totally absent in *Df(1)sc19* embryos. In ASC^{-} GMCs, Tap showed a prolonged delay and eventually turned on by stage 13 (Theodorou et al., 2022). Thus, the transcription factor ase was capable of activating the expression of the protein starting at earlier stages.

The enhancer of tap, KV21, was firstly studied in wt background. The immunostaining results showed PNS pattern at stages 9 and 11, but CNS and PNS pattern at stage 13 (Figure 13). The b-gal expression was found in a subset of NBs and in dpn^{+}, $pros^{+}$ and $b\text{-}gal^{+}$ cells (newly born GMCs).

The enhancer in *Df(1)sc19* showed no CNS staining, and a defective PNS staining (Figure 14). At stages 9 and 10, the absence of CNS staining was expected, as this was the pattern in wt as well. At the developmental stage 13, when the enhancer was activated, the deficiency affected the expression of the enhancer. Theodorou et al. (2022) found a different expression pattern in CNS, as they detected CNS signal from the stage 10. In early *Df(1)B57* embryos, the NB and GMC expression was lost, but they did detect limited expression in GMCs and midline from stages 13–14 onwards (not shown). The differences at wt stage 10 and *Df(1)sc19* stage 13 shows that further examination of the expression patterns in more stages should be conducted.

The comparison of the tapGFP and KV21 expression patterns show differences. The GFP of tap is detected only in GMCs, while the enhancer in NBs and GMCs. Concerning PNS, GFP had limited presence, while KV21 had strong signal. One can conclude that this enhancer does not recapitulate the GMC pattern of tap-GFP, instead it shows strong ectopic PNS expression. Either this enhancer is not acting on the tap gene (rather on another nearby gene), or the tap-GFP transgene is somehow defective.

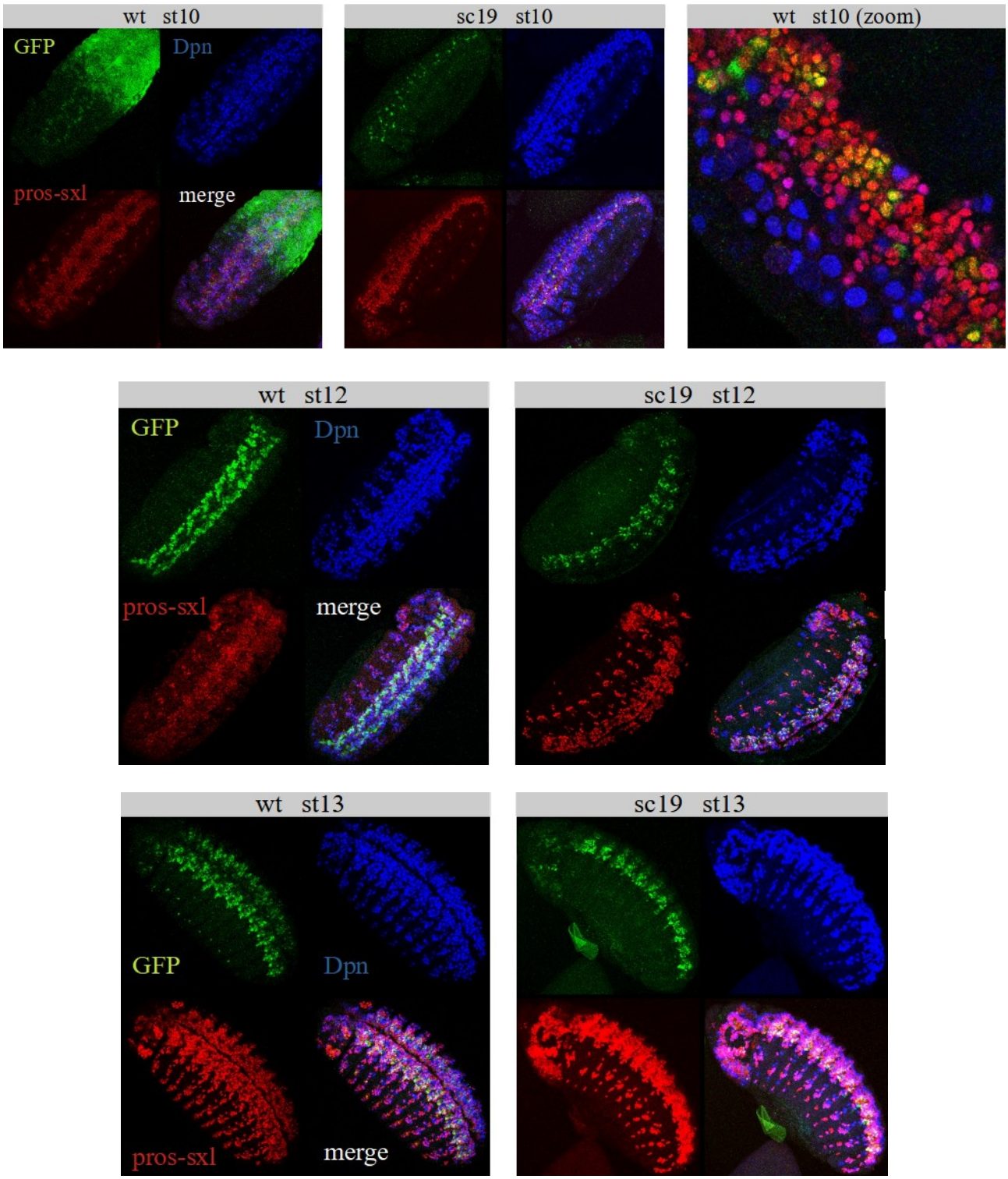

Figure 12: Immumostaining of tap-GFP protein of wild type (wt) and *Df(1)sc19* embryos at the developmental stage 10/11/12/13. Antibodies: g anti-GFP 488 (green), m anti-pros and anti-sxl 555 (red), gp anti-dpn 647 (blue).

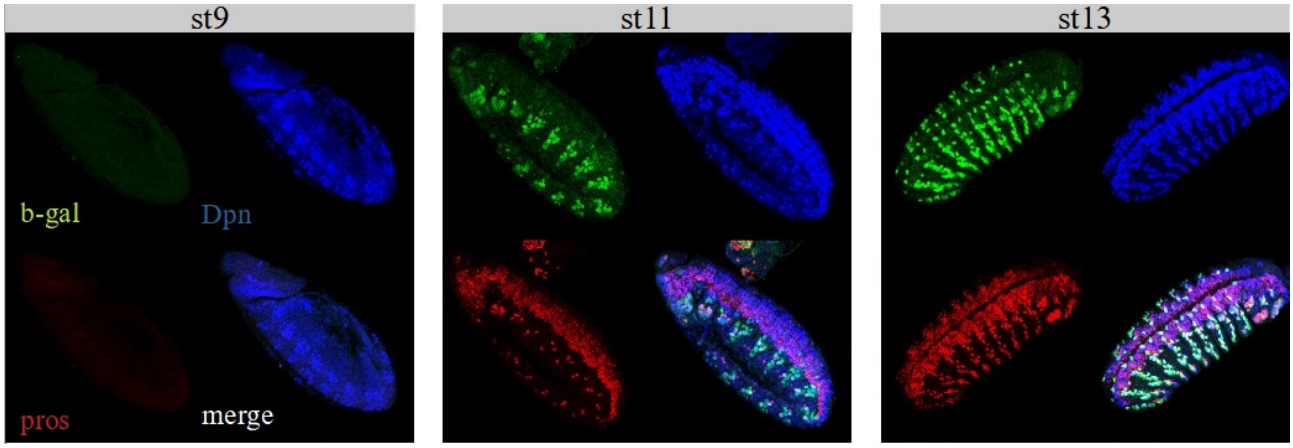

Figure 13: Immumostaining of KV21 at the developmental stages 9, 11 and 13. Antibodies: rb anti-b-gal 488 (green), m anti-pros 555 (red), gp anti-dpn 647 (blue).

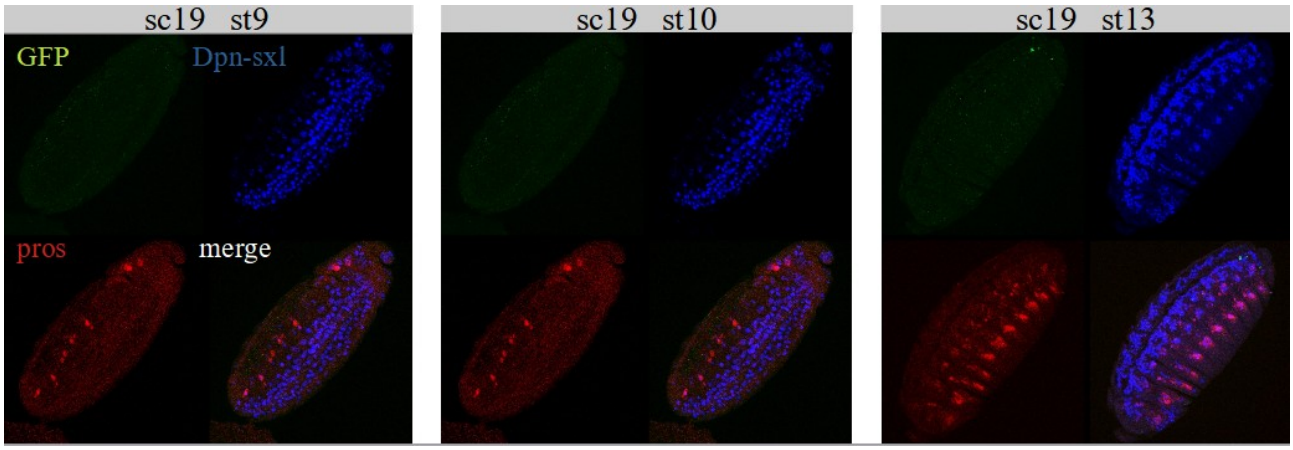

Figure 14: Immumostaining of KV21 of wild type (wt) and *Df(1)sc19* embryos at the developmental stages 9, 10 and 13. Antibodies: g anti-GFP 488 (green), rb anti-b-gal 555 (red), gp anti-dpn Cy5 and m anti-sxl 647 (blue).

KV23 (deadpan)

The gene of deadpan (dpn) encodes a basic helix-loop-helix protein containing a characteristic 'Orange' dimerization domain (bHLH-O). Its role is the transcriptional repression of genes that require a bHLH protein for their transcription (Bier et al., 1992; X. Li et al., 2017). In more detail, Enhancer of spit [E(spl)] and Dpn proteins are crucial in NB maintenance and proliferation. Both are expressed in NBs from embryogenesis onwards and have redundant functions in NB maintenance during development (Zacharioudaki et al., 2012).

The dpn protein was studied by Vasiliki Theodorou et al. (2022) in both deficiencies. In *Df(1)B57* background at stage 10 the expression levels were severely reduced, but from st11 onward rebounded. At *Df(1)sc19* background the delay was smaller, until stage 9, and from st10 onward the protein rebounded. Therefore Ase can activate dpn in a more timely manner in the absence of the other ASC proteins.

The results in Figure 15 show that the enhancer KV23 drove the expression of b-galactosidase in a subset of NBs in the VNC, as well as in the brain. Mutant embryos showed a moderate expression of the b-gal, especially in the CNS at stage 10. By stage 15 the expression levels of mutant embryos rebounded. In the *Df(1)B57* mutant, KV23 was never activated (Theodorou et al., 2022). Thus, ase bound in the enhancer and turned it on. The results of this experiment is from my rotation.

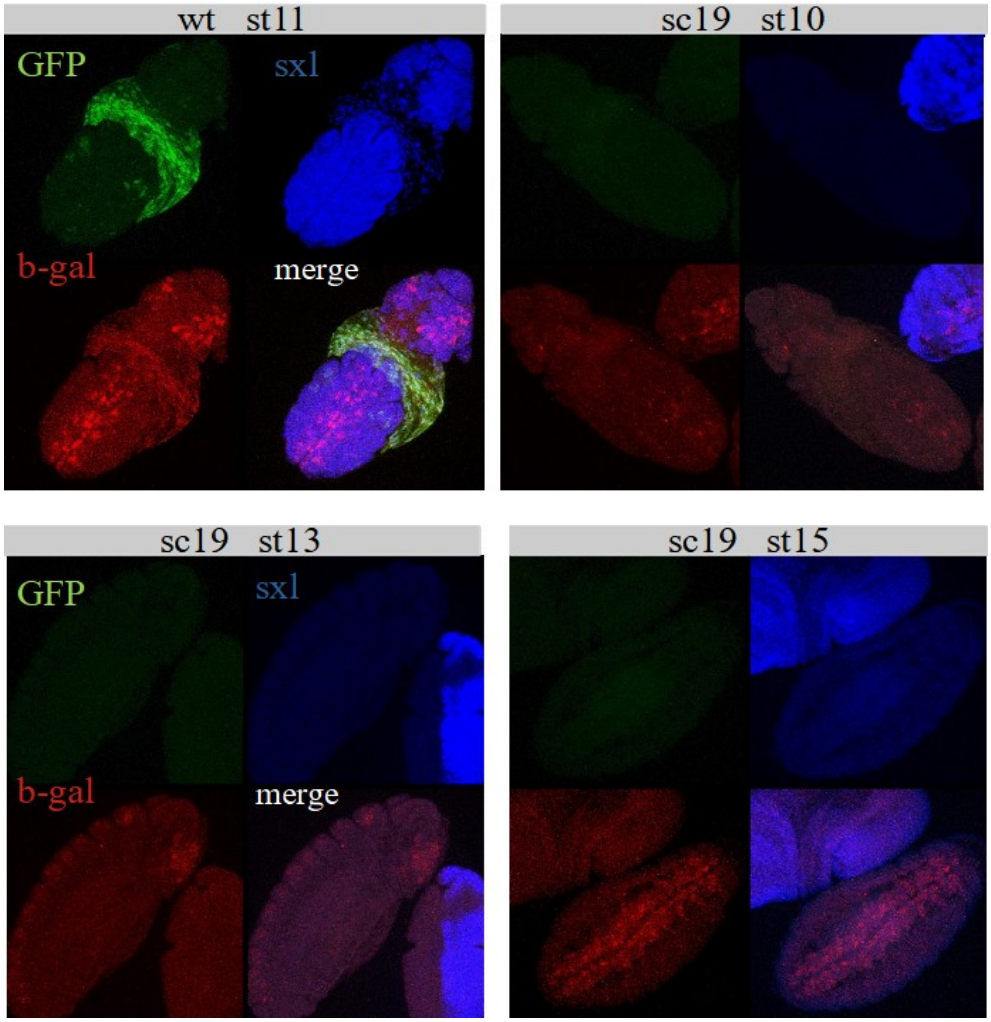

Figure 15: Immumostaining of KV23 of wild type (wt) and *Df(1)sc19* embryos at the developmental stage 10, 11, 13 and 15. Antibodies: g anti-GFP 488 (green), rb anti-b-gal 555 (red), m anti-sxl 647 (blue).

Worniu-GFP

The KV29 enhancer of the gene worniu (wor) was not further studied, but this was not the case for the protein of worniu tagged with GFP. Concerning the enhancer, its weak signal maybe was due to its cloned sequence (it is possible that the cloned sequence was not the whole sequence of the enhancer), or the cooperation of other enhancers was needed.

The protein wor-GFP showed in Figure 16 was present in all NBs and newly born GMCs in the CNS, brain from stage 9 to stage 15, and in PNS at stages 10-12. There were, also, a few wor+ cells that were dpn- and pros- (marked with an asterisk *).

The protein was also examined in both deficiencies, *Df(1)B57* and *Df(1)sc19*. Figures 17 and 18 show that deficiencies had not impact on the expression of the protein. It seems that wor-GFP is too strong and it overshadows Kr>GFP, and as a result the genotype of the males (no Sxl) was selected based on the Dpn/Pros pattern. Thus, from the above results, wor-GFP expression is proneural independent. It is worthy to note that, based on an immunostaining against the worniu protein performed previously in the lab, *Df(1)B57* delayed Wor expression, similar to Dpn. That's not the case here, probably due to *Df(1)B57* mis-genotyping or the characteristics the transgene had. Apparently, a careful comparison of the two stainings need to be done and/or new crosses of the wor-GFP line and the *Df(1)B57* line.

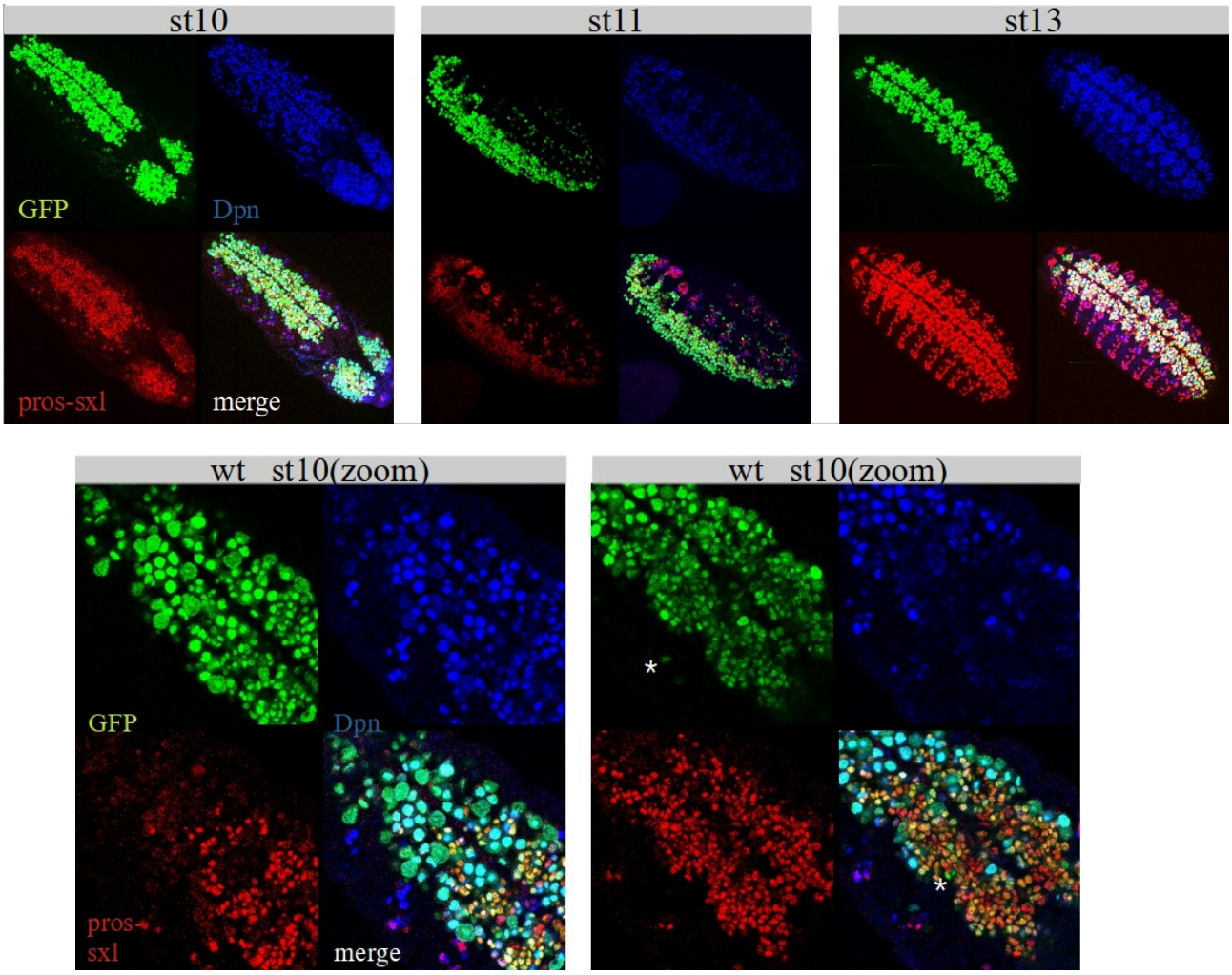

Figure 16: Immumostaining of wor-GFP embryos at the developmental stages 10,11 and 13. Antibodies: rb anti-GFP 488 (green), m anti-pros m anti-sxl 555 (red), gp anti-dpn 647 (blue). Sections at the level of NBs (left) and GMCs (right).

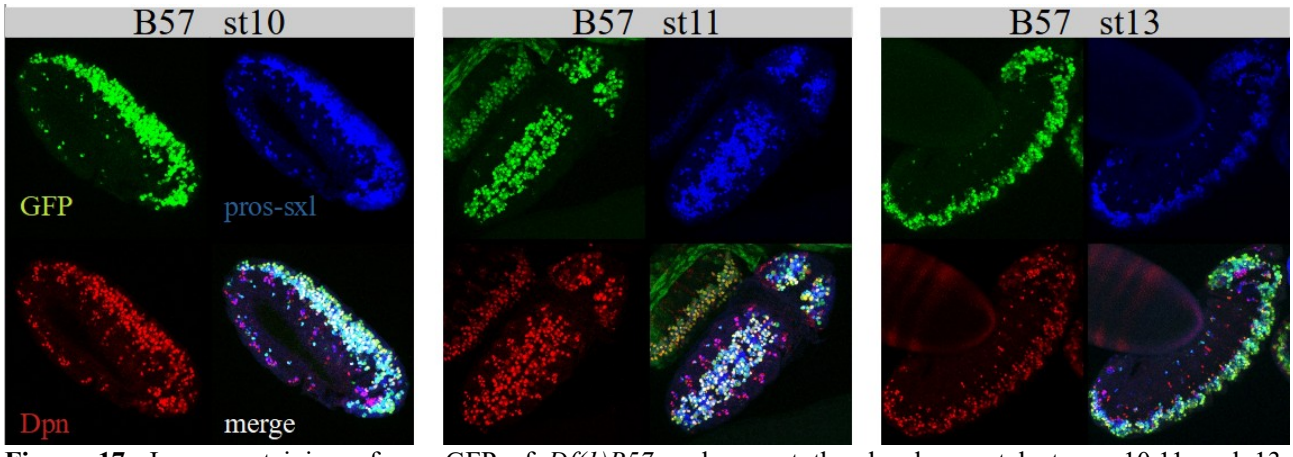

Figure 17: Immumostaining of wor-GFP of *Df(1)B57* embryos at the developmental stages 10,11 and 13. Antibodies: g anti-GFP 488 (green), gp anti-dpn Cy3 (red), m anti-pros and m anti-sxl 647 (blue).

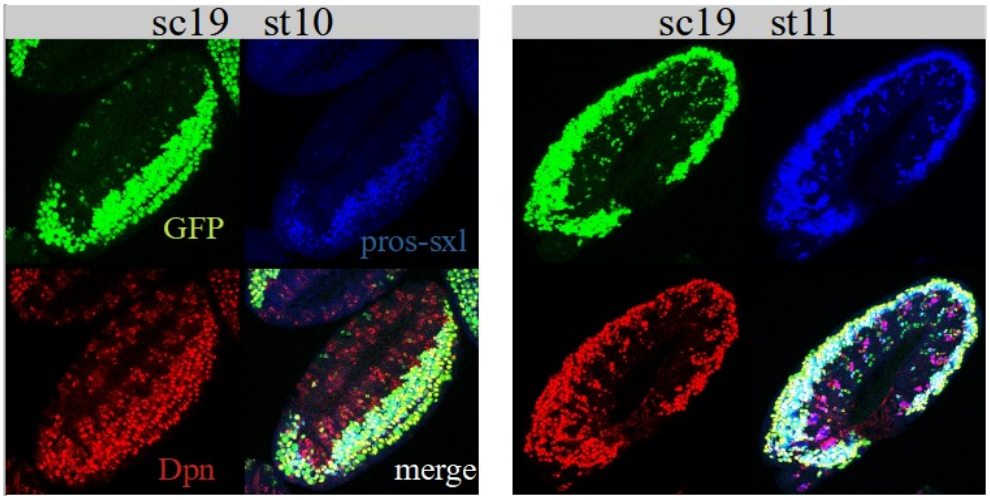

Figure 18: Immumostaining of wor-GFP of *Df(1)sc19* embryos at the developmental stages 10 and 11. Antibodies: g anti-GFP 488 (green), gp anti-dpn Cy3 (red), m anti-pros and m anti-sxl 647 (blue).

To summarize and discriminate the function of the ac, sc, and l'sc from ase were conducted all the above experiments. They showed that the are two classes of enhancers: the Ase-responsive and ase-non-responsive enhancers. The enhancers KV1 and KV8 were activated by Ase (Ase-responsive), while the KV4 and KV14 were not (ase-non-responsive enhancers). The rest enhancers, KV10, KV21 and KV23 have to studied further. The insc enhancer, KV1, that was the only activated in the *Df(1)B57*, there it was activated by other proneural factors.

The protein nervy tagged with GFP, in the presence of ase showed no activation in the CNS. The proteins scrtGFP, worGFP and tapGFP showed slight or no fluctuation in their expression patterns in wt and *Df(1)sc19* embryos. The bratGFP protein rebounded, when NBs rebound (st9). In all circumstances, PNS patterns showed no great variability, as ase is not the only present and responsible TF for the expression in the PNS (Table 3).

Table 3: Putative enhancers staining information in wt, DfB57 and Dfsc19 embryos, as well as the proteins the enhancers activate, in wt, *Df(1)B57* and *Df(1)sc19* embryos.

Enhancers	**wt**	**B57**	**sc19**	**Gene**	**wt**	**B57**	**sc19**
KV1	most NBs, brain and some PNS	st11: weak express during rebound	rebound stage 10l	insc	-	-	-
KV4	St10-13: subset of NBs and brain, PNS precursors	st10: lost	st10-13: lost in CNS	phyl	-	-	-
KV8	some NBs CNS, brain and PNS	st10: lost in CNS st12: rebound	st10: very few NBs st 12: rebound(?)	bratGFP	st9 onward: around GMCs (CNS+brain) ectodermally in all st	when NBs rebound and divide, around from GMCs (st10l)	when NBs rebound and divide, around from GMCs (st9)
KV10	some NBs CNS and brain (st 10 weak, st 11 strong) Strong PNS	lost in NBs, not in PNS	not sufficiently studied (st10)	scrtGFP	St9-10: all NBs CNS, brain, newly born GMCs, some SOPs	weak st9 rebound st11	almost as wt
KV14	st10-11: CNS, brain and PNS	st11: lost in CNS	st10-11: lost in CNS	nvyGFP	st10-16: some NBs, brain and strong	never rebound in CNS	st10-13: lost in CNS

					PNS precursors		
KV21	st11-13 some NBs in CNS and brain, pros+, dpn+ and bgal+ cells (maybe newly born GMCs), PNS strong st10 onward pros+,dpn+ and bgal+	lost in NBs and GMCs, st13-14: limited expression in midline and GMCs, PNS intact	st10-13: lost in CNS, same as wt in PNS	tapGFP	many GMCs, no NBs, no PNS	turned on st13	as wt
KV23	subset of CNS NBs, no PNS	never activated	st10-11: lost st13-15: rebound	dpn	st9: CNS and brain st11: +PNS	st9: stalling st11: rebound	st9: stalling st10: rebound
KV29	-	-	-	worGFP	st10 onward all NBs wor+ (CNS only), some midline, brain, most GMCs, some wor+ (dpn-pros-)in CNS and PNS	st 9: lost st10:some NBs st 11: all NBs	st10-11 as wt

Study of E(spl)-C genes targeted by Deadpan in dpn over-expression

In Drosophila E(spl) locus [E(spl) Complex) encodes seven genes: E(spl)mδ, mγ, mβ, m3, m5, m7, and m8 (Delidakis & Artavanis-Tsakonas, 1992; Knust et al., 1987). The seven paralogous bHLH-O proteins inhibit NB formation (Nakao & Campos-Ortega, 1996). The proteins initially are found in the nuclei of ectodermal cells in the ventral neurogenic region but not in the nuclei of delaminating neuroblasts (Jennings et al., 1994). At the stage of proneural cluster, when the cell, that will become the neuroblast, expresses Delta (Dl) the ligand of Notch receptor, activates the Notch signaling on the neighboring cells. The cleaved intracellular domain of Notch receptor, directly binds to Supressor of Hairless [Su(H)] (Hartenstein & Wodarz, 2013). In turn, Su(H) directly activates transcription of E(spl)-C genes in response to Notch receptor activity (Bailey & Posakony, 1995).

E(spl)m7 is inhibitor of neural fate, because it binds to proneural activators ac and sc, suppressing their activation mode. What is more, the direct DNA binding to target genes by E(spl)-C takes place, always aided by the co-repressor Groucho (gro) (Giagtzoglou et al., 2003). A second member of the complex, E(spl)m8 is a suppressor of NB fate and binds to gro, too (Paroush et al., 1994).

Dpn is a Hes protein, like the E(spl)s. Unlike E(spl), Dpn is highly upregulated in NBs and in fact it is used as an archetypal NB marker. It was observed that deadpan in over-expression generates numerous NBs and a hyperplastic VNC. Vasiliki Theodorou ChIP seq preliminary data against dpn showed that dpn binds in E(spl)-C genes, whose expression was also reduced in an RNA-seq experiment upon dpn overexpression (Figure 19). This raised the hypothesis that dpn is possible to suppress the suppressors of NB fate, like E(spl)-C genes or Notch. To address this, two genes, E(spl)m7 and E(spl)m8, were chosen in order to study if their expression is suppressed after dpn over-expression.

bib-Gal4 is active in the procephalic and ventral neurectoderm from stage 8 onwards and by stage 16 GFP is detected in the VNC and the mature epidermis, with bib-Gal4 over-expression not influencing NB specification. Induction of scAPAA, a stabilized variant of sc, and Notch resulted in phenotypes in agreement with the conventional model of mutual proneural-Notch antagonism in NB specification, rendering bib-Gal4 an appropriate driver to monitor the desired over-expressions (Theodorou et al., 2022).

Wild type embryos of m7-GFP are shown in Figure 20. E(spl)m7 was expressed in the neurectoderm, the place where NBs delaminate, and in the neuronal cluster at all cells surrounding the NB, except from the NB itself (Figure 19 zooms). The aforementioned expression pattern was studied at stages 9 to 11, but at stage 14 the expression had stopped. The cross E(spl)m7-GFP bibG4 x U8-1-1dpn was conducted, but the embryos did not have the dpn over-expression, so the expression pattern of m7 upon dpn overexpression is yet to be examined.

The E(spl)m8 protein in wt embryos is present in the neuroectoderm, and it is suppressed in the delaminating NBs. In dpn over-expression at st 9 E(spl)m8 was found in the neuroectoderm at wor+ cells and was absent from wor+, dpn+ NBs. By stage 10 and 11, the neuroectoderm expression of m8 in wor+ cells continues, but not all wor+ are m8+ cells. Likewise, the NBs did not express m8, but the proneural cluster around them expresses (Figure 21). Concerning E(spl)m8, the dpn over-expression did not change its expression levels, as in neuroectoderm dpn and m8 were concomitantly in the same cells, and in NBs the E(spl)m8 was suppressed as in the wt embryos.

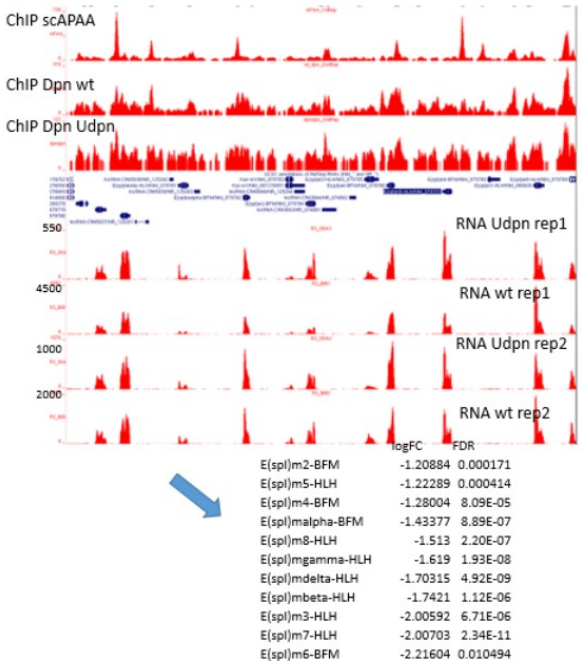

Figure 19: Preliminary data of ChIP sequencing against Dpn and Dpn over-expression and RNA sequencing upon Dpn over-expression, with an emphasis at the bottom of the reduced expression levels of the E(spl)-C genes. From Vasiliki Theodorou.

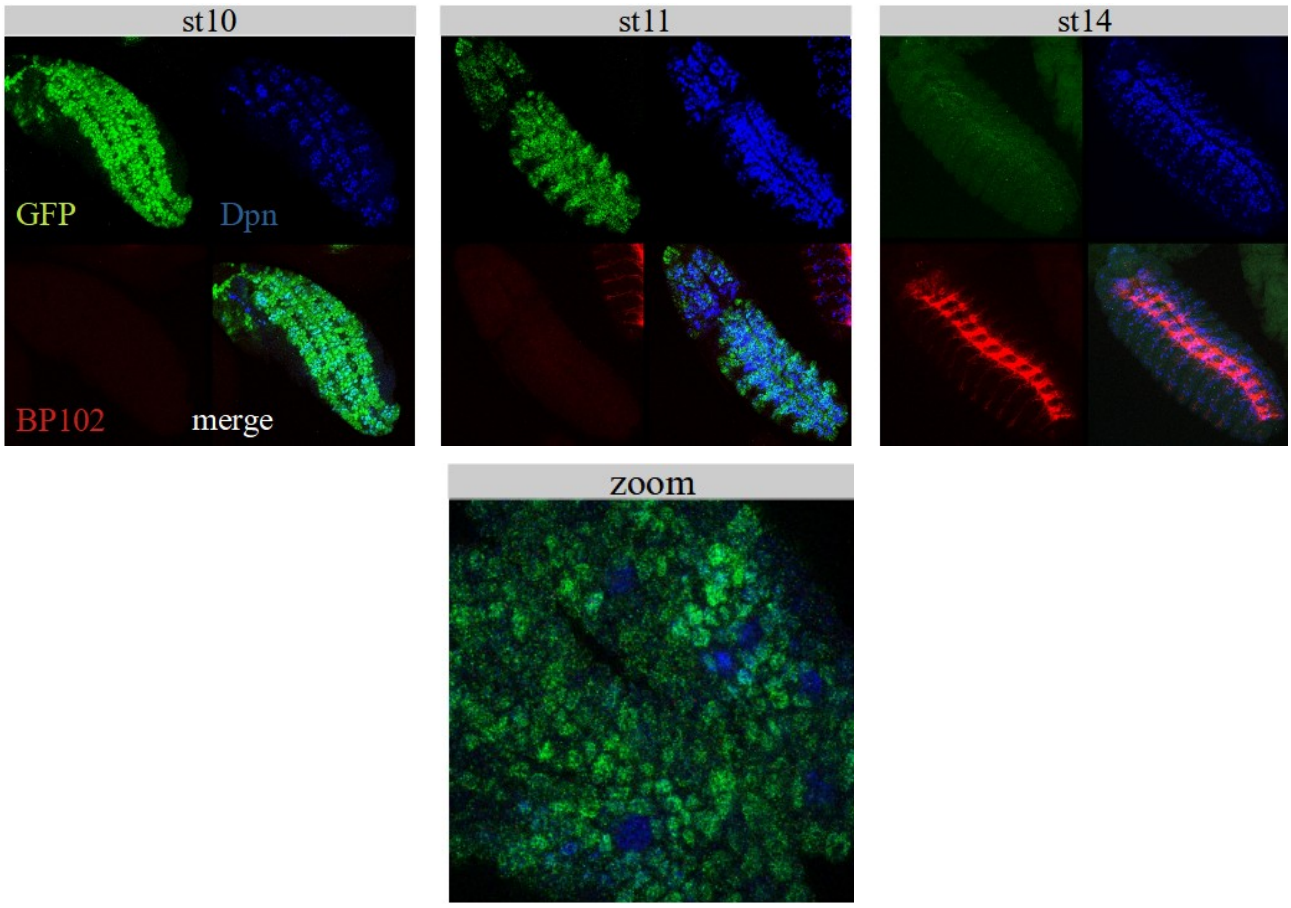

Figure 20: Immumostaining of m7GFP embryos at the developmental stages 10, 11 and 14. Antibodies: rb anti-GFP 488 (green), m anti-BP102 555 (red), gp anti-dpn 647 (blue).

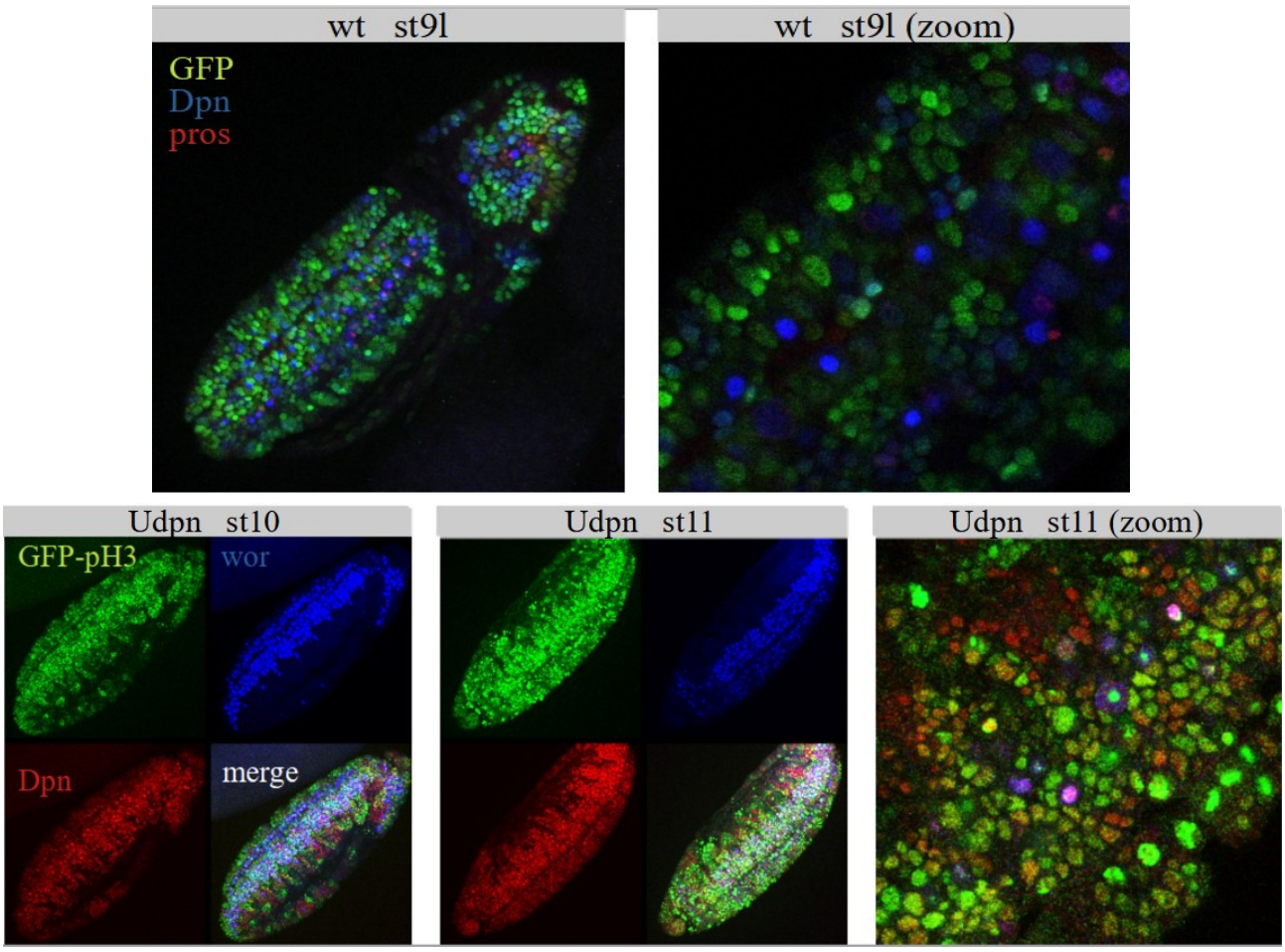

Figure 21: Immumostaining of wt and E(spl)m8GFP;bibG4 x U8-1-1dpn embryos at the developmental stages 9, 10 and 11. Antibodies: rb anti-GFP and anti-pH3 488 (green), gp anti-dpn 555 (red), rat anti-wor 633 (blue).

Over-expression of an extracellular domain deletion of Notch (UAS-NΔecd, abbreviated U-NΔE), mimicking Notch activation, exhibited reduced number of delaminated neuroblasts, severe CNS hypoplasia (stage 16) and complete embryonic lethality (Theodorou et al., 2022). Thus, we asked whether dpn over-expression induced neural hyperplasia can 'rescue'-dampen the U-NDE induced NB hypoplasia and whether this could be also monitored with the me-GFP expression pattern. Figure 22 shows a wt embryo and an embryo with dpn and notch over-expression at stage 10. At this stage, mutant embryo had an increase in Dpn positive cells that are worniu minus, wor+ NBs were not supernumerary and Notch overactivation did not influence the phenotype. Figure 23 shows embryos at later developmental stages, st13 and st15, when the co-existed dpn and notch overactivation resulted in numerous dpn positive cells and an intermediate phenotype of U-NDE U-dpn together with CNS hypoplasia.

In conclusion, Dpn do not supress one of the suppressors of the neural fate, the E(spl)m8 in Dpn over-expression. Although, Dpn dampen the severe CNS hypoplasia in UNΔE, in Dpn over-expression. Thus, Udpn did not seem to repress m8, but it could inhibit the ability of UNDE to eliminate NBs.

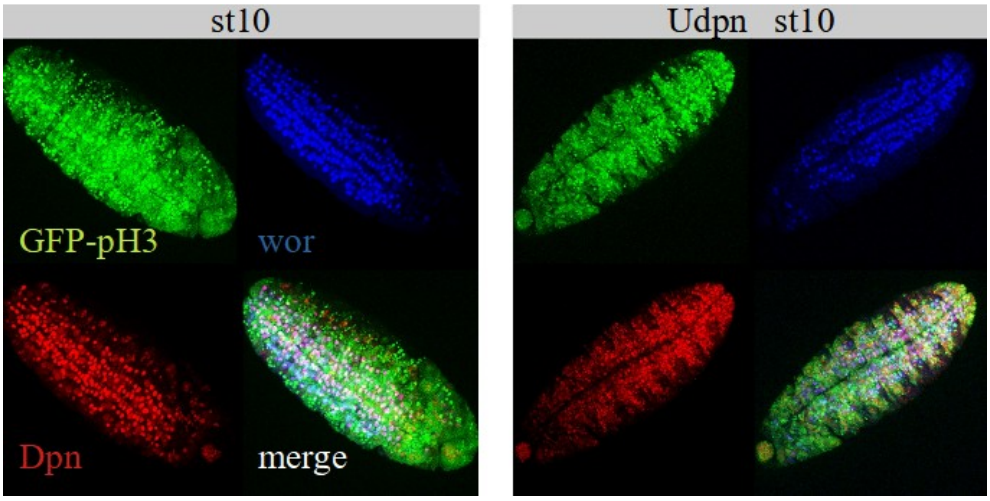

Figure 22: Immumostaining of bibG4;U-CD8-GFP x U-NΔE, U-dpn embryos at the developmental stage 10. Antibodies: rb anti-GFP and anti-pH3 488 (green), gp anti-dpn 555 (red), rat anti-wor 633 (blue).

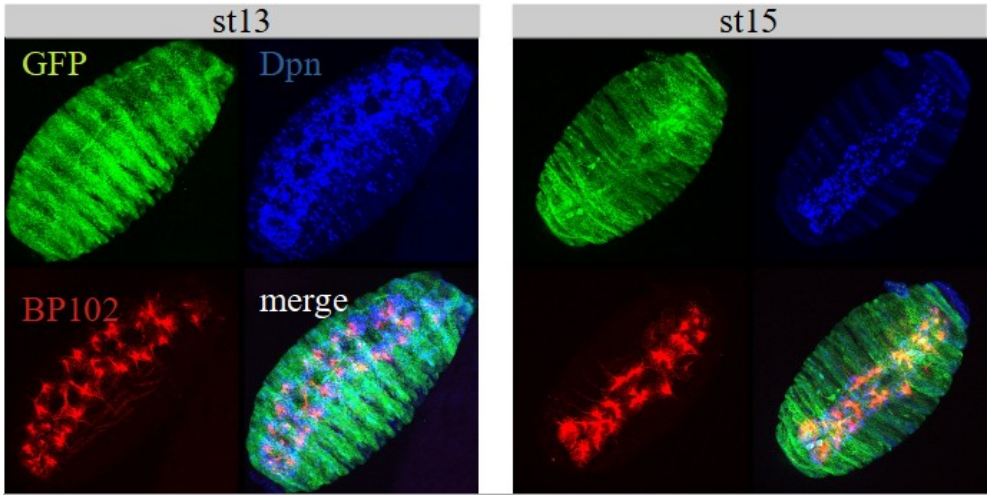

Figure 23: Immumostaining of bibG4;U-CD8GFP x U-NDE, U-8.1.1dpn embryos at the developmental stages 9, 10 and 11. Antibodies: rb anti-GFP 488 (green), m anti-BP102 555 (red), gp anti-dpn 647 (blue).

FACS sorting of embryonic worniu positive cells and cell culture

To further study the mechanism of how U-dpn induces neural hyperplasia, we asked whether the line wor-GFP could be used to monitor NBs in a cell culture. If the initial tries were successful, then U-dpn/CyO; worGFP/TM6B line would examined, so as to compare the differences in size, division, progeny in dpn over-expression embryos.

Firstly, we dissociated embryos of stages 7-11, using enzymatic and mechanical dissociation and we used the cell suspension of about 800 thousands cells to sort the GFP positive NBs. As seen in the Figure 23, the first diagram (FSC-A and SSC-A, logarithmic scale) corresponds to size and complexity of the embryonic cells, and the P1 gate was there for the living and bigger cells, defined by previous sorting. The Alexa Fluor 488-A and DsRed-A diagram was about the separation of GFP cells from the DsRed cells. The sample had only GFP cells, so the expected cells was under the diagonal line. Above this line would be the DsRed cells, while in the diagonal line are the auto-fluorescent cells or the cells with both fluorophores. From this diagram, based on the P1 gate too, a subpopulation that seemed to stands out from the rest cells was chosen as the gate P2. An other subpopulation that seemed to separate was the P4 gate. Both gates were cultured then, in order to verify where the NBs were. The last diagram, Alexa Fluor 488-A and SSC-A, was independent from the cell sorting, but verified that the cells in the P2 gate had fluoresced. The GFP cells are found between 10^3 and 10^5 , based on the intensity of the GFP, but also, are separated from the rest population. Gates are usually hierarchical organized, like a family tree, and this is the table showing. The P1 gate included 86% from the total cells, P2 the 1% and P4 the 14.2% of the P1. Last, P3 constituted the 1.9% from the whole cells.

After the first sorting, the cells from the gates P2 and P4 were again sorted, in order to test the purity of each population (Figures 25). Both subpopulations were not so pure, as their percentages were around 65% (P2) and 53% (P4). However, there were other attempts with better results.

FACS sorting duration was about an hour and then the sorted cells were cultured and imaged at the operetta or the microscope. Images from the operetta are shown in Figure 26, where GFP positive cells, possibly NBs are shown. More GFP positive cells were found in the P2 subpopulation, which was expected, as this subpopulation was more distinct than the P4, and showed more purity. Scanning and imaging results were not so successful, as endogenous GFP signal was weak and easily bleached by light, and as a result in a detected GFP positive cell (NB), after a minute of UV light, we could not detect any longer GFP. Furthermore, the operetta machine made the imaging process difficult, as the stage with the sample were moving in every scanning sequence, and the cells inside the plate changed their position and their focus every time. In conclusion, the processes of sorting and culture were complicated and the data preliminary. Apparently, corrections in the protocols of cell acquisition, sorting and culturing should be done.

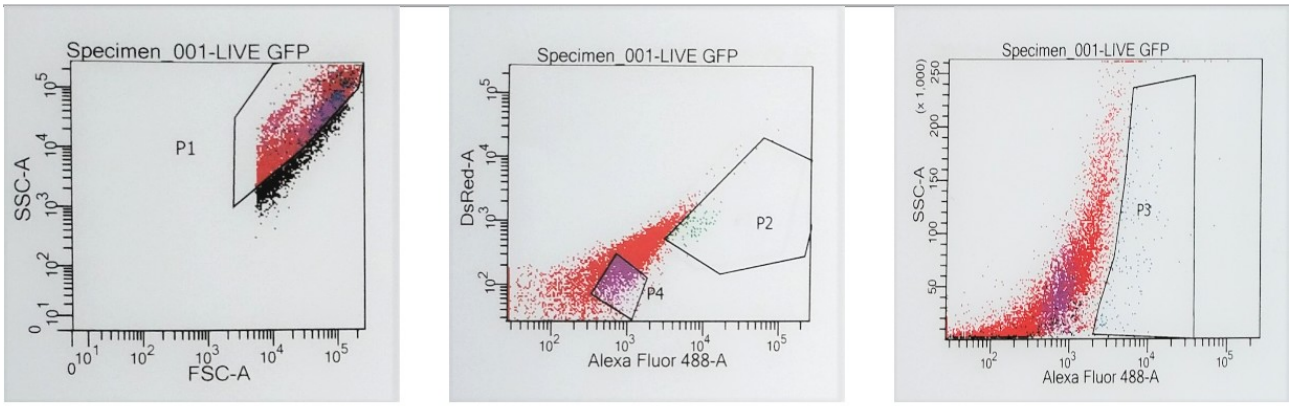

Tube: LIVE GFP

Population	#Events	%Parent	%Total
All Events	8,000	####	100.0
P1	6,882	86.0	86.0
P2	79	1.1	1.0
P4	1,136	16.5	14.2
P3	152	1.9	1.9

Figure 24: Indicative diagrams of worniuGFP positive cell sorting of whole embryos. Table shows how the gating was designed. Forward scatter (FSC) and Side scater (SSC).

Tube: AFTERW SORT P2_LIVE GFP

Population	#Events	%Parent	%Total
All Events	101	####	100.0
P1	98	97.0	97.0
P2	66	67.3	65.3
P4	4	4.1	4.0
P3	54	53.5	53.5

Tube: AFTER SORT P4_LIVE GFP_001

Population	#Events	%Parent	%Total
All Events	326	####	100.0
P1	311	95.4	95.4
P2	0	0.0	0.0
P4	172	55.3	52.8
P3	2	0.6	0.6

Figure 25: Indicative diagrams of cell sorting test purity of each cell subpopulation, P2 left and P4 right. The tables underneath shows the gating, as well as the percentage of purity of each cell population.

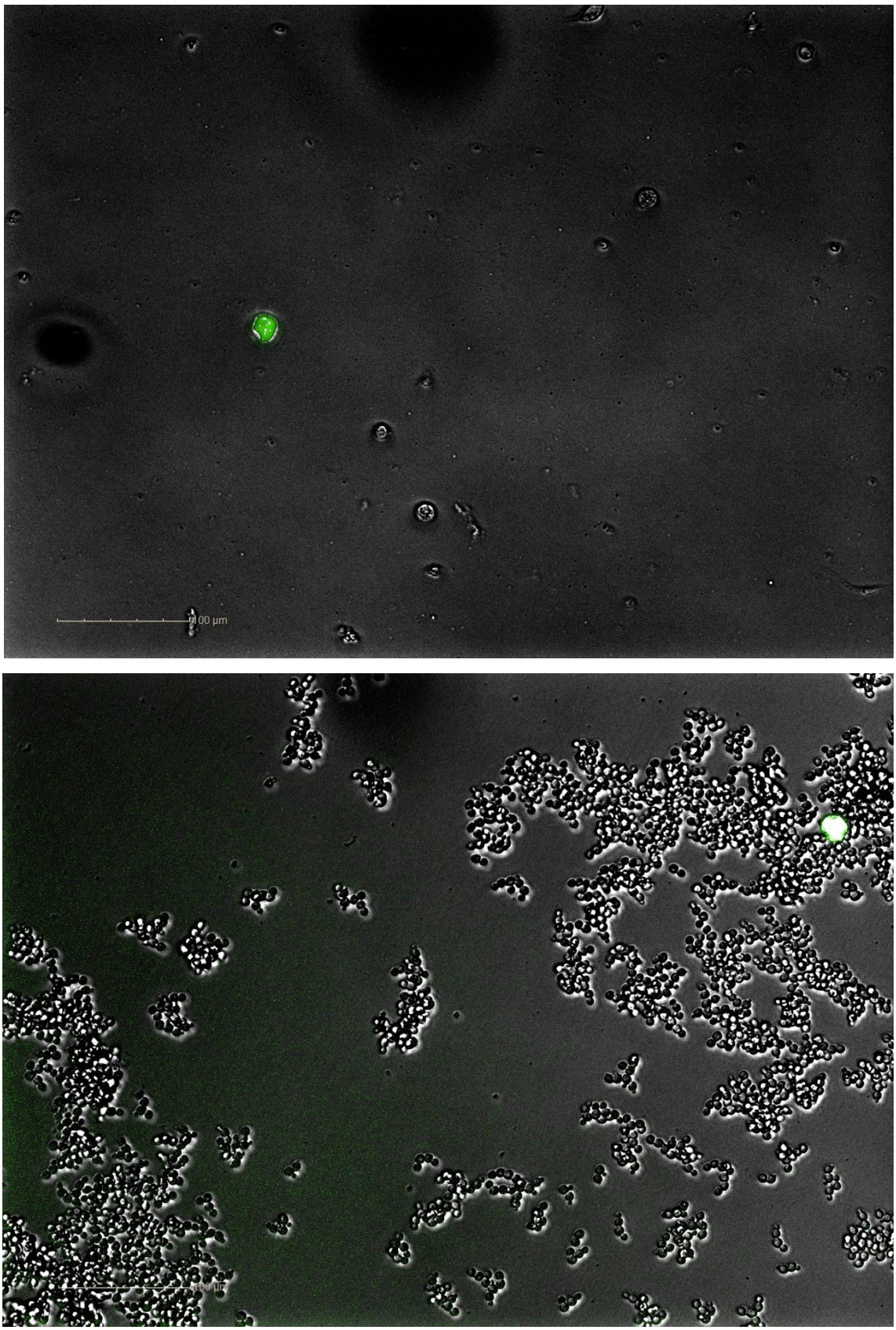

Figure 26: FACS sorted GFP^{+} cells, presumably NBs from P2 fraction, cultured in 48-well-plate in Schneider's medium, after 3 hours of plating (upper image) and 15 hours of plating (lower image). The images are from different experiments, conducted in different days.

Study of putative enhancers in later developmental stages (larva)

The designed and constructed KV lines include a possible enhancer upstream of a promoter and the β-galactosidase gene. The purpose of the X-gal staining was the semi-quantitative study of the enhancers, as the time that they need to become activated and start the transcription of the gene signifies their strength. In continuation of the X-gal experiments performed during my rotation including embryos of the KV lines, we wanted to examine the activity of the enhancers at larvae.

Two trials of each line were conducted and about 10 larvae were dissected for each experiment (Figure 27, Table 4).

Figure 27 shows the results of the X-gal staining protocol applied to 3rd instar wandering larvae, mainly the brain, the ventral nerve cord and the wing disks. In more detail, KV1 after one hour and 45 minutes appears strong staining in the central brain (CB) and the thoracic part of the ventral nerve cord (VNC), as well as there is a weak signal in the optic lobe (OL). KV4, the enhancer upstream of the phyllopod gene, appears a weak signal in the OL and strongly stained SOPs in the wing disk (WD). The strongest enhancer, KV8, showed strong signal at OL, central brain, and the thoracic part of the VNC and no signal at the WD, after one hour and 20 minutes of staining. The same time for staining was needed, also, for the KV21 enhancer that stained the OL only. The two possible enhancers of scratch, KV10 and KV19, showed weak staining of some NBs and SOPs at the wing disk and no staining, respectively. KV10 needed four hours for the weak staining pattern.

The two enhancers of the nervy showed deviation in the stained areas as well as the time, KV14 needed four hours for the central brain and VNC staining, while KV15 in an overnight staining apperead to have stained few SOPs at the wing disk. KV23 showed no staining in an overnight incubation. At last, KV29 after two and a half hours, showed weak staining of the central brain and the thoracic part of the VNC.

It is worthy to mention, that the characterization of each enhancer as a weak or strong is relative and results from the comparison between these enhancers. In other words, KV1, KV8 and KV21 needed less time than the other examined enhancers and had a strong effect of staining. On the other hand, KV19 and KV21 showed no staining patterns at all. Thus, these enhancers are not active in the larval stage or they are very weak. Another possible explanation is the cloned sequence not acting as an enhancer, but such a result have to be examined further and compared with embryo X-gal staining and with larval anti-bgal staining, which is more sensitive.

KV1 (insc)

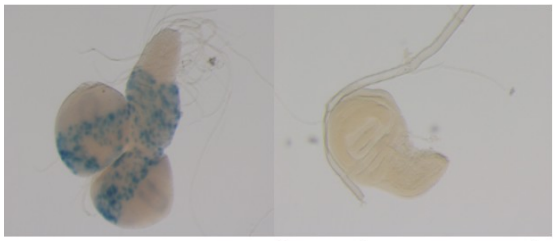

CB, VNC-th., OL weak 1.45h

KV4 (phyl)

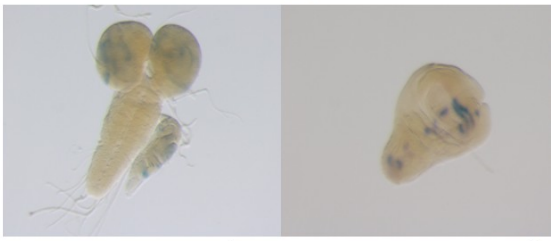

OL weak, WD- SOPs strong 2.20h

KV8 (brat)

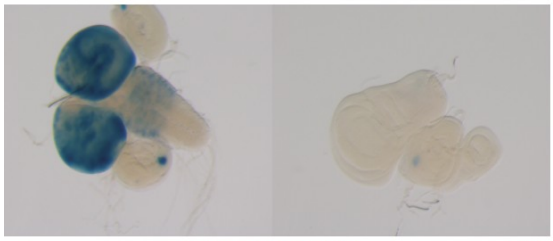

OL, CB, VNC-th, (no WD) 1.20h

KV21 (tap)

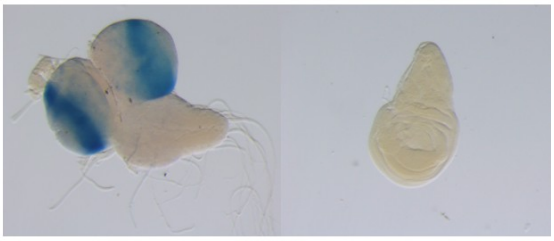

OL only 1.20h

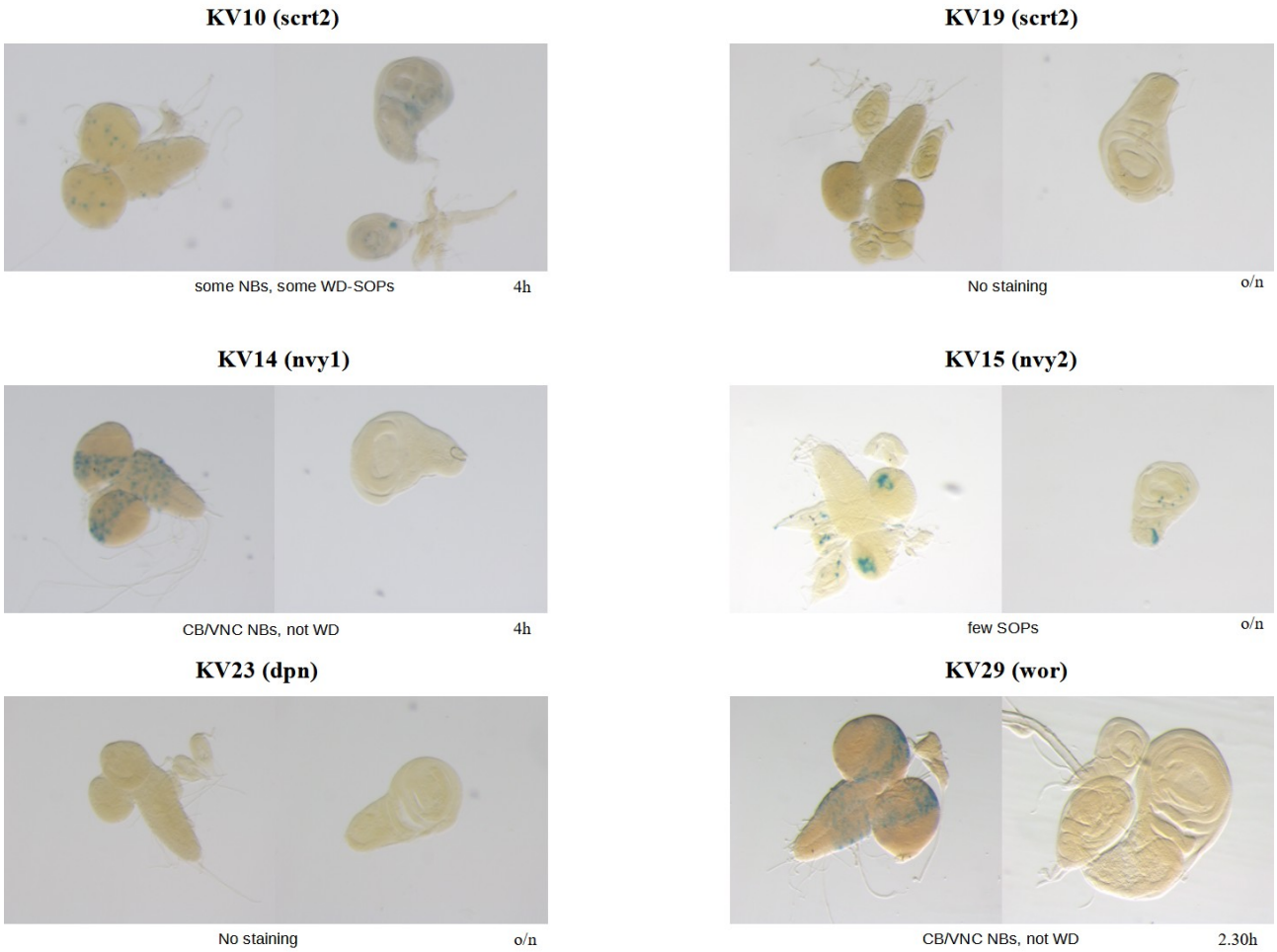

Figure 27: The staining results of each KV line of larval brain and wing disk (WD). Parentheses show the gene that enhancers activate and the time of the staining is showed at the right down corner. Central brain (CB), ventral nerve cord (VNC) and its thoracic part (th), optic lobe (OL), sensory organ precursors (SOPs) and neuroblasts (NBs).

Table 4: The two trials of X-gal staining and the time that was needed for the staining of each enhancer (coding name).

Code name of enhancers	Time of staining 1	Time of staining 2
KV1-1-1	1.30	2
KV4-3-1	2	2.40
KV8-10-2	1.10	1.35
KV10-17-1	o/n	4
KV14-16-1	1.10	4
KV15-8-3	o/n (2 days)	o/n
KV19-10-1	o/n	o/n
KV21-17-3	1.45	1
KV23-4-1	o/n	o/n

KV29-2-4	5	2

Study of the ASC-dependence of the KV10 enhancer in later developmental stages (larva)

Larval brain is used as a model of tumor formation and in our lab was used extensively for UNΔE induced tumors. Overexpression of NΔE for 24 hours leads to massive overproliferation of NBs throughout the CNS at the expense of neurons. The supernumerary Dpn-positive NB-like cells had a smaller size and were invading neuronal territories (deeper layers). Overproliferating neuroblasts of the dorsal brain lacked Ase expression, suggesting a type II origin, while overproliferating NBs in the ventral brain and VNC were both Dpn and Ase-positive, suggesting type I NBs (Zacharioudaki et al., 2012). Thus, we asked if there is any ASC dependency in Notch induced larval hyperplasias and if the KV enhancers could be used to monitor potential ASC contribution in growing tumors.

From all the possible enhancers, three were selected KV8, KV10 and KV14. The putative proneurals dependency would be examined in a different lack of all proneurals, the *Df(1)260-1*. However, the crosses of KV8 and KV14 with the *Df(1)260-1* were not successful, even the two attempts of generating the stock of the KV8 or KV14 together with the *Df(1)260-1*. To address its behaviour marcm clones were generated. The appropriate controls were studied as well. Figure 28 shows that GFP positive clones had no detectable effect in KV10 expression or cellular composition. Clones composition had one Dpn positive cell (NB) and its progeny, pros positive cells (GMCs). The line with the *Df(1)260-1*, used as control, showed the same results as the previous tested line (Figure 29). However, the generating of marcm clones needs a higher temperature, from 29 to 37ºC, so these experiments have to be tested again. It is worthy to say that, these 29ºC-marked lineages, might result not from mitotic recombination, but from spontaneous inactivation of Gal80, and thus they are not homozygous mutant for ASC (Goupil et al., 2021).

What is more, over-expression of Notch coupled with the lack of all proneurals was examined, in order to examine the ASC dependency in Notch induced tumors. Continuing to the Notch overactivation coupled to the *Df(1)260-1* or the Notch over-expression only as a control, GFP positive clones were smaller in size at 29ºC, but bigger and brighter in 37ºC. Again the clones did not show difference in the control and in the presence of deficiency. In these clones, almost all cells were dpn positive (Figures 30 and 31).

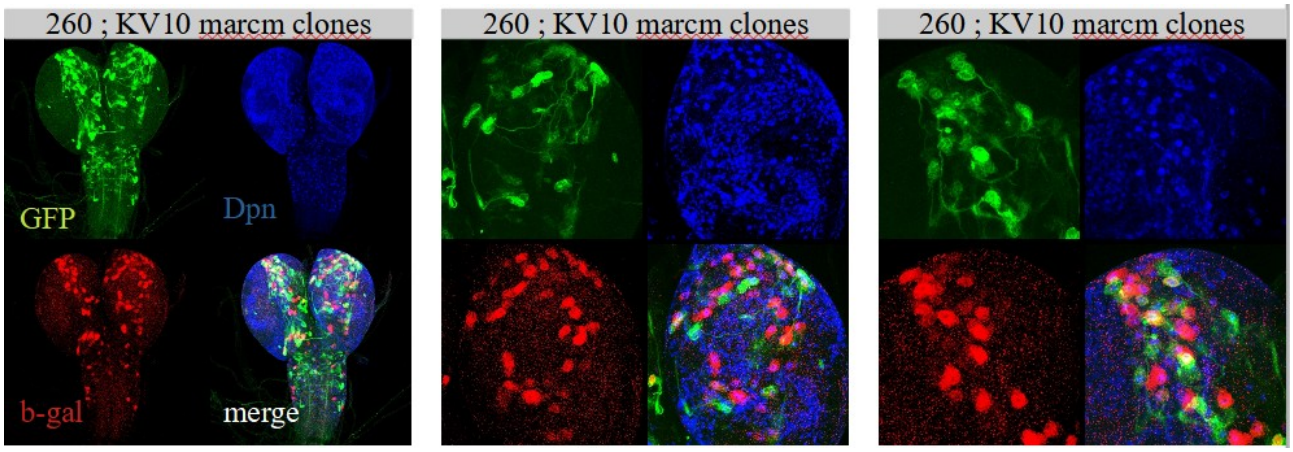

Figure 28: Marcm clones of 260/FM7; KV10/KV10 at 29ºC. Antibodies: g anti-GFP 488 (green), rb anti-b-gal 555 (red), gp anti-dpn 647 (blue).

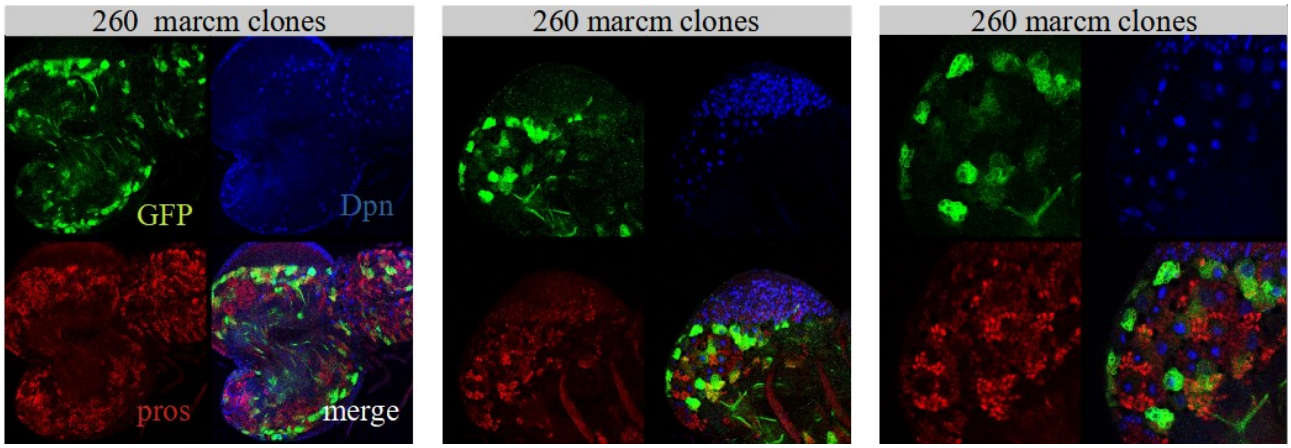

Figure 29: Marcm clones of 260/FM7; sp/CyO as a control at 29°C. Antibodies: rb anti-GFP 488 (green), m anti-pros 555 (red), gp anti-dpn 647 (blue).

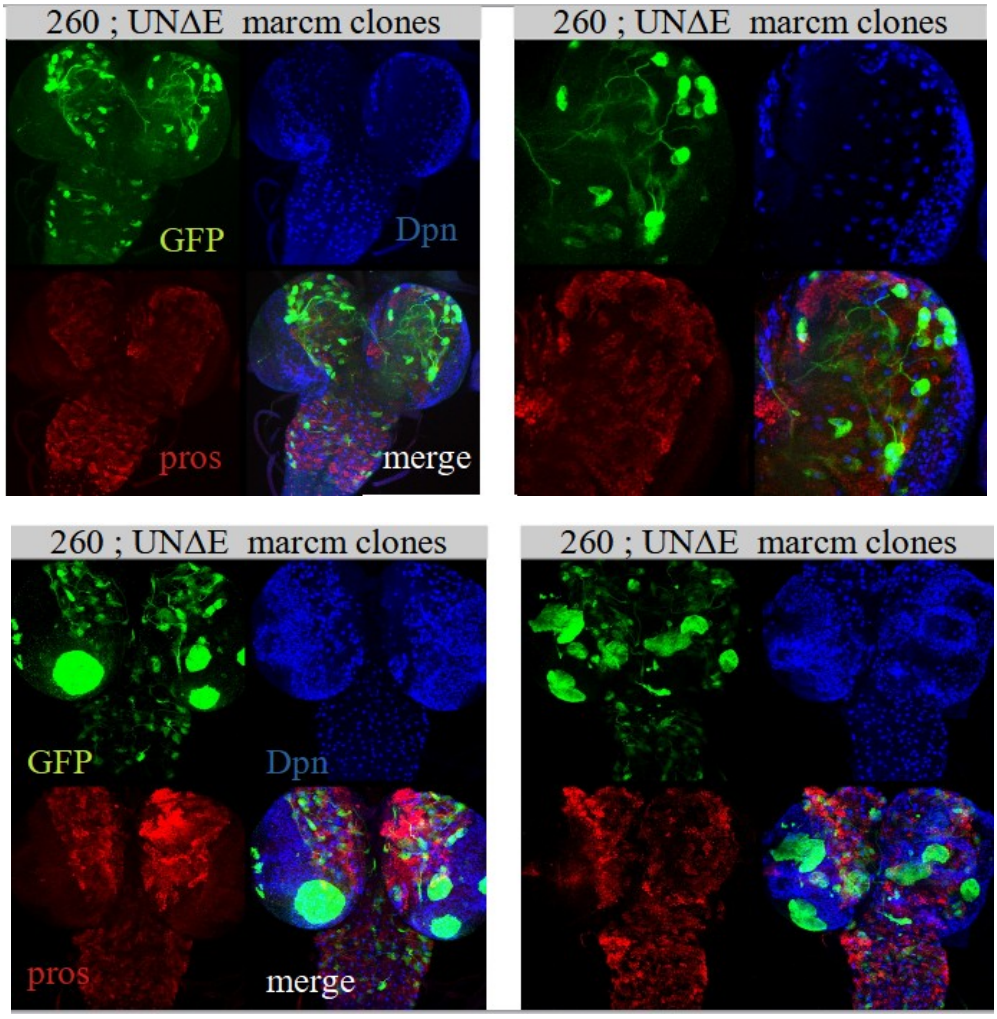

Figure 30: Marcm clones of 260/FM7;UNΔE/UNΔE, at 29oC (upper panels) and 37oC (lower panels). Antibodies: rb anti-GFP 488 (green), m anti-pros 555 (red), gp anti-dpn 647 (blue).

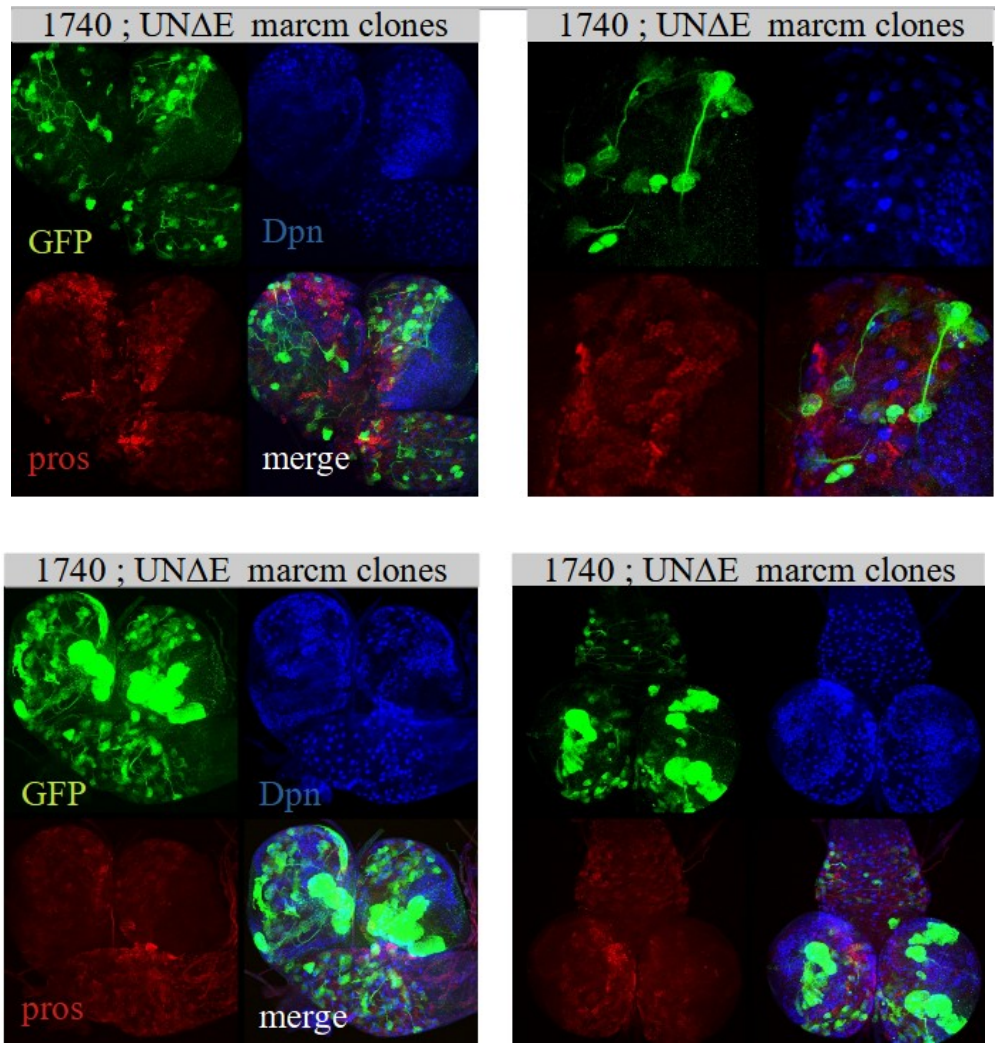

Figure 31: Marcm clones of 19A-FRT/19A-FRT;UNΔE/UNΔE, used as control at 29ºC (upper panels) and 37ºC (lower panels). Antibodies: rb anti-GFP 488 (green), m anti-pros 555 (red), gp anti-dpn 647 (blue).

Study of the downregulated gene of pumilio in Notch-induced clones at larva

Over-expression of activated Notch has been known to cause NSC hyperplasia in larvae, this is accompanied by induction of Hes genes; dpn and E(spl)mγ, and is suppressed by deletion of the E(spl) locus (Zacharioudaki et al., 2012). In these FLP-out clones, Type II lineages were severely affected, exhibiting a massive size increase. In Notch clones almost all cells expressed the neuroblast marker Dpn, with almost complete absence of differentiating cells. On contrary, type Is showed NSC hyperplasia with variable penetrance and expressivity. This is consistent with Notch signalling promoting NBs maintenance in larval brain (Magadi et al., 2020).

One last side project of my postgraduate thesis was the effect of the downregulation of the gene of pumilio (pumRNAi) in Notch clones. Although, there were at least four tries for generating Notch clones, this was not successful or repetitive. Indicative attempts are shown in Figure 28. The Notch-induced clones showed dpn positive cells in almost all cells, as Magadi et al. (2020) proposed (Figure 32). The first correction of the protocol was the temperature of the heatshock, from 29 to 37ºC, as it was proposed by Magadi et al. (2020). These results are yet to be examined.

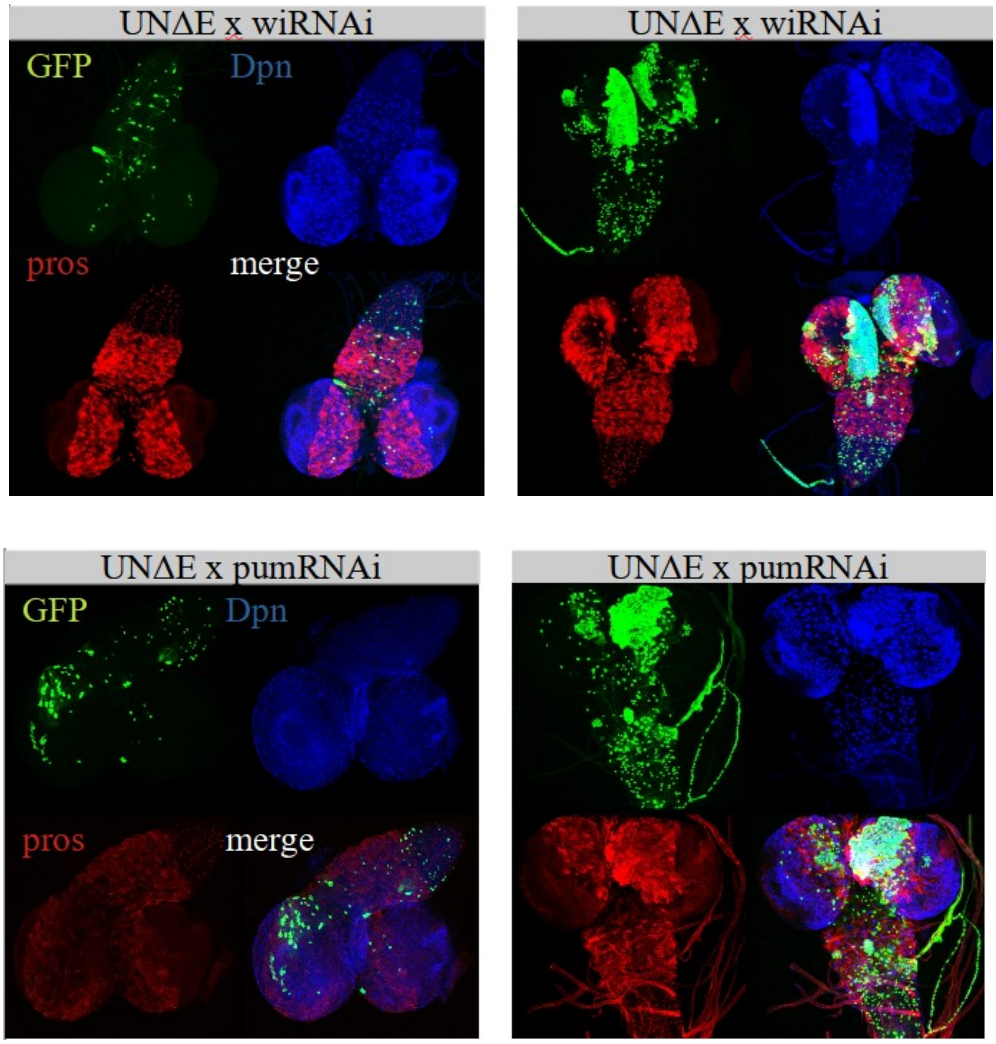

Figure 32: Notch-induced flip-out clones unsuccessful (left) and successful (right) in different genetic backgrounds, white RNAi (upper panels) and pumilion RNAi (lower panels). Antibodies: rb anti-GFP 488 (green), m anti-pros 555 (red), gp anti-dpn 647 (blue).

Discussion

Comprehensive study of the putative enhancers

The KV enhancer lines, that were studied earlier in *Df(1)B57* (Theodorou et al., 2022), were examined now in *Df(1)sc19*, in the presence of the transcription factor ase. This TF belongs to the proneural factors, together with ac, sc and l'sc, which induce the neural fate in the neuroectoderm of drosophila embryos. Ase is expressed in the delaminating neuroblasts, while the rest three proneurals earlier in the neuroectoderm. The loss of ase leads in a viable and fertile embryo with subtle bristle defects. Combining the later expression of ase and the mild defects of its null phenotype, it was suggested that ase NB expression is dispensable (Brand et al., 1993; Jarman et al., 1993). The *Df(1)sc19*, in which ase is not deleted, can give us an insight of the capabilities of ase.

In more detail, the enhancer of inscutable, KV1 was described as ase-responsive, because the TF ase activated it. The KV1 was, also, activated in *Df(1)B57* but at a later developmental stage presumably from other TFs. These unknown to us TFs maybe contributed to the activation of the enhancer in the *Df(1)sc19*, but the one stage earlier activation of the enhancer was from ase. On the other hand, the enhancer of phyllopod, KV4 was described as ase-non-responsive, while it was never activated in *Df(1)sc19* and its activation is ase independent. The brat-GFP gene and its enhancer KV8 were activated earlier in *Df(1)sc19*, and are both ase-responsive. Furthermore, the scrt-GFP was expressed in *Df(1)sc19* almost as in the wt embryos, and thus is ase-responsive, while its enhancer KV10 needs to be further examined. The nvy-GFP gene and its enhancer KV14 were described as ase-non-responsive, while they were never activated in *Df(1)sc19* and it seems that the activation of this gene, as whole, is ase independent. The enhancer KV21 and the gene that controls, tap, showed different expression patterns in the CNS and the PNS, and thus the results are not comparable. The gene dpn and its enhancer KV23 are characterised as ase-responsive, while the gene was expressed earlier in *Df(1)sc19* than in Df(1)B57, and the enhancer was never activated in *Df(1)B57* and was activated from ase in *Df(1)sc19*. Last, the wor-GFP showed no differences in its expression in both deficiencies and the wt, but previous immunostaining of wor in the lab showed delay in *Df(1)B57*, thus the expression of the transgene have to be studied again carefully.

In conclusion, ase could activate a couple of enhancers and almost all the genes that were studied. Especially the genes activated in *Df(1)sc19* were, also, activated in *Df(1)B57* by other transcription factors. It seems that ase can partially replace the rest proneurals, while in other circumstances the decisions made earlier in the neuroectoderm are so important that they are irreversible. All in all, ase is not a dispensable TF and is capable of activating enhancers and genes.

A further examination of more earlier or later stages should be done. However, X-gal staining of embryos and third instar larvae, as well as immunostaining of embryos, in wt and deficiencies (Theodorou et al., 2022), and larvae brains (Maria Kolonia thesis) are starting to give us a detailed picture of the behaviour of these enhancers.

Dpn overactivation and E(spl) genes behaviour

Preliminary data from Vasiliki Theodorou ChIP sequencing against dpn and dpn over-expression showed that dpn binds in genes of the E(spl) complex. The results from the RNA sequencing, that followed the ChIP-seq, showed that in Dpn over-expression the genes of E(spl)-C were downregulated. As a consequence, the possible suppressing role of dpn to E(spl)-C genes in dpn overactivation was studied. E(spl)m8-GFP, a transgene used as representative of the E(spl)m8 expression pattern (Piwko et al., 2019), showed no differences in expression in wt and dpn over-expression, while the E(spl)m7 were studied only in wt embryos. E(spl)m7 and m8 were detected in neuroectoderm and not in delaminating NBs until st11, and by st14 their expression was eliminated, as it was proposed by Jennings et al. (1994). Zacharioudaki et al. (2012) revisited the embryonic expression of E(spl)mγ and found NB expression from st11 until st13, and st13 loss from the neuroectoderm. We detect NB signal neither in E(spl)m8 nor in E(spl)m7, but loss of neurectoderm

expression at st14. Concerning the suppression of the E(spl) genes, it has been shown that escargot (Esg) and Scrt TFs, acting redundantly in PNS precursors, repress Notch target genes transcription [like E(spl)] (Ramat et al., 2016). The different results, from the foreseen ones from ChIP-seq and RNA-seq, were due to the presence of alternative suppressors of the E(spl)-C genes, besides to Dpn that did not seem to affect their expression, or due to construction of the transgene. The E(spl)m8-GFP may not comprise a putative Dpn responsive enhancer.

FACS sorting and cultured worGFP positive cells

Primary cultures are advantageous over established cell lines in Drosophila. In addition, individual NBs in vitro divide asymmetrically in a normal stem cell mode, producing a chain of progeny cells that inherit differential cell fates (Lüer & Technau, 2009). This, indicates that NBs have already commited in the neuroectoderm, and are able to cell-autonomously divide and produce their progeny (Lüer & Technau, 2009). Nevertheless, NBs require extrinsic signals from the overlying neuroectoderm to regulate spindle position and apical protein localization (Broadus & Doe, 1997), but the purpose of this experiment was not the spindle orientation. As a result, wor-GFP line was used for NBs culture, after cell sorting based on the GFP signal. The results was not so encouraging, as the GFP positive cells did not divide, or the dividing cells were not GFP positive. The possible causes are failures or mistakes in the procedure of cell acquisition, the FACS sorting itself, the culture conditions, even the time of imaging at operetta or the fluorescence microscope. Lüer and colleagues (2009) cultured single progenitor cells (st7-8) for 16 to 20 hours, which corresponds to the time required for normal embryos to fully develop (st 16-17). The same time window was used by us for the cell imaging at operetta, but as it was said this type of imaging created a series of problems. Apparently, the data from sorting and cell culture are preliminary, the protocols are not standardized and more tries should be done, in order to test NBs in different backgrounds, as it was the first speculation.

Semi-quantitative study of putative enhancers (X-gal staining of larvae)

To begin with, it would be useful, the KV enhancers tested with X-gal staining to be compared to the immunostaining results of larvae brains (Maria Kolonia postgraduate thesis). KV1 enhancer had the same pattern in X-gal and immuno- staining, same the KV8 showed no divergence. KV4 enhancer showed signal in optic lobe in both studies, but immunostaining showed VNC signal (abdominal hemisegments), too. The two scrt enhancers, KV10 and KV19, showed no differences in the two stainings. Concerning the two nervy enhancers, KV14 had the same signal in both studies, but KV15 showed weak signal in central brain, VNC and optic lobe in the immunostaining and no signal in X-gal. Maria Kolonia found KV21 expression in optic lobes, central brain and VNC, while X-gal staining detected only strong optic lobes signal. The next enhancer, KV23, appeared to be weakly expressed in only four regions of the central brain in immunostaining, while appeared with no staining in X-gal. Lastly, KV29 enhancer had the same pattern in both stainings, but immunostaining detected, also, weak optic lobe signal. Three from the tested enhancers, KV15, KV19 and KV23, need more examination as their signal was weak in immunostaining and absent in X-gal. The results from the X-gal staining in embryos (rotation report) showed that KV15 is active in the PNS, KV23 had strong signal in the CNS, while KV19 showed no staining pattern, even the 5 attempts for staining. Nevertheless, Theodorou et al. (2022), detected signal in CNS, PNS and midline of KV19, rendering KV19 an exclusive embryo acting enhancer.

In conclusion, immunostaining give a complete picture of the expression patterns and is more sensitive than the X-gal staining, and as a result the more accuracy in these data was expected. From the other hand, the aim of the X-gal is the measure of the expression strength.. All enhancers showed signal in larvae brains or embryos, even if in one of them their detected signal was weak or absent. Lastly, all the cloned putative enhancers have the accurate sequence to act as enhancers and are sufficient to drive b-gal expression in embryos and/or larvae, and most of them (except KV21)

recapitulate part of the expression pattern of the endogenous gene (whenever we have a comparison).

Enhancer KV10 and Notch over-expression in ASC deficiency background

From the desired KV8, KV10 and KV14, only the KV10 enhancer was able to be examined coupled with the *Df(1)260-1,* in order to monitor potential KV10 contribution in growing tumors. The KV10 enhancer with the absence of all proneurals showed neither different expression patterns nor different cell composition in Notch induced clones. Thus, the enhancer did not influence the Notch tumors.

In addition, Notch overactivation was studied in order to examine its dependency on proneurals. The Notch over-expression did not show any differences either in the expression patterns or the cell composition, compared to the controls in clones generated. Thus, the Notch over-expression is independent from the *Df(1)260-1*. Last, even if some initial results were obtained, the protocol temperature conditions have to be changed and more accurate conclusions to be draw.

pumilio RNAi effect in Notch over-expression

The Notch over-expression clones and how they are affected by the pumilio RNAi, was the purpose of these experiments. Unfortunately, the generating clones were not repetitive, mainly because the heatshock of the lines was carried out in a wrong temperature (29ºC instead of 37ºC, (Magadi et al., 2020). Another one possible explanation of the unsuccessful experiments may be the line carrying the actin flipase, which was not capable of generating clones.

Materials and methods

Growth and handling of flies

All the flies used in experimental procedures were grown in cylindrical, transparent, plastic tubes. Their food, a mixture of corn flour, water, agar and yeast, was in a solid form at the bottom of the vial, while the top was covered by cotton. Cotton lid provides the free exchange of the fresh air between the tube and the room and keeps the molds and mites out of the vial. Concerning the crosses of different Drosophila genotypes, the flies were kept at bigger cylindrical, transparent, plastic tubes (urine collectors-like tubes) with an adjustable cap (cages). The tube had small holes for the fresh air to come in and at the lid was the flies' food (upside down cage). This time, cap was half fulled with a solid mixture of agar and commercial cherry juice and on top there was fresh yeast. For further growing of a line, large, cylindrical, transparent, glass tubes were used, in the form of the plastic ones.

Temperature plays crucial role in Drosophila growing. The reproducibility of the experiments, also, require maintenance of the fly cultures at standard conditions. As a consequence, flies for immediate use, vials or cages, were kept at the controlled temperature of 25^{o}C and standard humidity levels. Stocks, flies that are long-term stored, are usually maintained at 18°C. This temperature slows down development to a generation time of about 20 days (Stocker & Gallant, 2008).

The handling of Drosophila requires anesthetized flies, so as to be easy the selection of desired individuals. The anesthesia was achieved by using CO_2. The CO_2 passed through a porous plate and formed a sea of gas. Thus, flies lying on the pad were anesthetized by the lack of oxygen and could be readily inspected and handled with fine paintbrushes. Flies can survive several minutes in this unconscious state. However, exposure to CO_2 for more than 20 minutes will result in lethality, and even before that, in the flies' fertility. Lastly, the flies, that were not usable anymore, were dumped into the "morgue" - a bottle filled with water and soap, fitted with a funnel (Stocker & Gallant, 2008).

KV enhancer lines

Three Chromatin Immunoprecipitation followed by deep sequencing (ChIP-seq) experiments, two against scAPAA and one against L(1)sc, was performed previously in the lab by Vasiliki Theodorou. Aim of this experiment, that was focused on stage 8- middle 11 embryos, was the finding of proneural TFs binding sites. Upon that, four replicated RNA-seq experiments and an H3K27Ac ChIP-seq from staged embryos were performed and the results were compared. Proneural TFs were found to bind in numerous regions in the genome. If these regions happen to have the open, accessible chromatin mark (H3K27Ac), also found in cis-regulatory elements, then this sequence may act as a plausible enhancer. In order to study the hypothesis that these regions were, indeed, working as enhancers of these specific TFs, 10 different regions whose protein product showed proneural dependency in mutated embryos were used to create transgenic lines of Drosophila melanogaster.

Those lines were designed and had the presumptive enhancer, a promoter, a reporter gene and the mini-white gene. In more detail, the enhancer had the sequence found from the ChIP-seq experiment, and the promoter was an hsp70 minimal promoter upstream of a lacZ reporter gene. Last, the mini-white gene was for the selection of the transgenic animals. When the transcription of this gene occured, β-galactosidase was detectable and the hypothetical enhancer was active (Theodorou et al., 2022)

Cherry juice agar plates

Materials

commercial cherry juice
agar

Procedure

Eight grams of agar and 250 ml of juice were boiled in a 500ml glass flask. The boiling took place in hotplate stirrer, with a stirrer inside the glass flask, in order to be homogeneous heating of the mixture. After the boiling procedure and the complete dilution of the agar in the juice, the mixture was transferred to 5cm diameter plastic agar plates. The plates were kept in room temperature to cool down and the agar to jell. After this, they were kept in 4ºC and used in cages for embryo collections.

Embryo Collections, Immunostaining and Imaging

Materials

1:1 commercial bleach and dH_2O
Heptane
10% formaldehyde
10x Phosphate Buffered Saline (PBS):

- NaCl: 137 mM
- KCl: 2.7 mM
- Na_2HPO_4: 10 mM
- KH_2PO_4: 1.8 mM

dH_2O
Methanol
0.2% Triton in 1xPBS (PT)
0.5% BSA(alboumin fraction) in PT (PBT)
Primary antibodies
Secondary antibodies
n-propyl gallate in glycerol (NPG)

Procedure

Embryo collections were made on cherry juice agar plates (lids). Embryos were transferred in sieves with fine paintbrushes, were dechorionated in 1:1 bleach and dH_2O for 2 minutes and were rinsed with tap water. Dechorionated emrbyos were transferred to 4 ml glass tubes containing fixative solution (1000µl dH_2O, 200µl 10xPBS, 800µl 10% formaldehyde, 2ml heptane) with paintbrashes and fixed for 16-18min with vigorous agitation (250rpm). Upon this, formaldehyde was discarded and 2ml methanol was added. Embryos were devitellinized with vigorous hand shaking in methanol for 30-60 seconds. After discard of heptane and three quick methanol rinses, samples were stored at -20ºC. On the day of immunostaining, embryos were rehydrated in 1ml PT. Three rinses with 1ml PT, and three 15 minutes washes with PT followed. Blocking was then conducted for at least 2 hours in 1ml PBT. Primary antibodies were diluted in 100µl PBT and incubated overnight at 4ºC with mild agitation. Next day, samples were washed extensively in PT; three rinses and three 15minutes wahes. After this, embryos were incubated with secondary antibodies dilluted in 100µl PBT for 3 hours at room temperature with mild shaking. After extensive PT washes, 80µl NPG mountant was added to each sample and incubated overnight at 4ºC. Embryos were then mounted on a microspope slide and imaged by confocal microscope. During the

immunostaining process the samples were protected from the light exposure and were covered with aluminium foil.

Larval dissections, X-gal staining and Imaging

Materials

1x PBS
1% glutaraldehyde in 1x PBS
X-gal buffer
X-gal with DMF
80% glycerol

Procedure

Larvae dissections were conducted in glass plate with 1ml PBS with a pair of forceps. 3rd instar larvae were selected, the posterior part (1/3) was cut and the rest 2/3 of its initial length was turned inside out. Tissues, such as the gut and the fat body, were removed carefully and the larvae carcasses left with the CNS and the developmental disks. After dissection, 15-20 larvae were transferred to 4 ml glass tubes containing 1ml of the fixative solution (1% glutaraldehyde in 1x PBS) and were left for fixation for 10 minutes with occasional swirl. After three quick 1ml 1x PBS rinses, samples were transferred to a 24-well plate with 300μl pre-warmed X-gal buffer and 12μl X-gal. The reaction (enzyme-substrate) was then conducted at 37ºC. The samples were occasionally checked in a stereoscope, if the reaction took place. When the blue colour showed, the reaction had to stop with three quick 1ml 1x PBS rinses. Then, the larval CNS and the wing disks were removed and mounted in 80% glycerol on a microspope slide and imaged by microscope.

Flip-out clones, Immunostaining and Imaging

Materials

10x PBS
dH_2O
10% formaldehyde
0.2% Triton in 1xPBS (PT)
0.5% BSA(alboumin fraction) in PT (PBT)
Primary antibodies
Secondary antibodies
n-propyl gallate in glycerol (NPG)

Procedure

Flies from the hs-FLP; act-FRT>STOP>FRT-Gal4, UAS-GFP stock were crossed with the appropriate UAS combinations for generating clones. Progeny underwent heat shock for 45 min at 29/37°C, 72 hours after egg lay (AEL). Three days later, ^{third} instar wandering larvae were selected and dissected (same process as in “Larval dissections, X-gal staining and Imaging”). The carcasses with the larval CNSs and wing disks were fixed (100μl PBS 10x, 500μl dH_2O, 400μl formaldehyde 10%) for 18 minutes, at room temperature, while shaking. Three quick 1ml 1x PBS rinses followed. Blocking was then conducted for at least 1 hour in 1ml PBT at room temperature, while shaking. Primary antibodies were diluted in 80μl PBT and larvae incubated overnight at 4ºC with mild agitation. Next day, samples were washed extensively in PT (three quick 1ml rinses and three 15min washes). After this, larvae were incubated with secondary antibodies dilluted in 80μl PBT for 2

hours at room temperature, while shaking. After extensive PT washes again, CNSs and wing disks were removed from carcasses and mounted in 35µl NPG. Samples imaged by confocal microscope. During the immunostaining process the samples were protected from the light exposure and were covered with aluminium foil.

Mosaic analysis (MARCM clones), Immunostaining and Imaging

Materials

10x PBS
dH_2O
10% formaldehyde
0.2% Triton in 1xPBS (PT)
0.5% BSA(alboumin fraction) in PT (PBT)
Primary antibodies
Secondary antibodies
n-propyl gallate in glycerol (NPG)

Procedure

Flies from hs-FLP, FRT tubP-Gal80, tubP-Gal4, UAS-GFP were crossed to appropriate FRT combinations for generating clones. Progeny underwent heat shock for 1/1.30 h at 29/37°C, 72 hours AEL, and CNSs were dissected out from wandering third instar larvae 3/4 days post clone induction. Dissection was conducted in glass plates with 1ml 1xPBS with a pair of forceps. CNSs were fixed (100µl PBS 10x, 500µl H_2O, 400µl formaldehyde10%) for 18 minutes, at room temperature, while shaking. Three 1ml 1x PBS rinses followed. Blocking was then conducted for at least 1 hour in 1ml PBT. Primary antibodies were diluted in 60µl PBT and larvae incubated overnight at 4ºC with mild shaking. Next day, samples were washed extensively in PT (three quick 1ml rinses and three 15min washes). After this, larvae were incubated with secondary antibodies dilluted in 60µl PBT for 2 hours at room temperature, while shaking. After extensive PT washes, CNSs and wing disks were removed from carcasses and mounted in 35µl NPG. Brains and disks imaged by confocal microscope. During the immunostaining process the samples were protected from the light exposure and were covered with aluminium foil.

Embryo FACS Sorting and cell culture

Fluorescent Activated Cell Sorting (FACS)

Typically, green fluorescent protein (GFP) is expressed in a tissue-specific manner using the UAS/Gal4 system, and cells are sorted based on their fluorescence signal. In NBs, however, this method is not applicable because the equal inheritance of Gal4 results in GFP expression in both daughter cells. Because cell size and GFP expression levels differ greatly between NBs and GMCs/neurons, the sorting is based on cell size, using forward scattering and fluorescence intensity. Flow cytometry analysis typically begins with creating gates to distinguish cells of interest. Forward versus side scatter (FSC vs SSC) gating is commonly used to identify cells of interest based on size and granularity (complexity). It is often suggested that forward scatter indicates cell size whereas side scatter relates to the complexity or granularity of the cell. However, it should be noted that forward scatter does not necessarily relate to size and side scatter is not really granularity. While these are an indication based on light refraction, it depends on the sample, the sheath fluid and the laser wavelength. This gating strategy can also be used to exclude debris as they tend to have lower forward scatter levels. They are often found at the bottom left corner of the FSC vs SSC density plot (Harzer et al., 2013).

Materials

1:1 commercial bleach and dH_2O
70% ethanol
10x Phosphate Buffered Saline (PBS)
dH_2O
0.2% Triton in 1xPBS (PT)
sterile1x trypsin in Ethylenediaminetetraacetic acid(EDTA) and PBS
Schneider's culture medium

Procedure

Embryo worniu-GFP staged collections (3-6h) were made on cherry juice agar plates. Embryos were transferred in sieves with fine paintbrushes, were dechorionated in 1:1 bleach and dH_2O for 2 minutes and were rinsed with tap water. Dechorionated emrbyos were rinsed with 70% ethanol, rinsed with tap water and transferred to 1.5ml tube with 1ml 0.2% PT. A spin (up to 3.000 rpm) followed, then PT was discarded and a new spin with 1ml 1xPBS was conducted. Pre-warmed at 37^{o}C trypsin was added to embryos for enzymatic homogenization. Simultaneously, gentle, short strokes using a pestle assisted the process of homogenization (mechanical homogenization) until all the embryo cells were suspended. The duration of the homogenization was maximum 4 minutes. The mixture of the suspended cells was transferred to a new 1.5ml tube through a mesh and a centrifuge at 3.000rpm for 1.5 minute followed. Embryo cells formed a pellet, so trypsin was discarded and cells resuspended to 1ml 1xPBS. Centrifuge at 2.000rpm for 4 minutes was performed and the pellet was resuspended again to 1ml 1xPBS. A second, identical centrifuge was performed and cells were resuspended to fresh 1ml 1xPBS. The cells were then sorted with Fluorescence-activated cell sorting (FACS) based on the endogenous expressing green fluorescent protein (GFP) tagged in the gene worniu (wor-GFP). Upon the sorting, cells were transferred to a 24-well plate and Schneider's culture medium was added. The next day the culture imaged by fluorescent microscope or operetta.
Our protocol relies on sorting of GFP-labeled cells that can be separated on the basis of their size and strength of GFP expression.

Gal4-UAS

A commonly used approach to express or knockdown specific genes in *Drosophila* is the so-called GAL4-UAS targeted expression system. GAL4 is a yeast transcription factor that is used to control the spatial and temporal expression of target genes, which consequently directs gene activity at a specific developmental stage and specific cells and tissues. In one parental strain, promoter regions for a particular gene are designed to drive the expression of GAL4 in some tissues. In another strain, the GAL4-binding upstream-activating sequence (UAS) is placed in front of the transgene. When these two strains are genetically crossed, their progenies express the transgene in specific tissues driven by the GAL4-UAS system (A. H. Brand & Perrimon, 1993). This system was used extensively in the fly strains.

Table 1: Crosses that were conducted during the thesis.

♀	♂
19A 260-1/FM7; sp/CyO	+; KV14-16-1/KV14-16-1
19A 260-1/FM7; sp/CyO	+ ; KV8-10-2 /KV8-10-2
19A 260-1/FM7; sp/CyO	+ ; KV10-17-1/KV10-17-1
sc19/FM7KrGFP	+ ; KV1-1-1/KV1-1-1
sc19/FM7KrGFP	+ ; KV4-3-1/KV4-3-1
sc19/FM7KrGFP	+ ; KV8-10-2/KV8-10-2
sc19/FM7KrGFP	+ ; KV10-17-1/KV10-17-1

sc19/FM7KrGFP	+ ; KV21-17-3/KV21-17-3
sc19/FM7KrGFP	tap-GFP
sc19/FM7KrGFP	odd-GFP
sc19/FM7KrGFP	+ ; + ; wor-GFP/wor-GFP
B57/FM7KrGFP	+ ; + ; wor-GFP/wor-GFP
+ ; + ; wor-GFP/wor-GFP	+ ; + ; wor-GFP/wor-GFP
U-8-1-1-dpn	E(spl)m8
U-8-1-1-dpn	E(spl)m7
U-CD8-GFP/ U-CD8-GFP; bibGAL4/bibGAL4	U-NDE-U-8-1-1/sp
19A 260-1/FM7; sp/CyO	hsFLP1-Gal80wFRT19A/y ; actGal4, U-CD8-GFP/actGal4, U-CD8-GFP
19A 260-1/FM7; UNDE/UNDE	hsFLP1-Gal80wFRT19A/y ; actGal4, U-CD8-GFP/actGal4, U-CD8-GFP
19A FRT/19A FRT ; UNDE/UNDE	hsFLP1-Gal80wFRT19A/y ; actGal4, U-CD8-GFP/actGal4, U-CD8-GFP
EqGal4/TM6B	1740/1740 ; UNDE/ UNDE or UNDE/CyO
19A FRT/19A FRT ; UNDE/ UNDE	EqGal4/TM6B
+ ; if/CyO-wg-lacZ ; MKRS/TM6B	+ ; + ; wor-GFP/wor-GFP
+ ; + ; wor-GFP/wor-GFP	+ ; if/CyO-wg-lacZ ; MKRS/TM6B→
+/CyO ; wor-GFP/TM6B	if/+ ; wor-GFP/TM6B→
	if/CyO ; wor-GFP/wor-GFP
+; U-8-1-1-dpn/CyO ; +	+ ; if/CyO ; MKRS/TM6B→
	U-8-1-1-dpn/if ; +/TM6B
if/CyO ; wor-GFP/wor-GFP	U-8-1-1-dpn/if ; +/TM6B →
	U-8-1-1-dpn/CyO ; wor-GFPTM6B

Table 2: Primary and secondary antibodies that were used for immunostaining. In parenthesis there is dilution used.

Primary antibodies	Secondary antibodies
rabbit anti-asense (1:50)	donkey anti-rabbit 488 (1:50)
rb anti-ase (1:50)	donkey anti-rb 555 (1:100)
rb anti-beta-galactosidase (1:100)	donkey anti-rb 555 (1:100)
rb anti-b-gal (1:100)	goat anti-rb 488 (1:50)
rb anti-Green Fluorescent Protein (1:100)	goat anti-rb 488 (1:100)
rb anti-phoshoHistone3 (1:150)	goat anti-rb 488 (1:50)
mouse anti-b-gal (1:50)	donkey anti-mouse 555 (1:50)
m anti-sex lethal (1:100)	donkey anti-m 647 (1:100)
m anti-sxl (1:100)	donkey anti-m 555 (1:100)
m anti-prospero (1:100)	donkey anti-m 555 (1:100)
m anti-cut (1:60)	donkey anti-m 555 (1:100)
m anti-BP102 (1:200)	donkey anti-m 555 (1:100)
m anti-groucho (1:100)	donkey anti-m 555 (1:100)
m anti-neurotactin (1:50)	donkey anti-m 555 (1:100)
guinea pig anti-deadpan (1:100)	goat anti-guinea pig 647 (1:100)
gp anti-dpn (1:100)	donkey anti-gp Cy5 (1:100)
gp anti-dpn (1:100)	donkey anti-gp Cy3 (1:40)
gp anti-dpn(1:100)	goat anti-gp 555 (1:100)
goat anti-GFP (1:50-1:80)	donkey anti-goat 488 (1:100)
rat anti-worniu (1:80)	goat anti-rat 633 (1:50)

Acknowledgements

At this point, I would like to thank Professor Christos Delidakis, who gave me the chance to be a member of the lab and helped me in every step and need of the postgraduate thesis. Also, I would like to thank my supervisor and postdoctoral fellow of the lab Dr. Vasiliki Theodorou, who helped me every single day in the conduction of the experiments and the writing of this thesis.
Furthermore, I would like to thank the postdoctoral fellows of the lab Margarita Stapountzi, Zoi Veneti and Eva Zacharioudaki for their assistance and advice throughout the year, as well as their kindness. PhD students Virginia Fasoulaki, Vassiliki Kapoulea and Chrysanthi Voutyraki were always there for me creating a pleasant working space. Lastly, the undergraduate students Eleni Aligianni, Leda Kavalieratou, Marialena Vathi, Asimenia Goniotaki and Anastasia Meligkounaki were the joy of the lab and we were working together harmonically.
In addition, I would like to thank the researcher and IMBB Group Leader Anastasios Pavlopoulos and the researcher and Staff Scientist Maria Monastirioti for being my committee in the master and for giving me advice.
Also, I would like to thank the postdoctoral fellow Elena Deligianni for the imaging in the operetta, and the research assistant Zaharenia Vlata for the FACS sorting procedure.
All in all, I would like to thank my family and friends who encouraged me throughout the year and helped my dreams to come true.

References

Alonso, M. C., & Cabrera, C. V. (1988). The achaete-scute gene complex of Drosophila melanogaster comprises four homologous genes. *The EMBO Journal*, *7*(8), 2585–2591. https://doi.org/10.1002/J.1460-2075.1988.TB03108.X

Apitz, H., & Salecker, I. (2014). A Challenge of Numbers and Diversity: Neurogenesis in the Drosophila Optic Lobe. *Http://Dx.Doi.Org/10.3109/01677063.2014.922558*, *28*(3–4), 233–249. https://doi.org/10.3109/01677063.2014.922558

Arnold, C. D., Gerlach, D., Stelzer, C., Boryń, Ł. M., Rath, M., & Stark, A. (2013). Genome-wide quantitative enhancer activity maps identified by STARR-seq. *Science*, *339*(6123), 1074–1077. https://doi.org/10.1126/SCIENCE.1232542/SUPPL_FILE/ARNOLD.SM.PDF

Arnold, C. D., Zabidi, M. A., Pagani, M., Rath, M., Schernhuber, K., Kazmar, T., & Stark, A. (2016). Genome-wide assessment of sequence-intrinsic enhancer responsiveness at single-base-pair resolution. *Nature Biotechnology 2016 35:2*, *35*(2), 136–144. https://doi.org/10.1038/nbt.3739

Bai, J., Sepp, K. J., & Perrimon, N. (2009). Culture of Drosophila primary cells dissociated from gastrula embryos and their use in RNAi screening. *Nature Protocols*, *4*(10), 1502–1512. https://doi.org/10.1038/NPROT.2009.147

Bailey, A. M., & Posakony, J. W. (1995). Suppressor of hairless directly activates transcription of enhancer of split complex genes in response to Notch receptor activity. *Genes & Development*, *9*(21), 2609–2622. https://doi.org/10.1101/GAD.9.21.2609

Banerji, J., Rusconi, S., & Schaffner, W. (1981). Expression of a beta-globin gene is enhanced by remote SV40 DNA sequences. *Cell*, *27*(2 Pt 1), 299–308. https://doi.org/10.1016/0092-8674(81)90413-X

Bier, E., Vaessin, H., Younger-Shepherd, S., Lily Yeh Jan, & Yuh Nung Jan. (1992). deadpan, an essential pan-neural gene in Drosophila, encodes a helix-loop-helix protein similar to the hairy gene product. *Genes & Development*, *6*(11), 2137–2151. https://doi.org/10.1101/GAD.6.11.2137

Brand, A. H., & Perrimon, N. (1993). Targeted gene expression as a means of altering cell fates and generating dominant phenotypes. *Development (Cambridge, England)*, *118*(2), 401–415. https://doi.org/10.1242/DEV.118.2.401

Brand, M., Jarman, A. P., Jan, L. Y., & Jan, Y. N. (1993). asense is a Drosophila neural precursor gene and is capable of initiating sense organ formation. *Development (Cambridge, England)*, *119*(1), 1–7. https://doi.org/10.1242/DEV.119.SUPPLEMENT.1

Broadus, J., & Doe, C. Q. (1997). Extrinsic cues, intrinsic cues and microfilaments regulate asymmetric protein localization in Drosophila neuroblasts. *Current Biology : CB*, *7*(11), 827–835. https://doi.org/10.1016/S0960-9822(06)00370-8

Cabrera, C. V., & Alonso, M. C. (1991). Transcriptional activation by heterodimers of the achaete-scute and daughterless gene products of Drosophila. *The EMBO Journal*, *10*(10), 2965–2974. https://doi.org/10.1002/J.1460-2075.1991.TB07847.X

Catarino, R. R., & Stark, A. (2018). Assessing sufficiency and necessity of enhancer activities for gene expression and the mechanisms of transcription activation. *Genes & Development*, *32*(3–4), 202–223. https://doi.org/10.1101/GAD.310367.117

Ceron, J., Tejedor, F. J., & Moya, F. (2006). A primary cell culture of Drosophila postembryonic larval neuroblasts to study cell cycle and asymmetric division. *European Journal of Cell Biology*, *85*(6), 567–575. https://doi.org/10.1016/J.EJCB.2006.02.006

Cohen, B., Simcox, A. A., & Cohen, S. M. (1993). Allocation of the thoracic imaginal primordia in the Drosophila embryo. *Development (Cambridge, England)*, *117*(2), 597–608. https://doi.org/10.1242/DEV.117.2.597

Crews, S. T. (2019). Drosophila Embryonic CNS Development: Neurogenesis, Gliogenesis, Cell Fate, and Differentiation. *Genetics*, *213*(4), 1111. https://doi.org/10.1534/GENETICS.119.300974

Cubenãs-Potts, C., Rowley, M. J., Lyu, X., Li, G., Lei, E. P., & Corces, V. G. (2017). Different enhancer classes in Drosophila bind distinct architectural proteins and mediate unique chromatin interactions and 3D architecture. *Nucleic Acids Research*, *45*(4), 1714. https://doi.org/10.1093/NAR/GKW1114

Delidakis, C., & Artavanis-Tsakonas, S. (1992). The Enhancer of split [E(spl)] locus of Drosophila encodes seven independent helix-loop-helix proteins. *Proceedings of the National Academy of Sciences*, *89*(18), 8731–8735. https://doi.org/10.1073/PNAS.89.18.8731

Feinstein, P. G., Kornfeld, K., Hogness, D. S., & Mann, R. S. (1995). Identification of Homeotic Target Genes in Drosophila Melanogaster Including Nervy, a Proto-Oncogene Homologue. *Genetics*, *140*(2), 573. https://doi.org/10.1093/GENETICS/140.2.573

Fernández-Hernández, I., Rhiner, C., & Moreno, E. (2013). Adult neurogenesis in Drosophila. *Cell Reports*, *3*(6), 1857–1865. https://doi.org/10.1016/J.CELREP.2013.05.034

García-Bellido, A., & De Celis, J. F. (2009). Anecdotal, Historical and Critical Commentaries on Genetics: The Complex Tale of the achaete–scute Complex: A Paradigmatic Case in the Analysis of Gene Organization and Function During Development. *Genetics*, *182*(3), 631. https://doi.org/10.1534/GENETICS.109.104083

Ghysen, A., & Dambly-Chaudiere, C. (1989). Genesis of the Drosophila peripheral nervous system. *Trends in Genetics*, *5*(C), 251–255. https://doi.org/10.1016/0168-9525(89)90097-8

Giagtzoglou, N., Alifragis, P., Koumbanakis, K. A., & Delidakis, C. (2003). Two modes of recruitment of E(spl) repressors onto target genes. *Development (Cambridge, England)*, *130*(2), 259–270. https://doi.org/10.1242/DEV.00206

Gonzalez, F., Romani, S., Cubas, P., Modolell, J., & Campuzano, S. (1989). Molecular analysis of the asense gene, a member of the achaete-scute complex of Drosophila melanogaster, and its novel role in optic lobe development. *The EMBO Journal*, *8*(12), 3553–3562. https://doi.org/10.1002/J.1460-2075.1989.TB08527.X

Goupil, A., Heinen, J. P., Rossi, F., Salame, R., Pennetier, C., Simon, A., Skorski, P., Lauzao, A., Bardin, A., Basto, R., & Gonzalez, C. (2021). Illuminati, a novel form of gene expression plasticity in Drosophila neural stem cells. *BioRxiv*, 2021.04.28.441783. https://doi.org/10.1101/2021.04.28.441783

Hales, K. G., Korey, C. A., Larracuente, A. M., & Roberts, D. M. (2015). Genetics on the Fly: A Primer on the Drosophila Model System. *Genetics*, *201*(3), 815–842. https://doi.org/10.1534/GENETICS.115.183392

Hartenstein, V. (1988). Development of Drosophila larval sensory organs: spatiotemporal pattern of sensory neurones, peripheral axonal pathways and sensilla differentiation. *Development*, *102*(4), 869–886. https://doi.org/10.1242/DEV.102.4.869

Hartenstein, V., Spindler, S., Pereanu, W., & Fung, S. (2008). The development of the drosophila larval brain. *Advances in Experimental Medicine and Biology*, *628*, 1–31. https://doi.org/10.1007/978-0-387-78261-4_1/COVER

Hartenstein, V., & Wodarz, A. (2013). Initial neurogenesis in Drosophila. *Wiley Interdisciplinary Reviews. Developmental Biology*, *2*(5), 701. https://doi.org/10.1002/WDEV.111

Harzer, H., Berger, C., Conder, R., Schmauss, G., & Knoblich, J. A. (2013). FACS purification of Drosophila larval Neuroblasts for next generation sequencing. *Nature Protocols*, *8*(6), 1088. https://doi.org/10.1038/NPROT.2013.062

Huang, M. L., Hsu, C. H., & Chien, C. T. (2000). The proneural gene amos promotes multiple dendritic neuron formation in the Drosophila peripheral nervous system. *Neuron*, *25*(1), 57–67. https://doi.org/10.1016/S0896-6273(00)80871-5

Jarman, A. P., Brand, M., Jan, L. Y., & Jan, Y. N. (1993). The regulation and function of the helix-loop-helix gene, asense, in Drosophila neural precursors. *Development*, *119*(1), 19–29. https://doi.org/10.1242/DEV.119.1.19

Jarman, A. P., & Groves, A. K. (2013). The role of Atonal transcription factors in the development of mechanosensitive cells. *Seminars in Cell & Developmental Biology*, *24*(5), 438. https://doi.org/10.1016/J.SEMCDB.2013.03.010

Jennings, B., Preiss, A., Delidakis, C., & Bray, S. (1994). The Notch signalling pathway is required for Enhancer of split bHLH protein expression during neurogenesis in the Drosophila embryo. *Development (Cambridge, England)*, *120*(12), 3537–3548. https://doi.org/10.1242/DEV.120.12.3537

Jiménez, F., & Campos-Ortega, J. A. (1990). Defective neuroblast commitment in mutants of the achaete-scute complex and adjacent genes of D. melanogaster. *Neuron*, *5*(1), 81–89. https://doi.org/10.1016/0896-6273(90)90036-F

Kaufman, T. C. (2017). A Short History and Description of Drosophila melanogaster Classical Genetics: Chromosome Aberrations, Forward Genetic Screens, and the Nature of Mutations. *Genetics*, *206*(2), 665. https://doi.org/10.1534/GENETICS.117.199950

Knust, E., Tietze, K., & Campos-Ortega, J. A. (1987). Molecular analysis of the neurogenic locus Enhancer of split of Drosophila melanogaster. *The EMBO Journal*, *6*(13), 4113–4123. https://doi.org/10.1002/J.1460-2075.1987.TB02757.X

Koshikawa, S. (2015). Enhancer modularity and the evolution of new traits. *Fly*, *9*(4), 155. https://doi.org/10.1080/19336934.2016.1151129

Kraut, R., & Campos-Ortega, J. A. (1996). inscuteable,A Neural Precursor Gene ofDrosophila,Encodes a Candidate for a Cytoskeleton Adaptor Protein. *Developmental Biology*, *174*(1), 65–81. https://doi.org/10.1006/DBIO.1996.0052

Kraut, R., Chia, W., Jan, L. Y., Jan, Y. N., & Knoblich, J. A. (1996). Role of inscuteable in orienting asymmetric cell divisions in Drosophila. *Nature 1996 383:6595*, *383*(6595), 50–55. https://doi.org/10.1038/383050a0

Larsen, C., Shy, D., Spindler, S. R., Fung, S., Pereanu, W., Younossi-Hartenstein, A., & Hartenstein, V. (2009). Patterns of growth, axonal extension and axonal arborization of neuronal lineages in the developing Drosophila brain. *Developmental Biology*, *335*(2), 289. https://doi.org/10.1016/J.YDBIO.2009.06.015

Lee, C. Y., Wilkinson, B. D., Siegrist, S. E., Wharton, R. P., & Doe, C. Q. (2006). Brat is a Miranda cargo protein that promotes neuronal differentiation and inhibits neuroblast self-renewal. *Developmental Cell*, *10*(4), 441–449. https://doi.org/10.1016/j.devcel.2006.01.017

Lehmann, R., Jiménez, F., Dietrich, U., & Campos-Ortega, J. A. (1983). On the phenotype and development of mutants of early neurogenesis inDrosophila melanogaster. *Wilhelm Roux's Archives of Developmental Biology 1983 192:2*, *192*(2), 62–74. https://doi.org/10.1007/BF00848482

Li, G., & Hidalgo, A. (2020). Adult Neurogenesis in the Drosophila Brain: The Evidence and the Void. *International Journal of Molecular Sciences 2020, Vol. 21, Page 6653*, *21*(18), 6653. https://doi.org/10.3390/IJMS21186653

Li, X., Chen, R., & Zhu, S. (2017). bHLH-O proteins balance the self-renewal and differentiation of Drosophila neural stem cells by regulating Earmuff expression. *Developmental Biology*, *431*(2), 239–251. https://doi.org/10.1016/J.YDBIO.2017.09.011

Lüer, K., & Technau, G. M. (2009). Single cell cultures of Drosophila neuroectodermal and mesectodermal central nervous system progenitors reveal different degrees of developmental autonomy. *Neural Development*, *4*(1). https://doi.org/10.1186/1749-8104-4-30

Magadi, S. S., Voutyraki, C., Anagnostopoulos, G., Zacharioudaki, E., Poutakidou, I. K., Efraimoglou, C., Stapountzi, M., Theodorou, V., Nikolaou, C., Koumbanakis, K. A., Fullard, J. F., & Delidakis, C. (2020). Dissecting Hes-centred transcriptional networks in neural stem cell maintenance and tumorigenesis in Drosophila. *Development (Cambridge)*, *147*(22). https://journals.biologists.com/dev/article/147/22/dev191544/226091/Dissecting-Hes-centred-transcriptional-networks-in

Martin-Bermudo, M. D., Gonzalez, F., Dominguez, M., Rodriguez, I., Ruiz-Gomez, M., Romani, S., Modolell, J., & Jimenez, F. (1993). Molecular characterization of the lethal of scute genetic function. *Development*, *118*(3), 1003–1012. https://doi.org/10.1242/DEV.118.3.1003

Nakao, K., & Campos-Ortega, J. A. (1996). Persistent Expression of Genes of the Enhancer of Split Complex Suppresses Neural Development in Drosophila. *Neuron*, *16*(2), 275–286. https://doi.org/10.1016/S0896-6273(00)80046-X

Ohno, S. (2001). Intercellular junctions and cellular polarity: the PAR-aPKC complex, a conserved core cassette playing fundamental roles in cell polarity. *Current Opinion in Cell Biology*, *13*(5), 641–648. https://doi.org/10.1016/S0955-0674(00)00264-7

Paroush, Z., Finley, R. L., Kidd, T., Wainwright, S. M., Ingham, P. W., Brent, R., & Ish-Horowicz, D. (1994). Groucho is required for Drosophila neurogenesis, segmentation, and sex determination and interacts directly with hairy-related bHLH proteins. *Cell*, *79*(5), 805–815. https://doi.org/10.1016/0092-8674(94)90070-1

Pi, H., Huang, S. K., Tang, C. Y., Sun, Y. H., & Chien, C. T. (2004). phyllopod is a target gene of proneural proteins in Drosophila external sensory organ development. *Proceedings of the National Academy of Sciences of the United States of America*, *101*(22), 8378–8383. https://doi.org/10.1073/PNAS.0306010101/ASSET/86642C4C-A940-475F-B240-5351615AC812/ASSETS/GRAPHIC/ZPQ0230450340005.JPEG

Pi, H., Wu, H. J., & Chien, C. T. (2001). A dual function of phyllopod in Drosophila external sensory organ development: cell fate specification of sensory organ precursor and its progeny. *Development*, *128*(14), 2699–2710. https://doi.org/10.1242/DEV.128.14.2699

Piwko, P., Vitsaki, I., Livadaras, I., & Delidakis, C. (2019). The Role of Insulators in Transgene Transvection in Drosophila. *Genetics*, *212*(2), 489. https://doi.org/10.1534/GENETICS.119.302165

Ramat, A., Audibert, A., Louvet-Vallée, S., Simon, F., Fichelson, P., & Gho, M. (2016). Escargot and Scratch regulate neural commitment by antagonizing Notch activity in Drosophila sensory organs. *Development (Cambridge)*, *143*(16), 3024–3034. https://doi.org/10.1242/DEV.134387/VIDEO-1

Reichardt, I., Bonnay, F., Steinmann, V., Loedige, I., Burkard, T. R., Meister, G., & Knoblich, J. A. (2018). The tumor suppressor Brat controls neuronal stem cell lineages by inhibiting Deadpan and Zelda. *EMBO Reports*, *19*(1), 102–117. https://doi.org/10.15252/EMBR.201744188

Requena, D., Álvarez, J. A., Gabilondo, H., Loker, R., Mann, R. S., & Estella, C. (2017). Origins and Specification of the Drosophila Wing. *Current Biology : CB*, *27*(24), 3826-3836.e5. https://doi.org/10.1016/J.CUB.2017.11.023

Roark, M., Sturtevant, M. A., Emery, J., Vaessin, H., Grell, E., & Bier, E. (1995). scratch, a pan-neural gene encoding a zinc finger protein related to snail, promotes neuronal development. *Genes & Development*, *9*(19), 2384–2398. https://doi.org/10.1101/GAD.9.19.2384

Schober, M., Schaefer, M., & Knoblich, J. A. (1999). Bazooka recruits Inscuteable to orient asymmetric cell divisions in Drosophila neuroblasts. *Nature 1999 402:6761*, *402*(6761), 548–551. https://doi.org/10.1038/990135

Singhania, A., & Grueber, W. B. (2014). Development of the embryonic and larval peripheral nervous system of Drosophila. *Wiley Interdisciplinary Reviews. Developmental Biology*, *3*(3), 193. https://doi.org/10.1002/WDEV.135

Stocker, H., & Gallant, P. (2008). Getting started : an overview on raising and handling Drosophila. *Methods in Molecular Biology (Clifton, N.J.)*, *420*, 27–44. https://doi.org/10.1007/978-1-59745-583-1_2

Terman, J. R., & Kolodkin, A. L. (2004). Nervy Links Protein Kinase A to Plexin-Mediated Semaphorin Repulsion. *Science*, *303*(5661), 1204–1207. https://doi.org/10.1126/SCIENCE.1092121/SUPPL_FILE/TERMAN_SOM.PDF

Theodorou, V., Stefanaki, A., Drakos, M., Triantafyllou, D., & Delidakis, C. (2022). ASC proneural factors are necessary for chromatin remodeling during neuroectodermal to neuroblast fate transition to ensure the timely initiation of the neural stem cell program. *BMC Biology*, *20*(1). https://doi.org/10.1186/S12915-022-01300-8

Tripathi, B. K., & Irvine, K. D. (2022). The wing imaginal disc. *Genetics*, *220*(4). https://doi.org/10.1093/GENETICS/IYAC020

Villares, R., & Cabrera, C. V. (1987). The achaete-scute gene complex of D. melanogaster: Conserved Domains in a subset of genes required for neurogenesis and their homology to myc. *Cell*, *50*(3), 415–424. https://doi.org/10.1016/0092-8674(87)90495-8

Wildonger, J., & Mann, R. S. (2005). Evidence that nervy, the Drosophila homolog of ETO/MTG8, promotes mechanosensory organ development by enhancing Notch signaling. *Developmental Biology*, *286*(2), 507–520. https://doi.org/10.1016/J.YDBIO.2005.08.026

Wodarz, A. (2002). Establishing cell polarity in development. *Nature Cell Biology*, *4*(2). https://doi.org/10.1038/NCB0202-E39

Wodarz, A., & Huttner, W. B. (2003). Asymmetric cell division during neurogenesis in Drosophila and vertebrates. *Mechanisms of Development*, *120*(11), 1297–1309. https://pubmed.ncbi.nlm.nih.gov/14623439/

Yamaguchi, M., & Yoshida, H. (2018). Drosophila as a model organism. *Advances in Experimental Medicine and Biology*, *1076*, 1–10. https://doi.org/10.1007/978-981-13-0529-0_1/TABLES/1

Yuan, L., Hu, S., Okray, Z., Ren, X., De Geest, N., Claeys, A., Yan, J., Bellefroid, E., Hassan, B. A., & Quan, X. J. (2016). The Drosophila neurogenin tap functionally interacts with the Wnt-PCP pathway to regulate neuronal extension and guidance. *Development (Cambridge)*, *143*(15), 2760–2766. https://doi.org/10.1242/DEV.134155/264058/AM/THE-DROSOPHILA-NEUROGENIN-TAP-FUNCTIONALLY

Zabidi, M. A., Arnold, C. D., Schernhuber, K., Pagani, M., Rath, M., Frank, O., & Stark, A. (2015). Enhancer-core-promoter specificity separatesdevelopmental and housekeeping generegulation. *Nature*, *518*(7540), 556. https://doi.org/10.1038/NATURE13994

Zacharioudaki, E., Magadi, S. S., & Delidakis, C. (2012). bHLH-O proteins are crucial for Drosophila neuroblast self-renewal and mediate Notch-induced overproliferation. *Development*, *139*(7), 1258–1269. https://doi.org/10.1242/DEV.071779